ABSTRACT

Title of Dissertation:	ACCESSIBILITY BASED EVALUATION OF COASTAL RURAL COMMUNITIES' VULNERABILITY TO COASTAL FLOODING AND THEIR ADAPTATION OPTIONS
	Zeinab Yahyazadeh Jasour, Doctor of Philosophy, 2022
Dissertation directed by:	Professor Allison C. Reilly, Department of Civil and Environmental Engineering

Global climate change and sea-level rise will cause significant risks to coastal communities. To make inclusive and cost-effective adaptation planning decisions, we need to understand who may be impacted and when. Currently, planning literature generally focuses on housing impacts; when will a house be inundated, and what adaptation strategies are useful to keep a house habitable? Housing, though, is only one of many types of infrastructures people need to reside in an area. Reliable roads are another. This dissertation conducts an analysis of parcel-level impacts of SLR on local residents' ability to reach key amenities such as emergency services, grocery stores,

and schools. Furthermore, it strategically evaluates where road protection should be implemented so that access is maintained in an equitable manner. Next, I use the accessibility analysis to identify the important roads for gathering high-resolution flood data to improve the accuracy of the analysis. I use Dorchester County, Maryland, U.S., as a case study. It is an extremely low-lying rural county and is expected to shrink in half by the end of the century due to SLR. The results from the case study indicate that some parcels are not expected to be inundated by SLR but are expected to experience accessibility impacts. Road protection appears to be a temporary strategy that can buy time for long-term adaptation strategies such as relocation. However, the protection strategies should be cautiously selected based on decision-makers priorities. The insight obtained by this dissertation highlights that when policy and decision-makers are deciding among adaptation strategies, they need to reach some level of consensus about assumptions for which a possible future is planned, and also the trade-off between increasing accessibility levels and balancing the distribution of accessibility among different demographic groups.

ACCESSIBILITY BASED EVALUATION OF COASTAL RURAL COMMUNITIES' VULNERABILITY TO COASTAL FLOODING AND THEIR ADAPTATION OPTIONS

by

Zeinab Yahyazadeh Jasour

Dissertation submitted to the Faculty of the Graduate School of the
University of Maryland, College Park, in partial fulfillment
of the requirements for the degree of
Doctor of philosophy
2022

Advisory Committee:

Professor Allison C. Reilly, Chair
Professor Gregory Baecher
Professor Michelle Bensi
Professor Tom Logan
Professor Katrina Groth, Dean's Representative

Dedication

To my respectful mom, Farideh.

To my beloved husband, Mohammad, and to my lovely daughter, Nora.

Acknowledgments

I would like to express my deepest appreciation to my advisor, Professor Allison Reilly, for her continuous support of my Ph.D. study and research. With her invaluable patience, motivation, and immense knowledge, she encouraged me to think critically and be innovative. She helped me grow as an independent researcher.

Special thanks to Professor Michelle Bensi for generously sharing her knowledge and experience.

I am grateful to my committee members, Professor Gregory B. Baecher, Professor Katrina Growth, and Professor Tom Logan, for their helpful comments and great suggestion.

I would like to thank my friends, group members, and peers for being helpful and supportive.

I wish to express my love to my mom, Farideh Alizadeh, and my siblings for their love and encouragement. A special thank is given to my daughter, Nora, who is an inspiration to achieve greatness. Finally, I would like to express my sincere gratitude to my husband, Mohammad Motalleb Najed, for his faithful love and strongest support. This endeavor would not have been possible without him.

Table of Contents

List of Tables

List of Figures

1 Chapter 1: Introduction

Global climate change brought on by greenhouse gas emissions is likely to cause heavier precipitation, increased temperatures, and more frequent extreme weather events (IPCC 2021; Mendelsohn et al., 2012). Sea-level rise, which is primarily caused by thermal expansion of the ocean as it is warmed and the melting of ice on land, is predicted to be among the more consequential impacts from climate change and will lead to significant human displacement and changes to ecosystem services (Nicholls, 2011; Pugh, 2004). There are also studies that demonstrate that climate change will change storm surge patterns which will increase the frequency and intensity of coastal flooding (Emanuel, 2005). While the localized impacts may vary, sea-level rise and more nuisance flooding will have serious impacts on communities (P. Jacobs et al., 2000). Coastal areas with shallow slope shorelines and proclivity to subsidence, such as the U.S. mid-Atlantic region, are especially threatened (Boon, 2012; McLean et al., 2001). Approximately 50% of the U.S. population (more than 164 million people) live or work in coastal counties (Moser et al., 2014), and more than 9.2 million people (about 3% of the U.S. population) reside in 100-year coastal floodplains (Crowell et al., 2010). The changes in temperature and rainfall patterns due to climate change also affect agriculture sectors worldwide. The changes in temperature and rainfall patterns due to climate change also affect infrastructure reliability. While global changes are likely to be small or moderate, regional changes could be significant in many parts of the world (Paudel et al., 2014). This highlights the importance of

understanding the risks from climate change and its impact on communities and provides a strong basis for investments in resilience actions.

In spite of many existing studies addressing the negative impacts of global changes on infrastructure components, the comprehensive evaluation of climate change and SLR on networked infrastructure and communities' well-being is missing (Wilbanks & Fernandez, 2014). A significant portion of the research in this field has explored the impact of SLR and coastal flooding on housing. For example, Pistrika & Jonkman (2010) and Cox et al. (2019) evaluate the impact of climate change and SLR on where individuals reside, and if a resident needs to relocate due to flooding, and when that may happen. Sadler et al. (2017) evaluate the percentage of the roadways with a high likelihood of flooding in the Hampton Roads area of Virginia under SLR and storm surge. However, the negative impact of flooding may not be limited to the inundated area; inundation of networked system components (e.g., roads, pipelines, or power assets) can cause cascading disruptions to large portions of the community. To better be prepared for climate change, it is necessary to understand who may be impacted by climate change and when this will happen.

Over the last two decades, more studies have focused on the role of flooding on the performance of transportation networks. On the East Coast of the U.S., more than 7,500 miles of roadways are currently threatened by nuisance flooding, which results in 100 million vehicle hours of delay annually (Jacobs et al., 2018). These numbers will increase in the future due to SLR (Wu et al., 2002). The negative impacts of flooding on transportation systems are usually evaluated in two different ways: assessment of

which roads will be inundated (Sadler et al. 2017, Ju et al. 2019) and evaluation of networked impacts of flooding in an aggregated spatial areas, such as longer travel times or losing access to a specific destination (Kermanshah & Derrible, 2017; Lu & Peng, 2011; Sohn, 2006). However, studying the roads and housing separately or focusing on single components does not provide a strong basis regarding which regions will be forced to adapt and when that may happen.

1.1 Resilience

Arguably, in order to build resilience to climate change and sea-level rise, it must first be defined with clear associated measures. Definitions of resilience vary from one field of study to another (Meerow et al., 2016), though core concepts center around individual and community well-being over time in the face of adversities, such as natural hazards and climate change. Resilience in the context of climate change adaptation is generally considered to be the capacity of a system to cope with hazardous events through response, adaptation, recovery, and learning (Change, 2014). Existing studies can be divided into two groups: one that concentrates on physical assets such as critical infrastructure and their ability to operate while responding to threats, and one that focuses on social characteristics that influence community recovery capacity (Bruneau et al., 2003; S. L. Cutter, 2014; Haimes, 2002; Hosseini Nourzad & Pradhan Anu, 2016a). Physical assets, including critical infrastructure, play a fundamental role in the operation and development of current societies, and their failure can result in a considerable reduction in serviceability and

can significantly cascade impacts on communities (Deshmukh et al., 2011). For example, disruption in a segment of a road network can have significant effects on the entire system. Therefore, it is necessary to evaluate the ability of these systems to withstand the stresses of hazard-related disruptions.

As the frequency and severity of disasters grow, there is increasing recognition of the fact that not all threats can be avoided. This highlights the importance of community resilience - a mechanism to ensure that minimum disturbances happen. In addition to physical assets such as road networks, the social units such as organizations, communities, and individuals also experience direct or indirect impacts of hazard-related damage and losses, and the socioeconomic and demographic characteristics of people and units influence their capacity to absorb losses, recover from adverse events, and to make changes that enhance their system resilience (Cutter, 2003). Ultimately, however, there is a significant knowledge gap in how the performance of the physical assets impacts community resilience and wellbeing. As the impacts of climate change are becoming recognized, and that inter-governmental agreement on climate mitigation is unlikely to be sufficient at preventing future climate extremes (Warner et al., 2009), policy-makers are looking towards not only mitigation strategies such as hardening but also considering adaptation strategies such as managed retreat from sea-level rise, or spreading risks through insurance (Siders, 2019; Warner et al., 2009).

The knowledge gap for building infrastructure and community resilience is especially significant for rural areas. Their limited resources combined with a wide-

scale flooding threat may cause more challenges for the residents in these areas to maintain their access to critical services. In the case of mitigation and hardening of the roads, rural communities face more problems due to the sparse roadway network that offers fewer alternatives for motorists.

The knowledge gap for building infrastructure and community resilience is often especially significant for rural areas. Their limited resources, often combined with a wide-scale flooding threat, may cause more challenges for the residents in these areas to maintain their accessibility to critical services. While both urban and rural areas are vulnerable to flood hazards and SLR, research on adaptation to SLR mostly focuses on urban areas because the greatest losses in property value are more possible in urban areas(Weiss et al., 2011). Rural communities also tend to be home for populations that are more vulnerable to SLR impacts due to poverty and being isolated from central planning agencies (Donner & Rodríguez, 2008; Hardy et al., 2017). The economic impacts of flooding could be more significant in rural areas than urban areas due to more self-employment and more dependency on natural resources (Twigger-Ross et al., 2005). Rural areas also have fewer facilities per capita, and the loss of services and shops can disproportionately impact small communities. In terms of health, physical injuries may become worse because of the longer distance to services and also loss of access due to flooded roads. Moreover, during and after floods, rural communities may receive less attention due to having less political visibility than urban residents (Bukvic & Harrald, 2019).

Understanding the impact of climate change, especially sea-level rise, and storm surge flooding, at a finer spatial resolution in coastal communities, especially rural areas, can enable decision-makers, policymakers, and other experts to make more informed decisions regarding mitigation and adaptation strategies and to help improve the resilience of the communities.

1.2 Dissertation objectives

The main objective of this dissertation is to conduct a comprehensive evaluation of how sea-level rise and storm surges intersect with roads in rural communities and how these disruptions impact local residents. I also advance techniques that inform how to effectively build local resilience through roadway improvements and local monitoring. Through a series of three research questions, the body of work broadly advances the field of resilience engineering through both the methods that are used to evaluate local impacts and how the results demonstrate a reconsideration of adaptation trigger points.

The research questions and associated research activities are discussed briefly in the subsections below, and details are provided in Chapters 2-4. In addition, research on the impact of climate change on agriculture in rural coastal counties is provided in Appendix A. Chapter 5 responds to the research question raised in each chapter and summarizes the main findings of each section. Furthermore, it also describes the limitations and future directions of this dissertation.

1.3 Research Question 1: Roadway flooding as a bellwether for household retreat in rural, coastal regions vulnerable to sea-level rise

Coastal flooding will significantly impact the road networks in low-lying rural coastal areas, and this will impact residents' daily lives. The localized impacts of flooding will vary, though the threat is expected to increase due to SLR (Azevedo de Almeida & Mostafavi, 2016; Fang et al., 2020). In the U.S., almost 50% of the population live or commute to the coastal counties, and their daily lives rely on transportation networks. Floods and inundation from storm surges and sea-level rise not only damage buildings and businesses; they also can significantly disrupt networked infrastructure, including roads and powerlines. A disruption in one segment of a networked system can have cascading impacts and ultimately has the potential of negatively impacting the entire system. To date, a significant portion of the research evaluating the impact of repetitive coastal flooding and SLR focuses on residential structures flooding and mitigation (Cox et al., 2019; Pistrika & Jonkman, 2010). The assumption is that household inundation is an adaptation trigger point that will force relocation. However, repetitive temporary loss or permanent loss of critical networked infrastructures, such as roadways and electricity, impact individual's ability to reside and access economic opportunities in flood-prone places and are each likely to influence migration from coastal, flood-prone areas even if houses themselves are not flooded (Cole, 2008).

This chapter focuses on road infrastructure and the impact that SLR could have on local residents as a result of roadway flooding. Over the past decades, more emphasis has

been placed on the impact of flooding on local residents. I will focus on the impacts of the flood on communities using accessibility analysis. Accessibility is described as an ability to reach desired destinations such as grocery stores. The following gaps are identified:

- At present, there is not a body of literature that examines the relationship between the failure of critical infrastructure services such as transportation networks and parcel inhabitation.
- Most accessibility evaluations are conducted at spatially aggregated scales, such as census tracts, which can easily mask important information about some neighbors or parcels.
- Existing studies that consider roadway flooding use a limited number of flooding scenarios, such as 1 meter of water or a 100-year flood scenario which cannot provide a comprehensive understanding of the threat.

The following research questions are explored in Chapter 2 to address the knowledge gaps in the existing literature.

- How do different SLR scenarios with different exceedance probabilities impact parcel-level accessibility and travel distance in the rural coastal regions?
- Which parcels may experience the impacts of flooding, regardless of whether their structure floods?

- What is the warning time between accessibility loss and future household inundation for each parcel in the area?

To address these research questions, a computational-geospatial framework is developed that assesses the parcel-level accessibility to everyday facilities, including emergency services, and the impacts that SLR will have on that access. The focus of this work is on parcel-level impacts, as a coarser spatial aggregation can mask distributions, causing some parcels to appear less vulnerable to SLR-related transportation disruptions than they truly are. This allows me to identify parcels that may experience the impacts of flooding, regardless of whether their structure floods. It also helps us to define the warning time between accessibility loss and future household inundation. Finally, this framework has been implemented in a realistic case study in Dorchester County, MD.

- More details of the study are provided in Chapter.2.

1.4 Research Question 2: Bridging adaptation resources across the urban-rural divide: A comparison of equity-focused roadway investment strategies against flooding

Coastal communities are increasingly facing disruptions as a result of sea-level rise-induced coastal flooding (Wu et al., 2002). Inundation of transportation infrastructure can affect travel to critical services and economic opportunities (Alabbad et al., 2021). Flooding of only a few road segments may disconnect some parts of the community or increase the distance to reach key amenities (Sohn 2006). Roadway

inundation can be more problematic in rural areas, which have more sparse road networks and offer fewer alternative routes to access services.

A well-known and standard approach for investing mitigation resources is to protect high traffic volume roads under the threat of inundation. This approach is practical and politically defensible, though it may not result in maximal accumulated benefits. Specifically, because this method is not considering a systems-level perspective, it is not evaluating the ability of all residents to get to key facilities, such as fire stations. Moreover, ignoring the spatial distribution of floods in a network and protecting high traffic volume roads without investigating the network-wide impact of other road inundation may offer limited benefits (Alipour et al., 2020; Douglas et al., 2017).

Over the past decade, most of the studies that explored optimal systems-level resource allocations for road armoring in flood-prone areas end up emphasizing the protection of urban regions for reasons of efficiency. This leads to uneven distribution of the benefits among groups of the communities, especially in rural areas. The following gaps are identified in the literature:

- Existing approaches simplify their analysis by evaluating the impact of protection strategies on network performance by simply adapting one road segment at a time, as opposed to the impact that a suite of roadway adaptations may offer.Studies that focus on protection strategies and transportation equity consider the spatial distribution of benefits among different sociodemographic

and socioeconomic groups, but to the best of the author's knowledge, none of them aim to balance access between rural and urban communities.

- Further, these studies use performance measures, including road volume and capacity, and not accessibility, and thus do not consider each resident’s basic need of travel during periods of extremes.
- Most of the existing studies on optimal protection strategies do not provide information about the robustness of their strategies under other flood scenarios with different return periods.

The following research questions are explored in Chapter 3 to address the knowledge gaps in the existing literature.

- How will different storm surge scenarios impact parcel-level accessibility in the rural coastal regions?
- What are optimal road protection strategies under different budget limits to address the following objectives?
    - Maintain accessibility of more parcels.
    - Improve the accessibility share of all block groups, considering all the same.
    - Improve the accessibility share of all block groups, considering different weights.
    - Balance accessibility of parcels in rural and urban block groups.

    - Balance accessibility of parcels in vulnerable and non-vulnerable block groups.
- How robust are the protection strategies under different storm surge flooding scenarios?

To address these research questions, a framework is developed that evaluates the benefits and burdens of road protection strategies under different flood scenarios on a rural community. The focus of this work is to consider transportation equity by finding the optimum protection strategies that distribute the benefits evenly among different groups of the community. This study also aims to evaluate the impact of combinations of roadway adaptations instead of studying the links individually and independently. For this reason, two different storm surge flooding scenarios (10-year and 100-year) are used and compared, and also different budget limits are considered.

More details of the study are provided in Chapter 3.

1.5 Research Question 3: Identification of Critical Road Segments that reduce uncertainty surrounding access to emergency services if monitored

Road networks are a key infrastructure service for communities, designed to provide reliable access to opportunities and to critical services. During disasters and other emergency situations, roads are vital resources that play a significant role in rescue operations, evacuation, community recovery, and reconstruction. However, they often fail to maintain their original orientation due to being highly exposed to flood inundation, resulting in transportation network performance degradation. The

disruption of links is not equal in terms of their impact on network performance; the failure of certain links can be highly problematic in a resident's accessibility, while others only result in longer trips for a few residents. A challenging issue for decision-makers and stakeholders during periods of high tides and heavy precipitation is not knowing which roads will flood, and thus should be avoided. In rural areas, the sparse network can mean that alternative routes are considerably longer, and this can be particularly problematic for emergency vehicles which rely on speed.

This work "flips" the threat-consequence modeling paradigm to investigate where the impacts of floods on a road network are most consequential (in terms of lack of access and longer routes) in order to inform where localized monitoring and finer-scale, computationally intensive hydrodynamic modeling should take place. The project was born from the question "where should we improve the accuracy of our hydrodynamic modeling?" which requires better forensic investigation of localized water conveyance infrastructure (e.g., location of culverts), closer monitoring of actual hydraulic conditions, and finer-scale hydrodynamic modeling. Having better localized information about the potential flooding can help inform motorists and emergency managers with trip-planning.

In order to better inform decision-makers, this work leverages the transportation network and evaluates the network-wide impacts of certain links failure based on accessibility changes. Then uses the results to identify the critical links to understand where more accurate flood data maximizes information about the consequences of floods. Previous studies have mostly focused on links with a higher chance of flooding

or the limited high traffic volume roads to identify the critical links for gathering more accurate data. The following gaps are identified:

Existing approaches that aim to identify critical links simplify their analysis by evaluating the criticality of an individual link on a network at a time as opposed to the analysis of a combination of roadways.

- Most studies that focus on candidate links for more accurate data consider a deterministic flood water amount and ignore the uncertainty of the flood depth.
- To the author's best knowledge, no previous work uses the consequences of flooding on transportation networks to identify the critical links for which more accurate hydraulic understanding is warranted.

The following research questions are explored in Chapter 4 to address the knowledge gaps in the existing literature.

- Can an accessibility analysis of a roadway network help to inform where the accuracy of hydrodynamic models should improve?
- How do varying storm surges with different confidence limits impact motorists and emergency managers?

- Which roads are most critical to install flood monitoring equipment, so as to provide maximal information to the most local residents and emergency services?

To address these research questions, a framework is developed that first determines the road links that may flood under a 1-year flood scenario under different uncertainty analyses (confidence limits). I then evaluate parcel-level access to understand the value of gathering accurate flood data. I also use different budget limits to evaluate the sensitivity of the results to the number of monitoring equipment.

More details of the study are provided in Chapter 4.

2 Chapter 2: Roadway Flooding as a Bellwether for Household Retreat in Rural, Coastal Regions Vulnerable to Sea-level Rise

2.1 Introduction

While localized impacts will vary, the threat of coastal flooding is expected to increase due to periods of heavier precipitation and sea-level rise (SLR) (Azevedo de Almeida and Mostafavi, 2016; Fang et al., 2021). In the U.S., more than 164 million people (approximately 50% of the population) live or work in coastal counties (Moser et al., 2014), and more than 9.2 million people (approximately 3% of the population) reside in 100-year coastal floodplains (Crowell et al., 2010). However, this figure does not fully reflect the extent to which coastal flooding impacts Americans (and people throughout the world) now and into the future. Floods not only damage homes and businesses; they also can significantly impact networked infrastructure, including roads and pipelines. A disruption in one segment of a networked system can have ripple effects on the entire system. For example, an individual who resides outside a floodprone coastal area may rely on surface transportation with segments inside flood-prone areas, forcing repetitive detours and longer travel times - if they can reach their destination at all. This is particularly concerning when considering a potential lack of access to emergency services. In some instances, repetitive loss of infrastructure may prove to be a bellwether for future residential inundation.

To date, a significant portion of the research (and government planning documents) that explore how individuals and communities may be impacted by

repetitive coastal flooding and SLR focuses on where individuals reside (Cox et al., 2019; Hauer et al., 2016; Pistrika & Jonkman, 2010), and if and when a resident would be forced to relocate under different climate scenarios. However, residential structures are only one of many types of infrastructure required for individuals to maintain residence; repetitive temporary loss or permanent loss of other critical infrastructures, such as roadways, electricity, and access to healthcare impact residents' ability to recover after floods and are each likely to influence migration from coastal, flood-prone areas even if houses themselves are unaffected (Cole, 2008). This is a particular issue, given that more than 60,000 miles of roads in the U.S. are within FEMA's coastal flood zone (Douglass & Krolak, 2008). Furthermore, in rural areas, especially areas with highly fractal coastlines, large-scale coastline protection is infeasible.

Coastal flooding and its impact on networked infrastructure could also create and exacerbate existing regional and economic inequalities. The transportation literature has consistently highlighted how low- and moderate-income communities, along with communities of color, consistently experience poorer access and other transportation quality metrics (Ermagun and Tilahun, 2020; Zuo et al., 2020). More recently, there has been an emphasis on evaluating the distributional impacts of disruptions and investments in transportation infrastructure (Bills and Walker, 2017; Kelobonye et al., 2019). It is reasonable to hypothesize in areas with coastal flooding that, repetitive loss of infrastructure services, such as transportation access, may induce retreat among the wealthy before their house is threatened and, conversely, limit economic and job opportunities among the most vulnerable who are unable to relocate

without assistance. Understanding which regions will be forced to adapt and when can support long-term regional planning and enable just transitions.

The work in this paper specifically focuses on road infrastructure and the impact that SLR could have on local residents as a result of roadway flooding. However, the approach is flexible enough to consider any networked infrastructure (e.g., electricity or water) and the impacts that disruptions in one area of the network could pose on other areas. I create and implement a computational-geospatial framework that evaluates parcel-level accessibility to everyday amenities and facilities, including emergency services, and the impacts that SLR will have on that access. Accessibility, here, refers to the availability of a route connecting a specific location (e.g., a parcel) to a desired destination and, if a route exists, the travel distance of that route (Litman, 2008). The focus of this work is on parcel-level impacts, as opposed to impacts at more aggregated geospatial levels such as census tracts - which is a more common approach due to previous computational limitations (Logan et al., 2019). This allows us to pinpoint which parcels may experience the impacts of flooding, regardless of whether the structure on the parcel floods. It also supports questions about when limited accessibility becomes a bellwether for future household inundation. The framework is illustrated using Dorchester County, Maryland. Dorchester County has 1,700 miles of shoreline and is highly vulnerable to SLR (Cole, 2008). It is expected to lose approximately 60% of its landmass by 2100 (Chanse, 2016).

This work expands upon the literature in three ways. First, it provides a framework for quantifying parcel-level accessibility to critical facilities (here,

emergency services, grocery stores, and schools) for different SLR scenarios. Second, it identifies when parcels will be inundated by SLR under different climate scenarios in order to quantify the warning time that residents have between accessibility loss and parcel inundation. Third, this approach is demonstrated using a realistic case study in Dorchester County, MD.

2.2 Literature review

2.2.1 Transportation Resilience to Flooding

Over the past two decades, in both the literature and in practice, there has been a shift in emphasis from hazard avoidance to impact reduction and whole-community resilience (S. Cutter, 2016; Sharifi, 2016). The idea is that it is both too costly and, in many ways, impossible to avert impacts from all possible threats, but that there are ways to empower communities to withstand and overcome them. To achieve this ideal, communities must act as a system to manage and minimize risks and improve their ability to recover (Gillespie-Marthaler et al., 2019). Policymakers, too, have adopted this approach, and many have turned their attention to efforts to strengthen communities against various types of disasters (Reiner & McElvaney, 2017). However, to improve resilience, I need to measure it (S. L. Cutter et al., 2010). At present, efforts to measure community resilience are inconsistent and differ on what should be measured (Cutter, 2014). The existing studies can be divided into two camps: one that focuses on a region's physical assets, such as critical infrastructure and its ability to operate while resisting threats, and one that focuses on social factors that impact

community recovery capacity (Bruneau et al., 2003; S. L. Cutter, 2014; Haimes, 2002; Hosseini Nourzad Seyed Hossein & Pradhan Anu, 2016b). The methodology presented in this work makes progress in bridging this divide by identifying the parcels (and thus residents) who are most affected by flooding and infrastructure disruption. While resilience indicators are usually provided at a community-level resolution, my work focuses on much more granular scales.

There are multiple ways researchers have quantified transportation network resilience, including reliability, robustness, and vulnerability measures (Jenelius & Mattsson, 2012; Nagurney & Qiang, 2012; Vromans et al., 2006). These metrics tend to focus on the functionality of the network and not on its users. Accessibility and mobility are two additional concepts used in transportation planning to evaluate performance changes in transportation systems and the impact on members of the community (Ross, 1999). While not usually discussed in a disaster context, both can indicate resilience from the perspective of individuals. Accessibility describes an ability to reach a destination. When a disruption occurs on a road network, such as one or more road closures, residents could lose their ability to access particular destinations such as workplaces or grocery stores if no alternative route exists (Taylor & Susilawati, 2012). This can often be the case in rural areas which may have limited alternative routing options. If at least one route to the destination remains viable, the travel distance may be longer. Taylor and Susilawati (2012) explored this concept using an inverse of accessibility (remoteness) metric in their analysis to capture the impact of link failures on rural populations' ability to access services and facilities. On the other hand,

mobility describes the physical movement and is usually measured in terms of distance or speed of travel from an origin to a destination, and often includes the impacts of congestion due to vehicle rerouting (Litman, 2008). In some instances, it is possible that some destinations are still accessible despite road disruptions, though the distances to those destinations may be longer due to detours and the time to those destinations is longer due to congestion.

Over the past decade, more emphasis has been placed on the role of flooding on the functionality of transportation infrastructure. Flooding is increasingly problematic on coastal roads both in the U.S. and globally (Douglass et al., 2014). Flooding can originate in multiple ways, including pluvial and fluvial sources, but increasingly, tidal nuisance flooding is an additional stressor, and its frequency will increase significantly by the end of the century. Jacobs et al. (2018) find that tidal nuisance flooding threatens over 7,500 miles of roadways across the East Coast of the U.S. and likely causes 100 million vehicle hours of delay annually. SLR also increases the mean sea-level height upon which surge builds, meaning storm surge heights will increase and penetrate farther inland in the future (Wu et al., 2002).

A suite of work, including Castrucci and Tahvildari (2018, 2017), Jacobs et al. (2018), Ju et al. (2019), and Sadler et al. (2017), evaluates *what* will be inundated by floods by overlaying flood inundation with the geo-positioning of infrastructure. For example, Sadler et al. (2017) assess the percentage of the roadways with a high likelihood of inundation in the Hampton Roads area of Virginia under SLR and storm surge. Ju et al. (2019) quantify the percentage of the population, lifeline infrastructures

(including roads), emergency response assets, and developed land that are exposed to different flood scenarios in the San Francisco Bay Area. Jacobs et al. (2018) consider both spatial and temporal inundation of road assets for the entire eastern seaboard of the U.S. resulting from nuisance flooding and combines these inundation metrics with current roadway demand to equate future impacts.

Many approaches additionally consider networked impacts of flooding and how users of the system could be impacted in terms of longer travel times or inability to reach a destination. These approaches are usually conducted at spatially aggregated levels and not for individual parcels. For example, Sohn (2006) calculates the accessibility score for each county in Maryland as a function of its population, the shortest travel distance, and the average traffic volume between the county and all other counties both under normal conditions and a 100-year flood. However, this analysis evaluates county-level impacts and only considers state and federal roads, meaning adaptation (e.g., traffic diversion) that uses local roads is not considered. Lu and Peng (2011) identify the most vulnerable traffic analysis zones in Miami, Florida, for two different SLR scenarios, as measured by the travel time from one zone to another after inundation relative to before. This measure is then summed over all zones and weighted by population. This work considers the entire road network, though individual impacts are not evaluated. Lu et al. (2015) expand on their 2011 work to include a more sophisticated gravity model that considers how vehicles will be rerouted to avoid water and thus compute the impact on traffic and travel delays. Kermanshah and Derrible (2017) is similar in that it focuses on the travel between urban neighborhoods due to

floods but also consider how topological properties of the road network evolve as a result of flooding.

Andersson and Stalhut (2014), Coles et al. (2017), Fereshtehpour et al. (2018), and Green et al. (2017) are specific in that they consider how floods impact emergency response, though they generally focus on a limited number of origins and destinations. For example, Fereshtepour et al. (2018) compute how travel times would increase between a fire station and six health care facilities in Lower Manhattan, NY, for 100-year coastal and pluvial flood events, though they do not consider how these floods would impact congestion - a potential shortcoming in a heavily urbanized region. Similarly, Green et al. (2017) evaluate the accessibility of emergency responders during different flood scenarios in Leicester, UK. They identify the percentage of the region that is accessible to ambulance, fire, and rescue service stations within 8 and 10 minutes (legislative mandates for emergency services) for pluvial and fluvial floods, though do not evaluate the impact of floods on residents.

In some of the most refined work yet, Sun et al. (2020), Hummel et al. (2020), and Sun et al. (2021) go beyond examining a few origins and destinations to evaluate how flooding and localized flood protections could impact commuters in the San Francisco Bay. To do this, they merge high-resolution hydrodynamic models of inundation with an agent-based transportation simulation model to compute traffic delays for a deterministic future SLR scenario. They, however, consider only a small fraction of commuters due to computational constraints (though road capacity is proportionally constrained) and the works assume user equilibrium is achieved, though

this may not occur during times of disruption. Thus, some travel time estimates could be underpredictions.

2.2.2 SLR and Residential Adaptation

As property damage from coastal flooding continues to rise, finding tolerable and cost-effective strategies that mitigate or prevent these losses completely is becoming a key priority for communities (Highfield et al., 2014; Warren-Myers et al., 2018). In practice, the dominant strategy is to identify and implement hardening strategies that enable individuals to remain in their homes. This includes shoreline protection and beach nourishment, seawalls and levees, and structural approaches that raise or armor a house (Longenecker, 2019; Peacock, 2003; Rao et al., 2015). While many of the strategies are evaluated in aggregate or at community-level, such as acquiring and conserving open space (S. D. Brody et al., 2017; Calil et al., 2015), and levees (Longenecker, 2019), there is growing recognition of the importance of parcel-level evaluation. For example, Andreucci and Aktas (2017) assessed the vulnerability of coastal communities to the impacts of SLR in Connecticut. Their analysis revealed important information about efficient ways to protect homeowners from the adverse impacts of floods. This specific information can easily be masked by aggregated analyses at the community-level (Highfield & Brody, 2013). Brody et al. (2014) assessed the impact of adjacent land use and land cover on flood damages recorded on 7,900 properties in Texas. The influence of proximity and built environment factors can be more thoroughly assessed in parcel-level analysis.

The unavoidable impacts of climate change and SLR on coastal communities will demand adding retreat to the adaptation strategies that up to now focus more on structural protection and recovery. Retreat allows residents to build new beginnings in safer places and helps create public amenities by removing homes in flood-prone areas and restoring the land for natural floodplain uses (Freudenberg et al., 2016). Despite the importance of this adaptation strategy, few studies have focused on retreat decisions (Hecht & Kirshen, 2019). Kirshen et al. (2008) find that it is economically advantageous to use structural protections, such as seawalls, in highly developed areas. Less structural approaches, such as retreat and floodproofing, can be more cost-effective and flexible in responding to uncertain climatic changes in more rural areas, but uncertainty in the expected rate of SLR makes planning difficult. They also note that retreat is an expensive strategy, particularly in areas with high-value properties, which makes it less desirable unless substantial flooding has occurred (Kirshen et al., 2008). Bier et al. (2020) argue that the government could encourage residents at-risk of SLR inundation to relocate before flooding happens using subsidies. However, there are many important factors other than economic costs, such as losses in social networks, access to healthcare, employment, and physical and mental health affecting the relocation (McMichael et al., 2012). Song and Peng (2017) study the impact of people's risk perception, hazard experience, threat, and adaptation appraisal on households' likelihood to relocate away from low-lying coastal areas threatened by SLR. Their results show that households who believe SLR is happening and have experienced inundation due to sea-level changes have a higher willingness to relocate. Households

with existing adaptations such as seawalls and flood insurance are reluctant to relocate. At present, there is not a body of literature that examines how retreat intersects with issues related to transportation access or failures in other infrastructure services that support parcel inhabitation.

2.3 Methodology

The work presented in this section describes the framework for quantifying parcel-level accessibility to essential facilities under different flooding conditions, with a specific focus on SLR. An overview of the approach is presented in Figure 2.1. For each flood scenario discussed below, I overlay its water depth for the entire region onto the road network to identify which links (i.e., roads) within the network are inundated. I then evaluate whether residents at each parcel are able to reach essential destinations (specifically fire stations, grocery stores, and schools) during each scenario and, if so, the distance to the closest facility in each class. This work additionally considers (1) when residents lose accessibility to critical facilities due to SLR under different climate scenarios and (2) when the centroid of a parcel will become inundated by SLR and compares this to when the resident at that parcel will lose transportation access. This work is conducted in a geospatial computational framework designed and built in the computer language R.

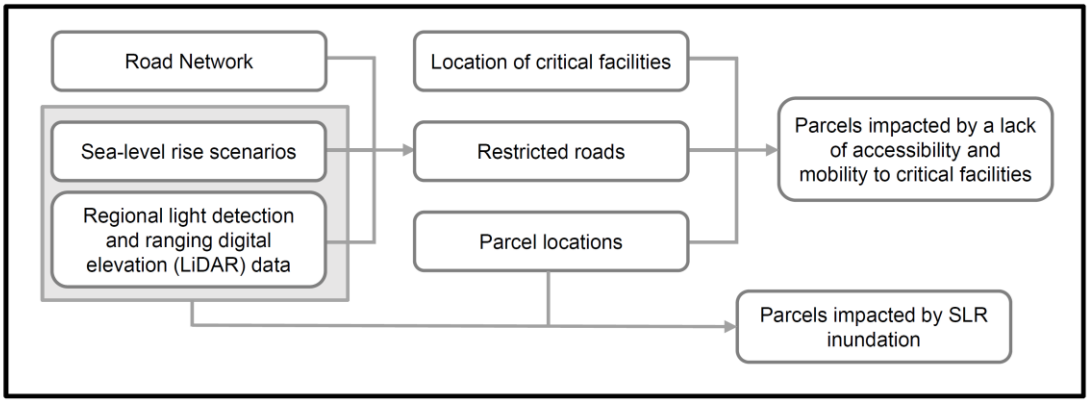

Figure 2.1. Framework

2.3.1 SLR Inundation Scenarios

We consider the impact of relative sea-level rise (RSLR) - or localized sea-level rise that additionally considers changes in land movement and ocean circulation patterns - on accessibility in the region. The computational platform is flexible enough to consider alternative or additional sources of flooding, such as storm surge. Because ocean rise is not expected to be uniform across the U.S. and the world (Boesch et al., 2013), I rely on recent RSLR projections developed by the State in partnership with the University of Maryland Center for Environmental Science. This work offers probabilistic projections through 2150 by downscaling global SLR projections to localized coastal areas in Maryland (Boesch et al., 2018). See Table 2.1. SLR scenarios used in the analysis.. Multiple states, including California and New Hampshire, have put forth similar studies (New Hampshire Coastal Risk and Hazards Commission, 2016; *State of California Sea-Level Rise Guidance*, 2018). The analysis includes exceedance probabilities for the central probabilistic estimate (i.e., 50%), the most likely range (i.e., 17% - 83%), and 1% and 5% levels for the years 2030, 2050, 2080,

and 2100. For the years 2030 and 2050, there is one estimate of RSLR, but for the years 2080 and 2100, the report considers three climate change scenarios (Representative Concentration Pathways (RCP) 2.6, 4.5, and 8.5). I exclude the RCP 2.6 scenario because of the general consensus of its improbability (Mora et al., 2013). While some argue that RCP 8.5 is unrealistically conservative, I include it to show the potential worst-case scenario (Hausfather & Peters, 2020).

Multiple tidal datums exist. Some organizations, including NOAA, tend to use the Mean Higher High Water (MHHW) datum when reporting on RSLR (Zervas, 2009). MHHW represents the daily average of the higher high-water height. It is possible that areas that are inundated during the worst high tide are not flooded during the rest of the day. To better capture sustained inundation, I use the Mean Sea Level (MSL) datum, which presumes that an area that is inundated under MSL conditions is inundated for at least (approximately) half of the day. To develop SLR inundation maps for my case study region, RSLR projections (e.g., 0.4 m) for the given years and exceedance probabilities under consideration are added to the mean sea level relative to the baseline of the year 2000, consistent with Boesch et al. (2018).

Table 2.1. SLR scenarios used in the analysis.

Year	RCP	Exceedance probabilities considered
2030	-	1%, 5%, and "likely range" (17% and 83%)
2050	-	1%, 5%, and "likely range" (17% and 83%)
2080	4.5	1%,5%, and "likely range" (17% and 83%)
	8.5	
2100	4.5	1%, 5%, and "likely range" (17% and 83%)
	8.5	

To understand which roads are inundated, this study overlays water levels raster files with a Digital Elevation Model (DEM) of the study region developed using USGS LiDAR data to compute flood depth ("Maryland's GIS Data Catalog," 2019). More specially, I use a "bathtub" approach to model the impact of RSLR, which assumes that all inland locations with elevations less than the RSLR depth are inundated by water. The hydraulic connectivity is not considered but could be in future work. This is hydrodynamically reasonable in my study region, given that the region is a large estuary with a shallow slope coastline and numerous tidally influenced streams, though it could result in unrealistic flooding in low-lying areas that are not tidally-influenced or directly impacted by RSLR. This limitation could be addressed in future work with the incorporation of hydrodynamic model results to calculate water depths and delineate inundation areas. Once the inundation data is overlaid onto the region, the maximum inundation depth for each road segment is computed, along with the depth of the water at the centroid of each parcel. (We assume that residences are at the centroid of each parcel and that they are at ground elevation, but this could be easily modified with additional data.) This approach assumes that even if a narrow section of the road is inundated by a depth above the prescribed depth parameter (described below), the road is impassable. This approach is completed using the 'raster' package (Hijmans et al., 2021) in the computing language R (R Core Team, 2019). This enables faster accessibility analysis later on.

2.3.2 Road Network

The transportation network is built *in silico* using TIGER/Line Shapefiles road network data from the United States Census Bureau (U.S. Census Bureau, 2017), which includes all the federal, state, and local roads in the U.S. It also provides information about the road function and detailed road geometry. This data was merged with state LiDAR data on centerline roadway elevation. Because I specifically consider household-level accessibility to local critical facilities, I assume the parcel to be the origin and the facilities (grocery stores, schools, and fire stations) to be the destinations. It is straightforward to consider additional destinations. For both origins and destinations, the entrance to the parcel is found by identifying the location on the road network that minimizes the distance between the center of the parcel and the road.

Travel restrictions on roads due to flooding have been addressed in previous studies using a binary variable - flooded or not - which means any road link located in a flooded area is restricted (Sohn, 2006; Suarez et al., 2005). Some studies have added a flood depth threshold, whereby travel on the road is restricted once the water level is above a prescribed threshold (Fereshtehpour Mohammad et al., 2018; Green et al., 2017; Jotshi et al., 2009). I use this approach and more details are provided momentarily. Some studies additionally consider speed reductions when the water depth is low enough for a vehicle to traverse the road segment, but the water slows travel (Jotshi et al., 2009; Pregnolato et al., 2017). While I recognize that speed reduction for flood levels in a certain range is potentially important, I exclude speed

reduction factors for now. My models show that impassable roadways have a much more significant impact on accessibility than speed reductions.

Many studies have evaluated what are "safe" thresholds for traversing flooded roads, while acknowledging that no threshold other than 0 cm, is truly safe. SmartDriving – a U.K. driving school - recommends motorists not traverse roads with a water depth greater than 15 cm, as it could result in a loss of vehicle control (SmartDriving, 2021). Fire trucks, on the other hand, have a tolerance for traversing at most 25 cm of floodwaters depth due to their size, weight, and power (Dawson et al., 2011b; Green et al., 2017; Pregnolato et al., 2017). (This is not to say it is recommended that fire trucks and cars traverse flooded roads. For example, conversations with local fire and rescue squadrons report significant vehicle corrosion due to salt water.) For the purposes of this study, I use two different thresholds: roads with flood depth greater than 15 cm are considered closed when considering the accessibility to critical facilities such as grocery stores and schools; roads with flood water greater than 25 cm are considered closed when considering the accessibility to emergency services such as fire stations and hospitals.

Some studies that explore the impact of floods on roadways additionally consider how road demand and traffic congestion might change (e.g., de Oliveira et al., 2014); Feng et al., 2019). I do not consider this in my analysis because my study region is extremely rural, and congestion is not a significant concern - accessibility is. However, this implies that my metric that measures changes in travel distance may

underestimate the true impact due to longer travel times from road flooding and congestion.

Once the network is built that includes road segments closed due to inundation, I apply a shortest path algorithm (i.e., Dijkstra's algorithm) to establish whether a parcel is able to reach a particular destination and, if so, the distance that is required. This is then compared to what the distance would have been without flooding. Dijkstra's algorithm is a widely used method for identifying shortest paths and is also computationally efficient (Sniedovich, 2010). This is repeated using the R packages 'shp2graph'(B. Lu & Lu, 2018) and 'igraph' (v1.2.6; Csardi and Nepusz, 2006) for all inundation scenarios under consideration.

2.4 Study area

Our study area focuses on Dorchester County, Maryland, and small portions of some neighboring counties to capture critical facilities that residents in Dorchester County may rely on (Figure 2.2). This area, along Maryland's Eastern Shore, is extremely low-lying and, as a result, experiences repetitive flooding that frequently isolates residents and forces them to plan trips in advance so as not to be stranded by rising tides. It has several long, narrow peninsulas and numerous creeks, streams, and man-made tidally influenced "tax ditches" dug mostly by enslaved people. In many places, roads are paved dikes that cross through tidal marshes (Cole, 2008). The county is rural with a small urban center in the City of Cambridge. As of 2010, the county's population was 32,623. The population primarily relies on private vehicles. A public

transit operator (Delmarva Community Transit) exists in the region, though service is infrequent and the routes primarily connect Cambridge to towns in adjacent counties.

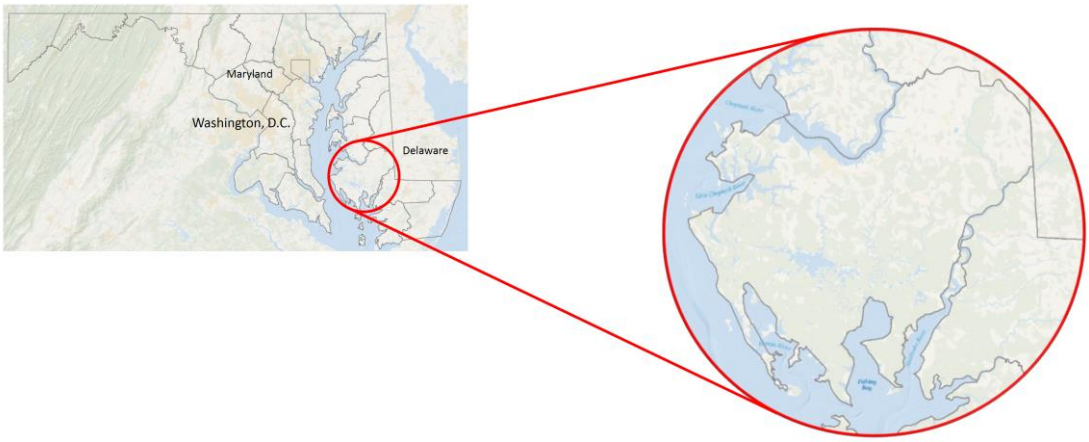

Figure 2.2. Case study location (ESRI, 2021)

SLR poses a significant risk to Dorchester County's people and infrastructure, and its impacts are already apparent in shoreline erosion and the increased frequency of "sunny day" flooding. The county's land area is expected to shrink in half by the turn of the century due to SLR (Cole, 2008). Limited economic and political resources constrain Dorchester County's options for adapting to SLR (Miller Hesed & Paolisso, 2015), and state and local officials and residents must make challenging decisions about what to protect and what to abandon. While the ethics of this point are debatable, the cost to maintain many roads and the culverts and ditches that drain them will soon become more expensive than the value of the properties that they serve (Cole, 2008). Table 2.2. Projected relative mean SLR estimates above 2000 levels for Dorchester County based on the Cambridge, MD tide gauge station. Columns show different exceedance probabilities, and rows correspond to different years and emissions (Boesch et al., 2018). presents the mean RSLR estimates for four exceedance

probability and two climate scenarios for Dorchester County. Under the RCP 4.5 scenario, the most likely range of relative mean SLR is between 0.43 m and 0.82 m by 2080 and between 0.55 m and 1.01 m by 2100. Under the RCP 8.5 scenario, the numbers shift to between 0.52 m and 0.98 m by 2080 and between 0.67 m and 1.34 m by 2100.

Table 2.2. Projected relative mean SLR estimates above 2000 levels for Dorchester County based on the Cambridge, MD tide gauge station. Columns show different exceedance probabilities, and rows correspond to different years and emissions (Boesch et al., 2018).

Year	Emissions Pathway	1% probability RSLR meets or exceeds (m)[1]:	5% probability RSLR meets or exceeds (m):	Likely probability range (i.e., 17% - 83%) RSLR meets or exceeds (m):
2030	**N/A**	0.40	0.34	0.12 - 0.27
2050	**N/A**	0.73	0.64	0.27 - 0.52
2080	**RCP 4.5**	1.28	1.01	0.43 - 0.82
	RCP 8.5	1.46	1.16	0.52 - 0.98
2100	**RCP 4.5**	1.77	1.34	0.55 - 1.01
	RCP 8.5	2.16	1.65	0.67 - 1.34

We include critical facilities in neighboring counties that are within a 15-minute drive of at least one resident in Dorchester County to more realistically capture the critical facilities that residents may rely on. I then evaluate whether residents at each parcel in Dorchester County are able to access at least one facility among each class of critical facilities (i.e., fire stations, grocery stores, and schools) and if so, I compute the network distance between the parcel and the closest facility. As an example, I evaluate

[1] There is a 1% chance that sea-level rise would exceed the corresponding amount for each S LR scenario (e.g., there is a 1% chance SLR would exceed 0.40 m in 2030).

whether routes exist between a given parcel and all grocery stores, and if at least one route does, I identify the grocery store that is closest. As a result of inundation and road configuration, that grocery store may not be the shortest Euclidean distance. While this work only considers accessibility to fire stations, grocery stores, and schools, other key public accommodations, such as hospitals, pharmacies, and important civic buildings could additionally be considered.

2.5 Results

The results are organized as followed: I first show the results for the scenario with no inundation. This forms the model baseline. I then present results for potential accessibility loss for possible climate futures. Finally, I compare these results to when parcel inundation is expected to evaluate the potential for forewarning due to accessibility reduction.

2.5.1 Baseline scenario

Figure 2.3 shows the distance required by residents, under dry conditions, to reach their closest (a) fire station, (b) grocery store, and (c) school. No resident lacks accessibility to any class of critical facility. Each box represents one parcel, and the darker the green, the closer the parcel is to the critical facility. Conversely, the orange parcels are further from their closest facility. These figures demonstrate which residents are access-poor for each class of service. The southern part of the county is more rural and isolated than other parts, and thus residents must travel greater distances to reach their closest fire station and school in particular - sometimes 30 km or more. The ogive

(i.e., the empirical distribution function) in Figure 2.4 shows the distribution of the distance that residents must travel to reach the closest critical facility in each class. This plot indicates that nearly 90% of the residents live within 10 km of fire stations, but this number decreases to 80% for schools and grocery stores.

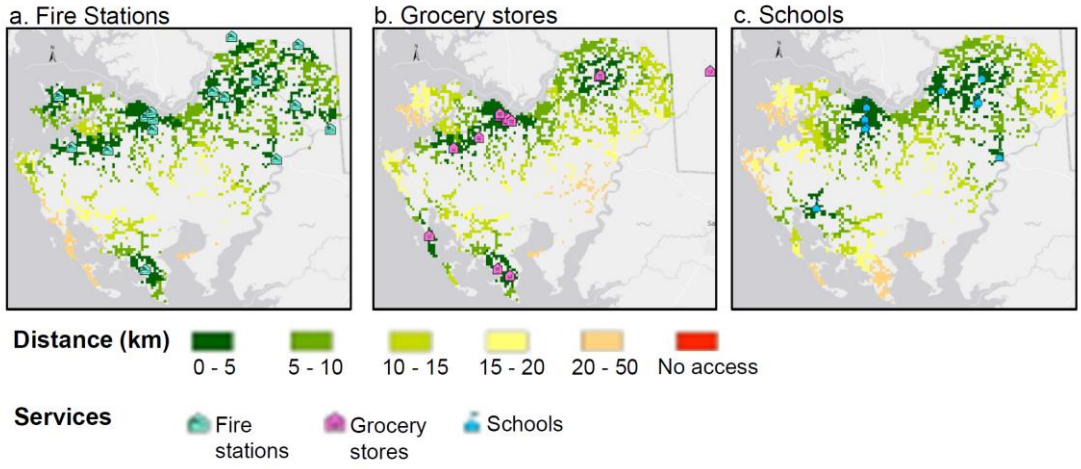

Figure 2.3. Distance from residents' parcels to their closest (a) fire station, (b) grocery store, and (c) school, respectively, assuming 2000 mean sea-level. Between 2000 and 2020, the mean sea-level has risen approximately 0.5 feet in this region.

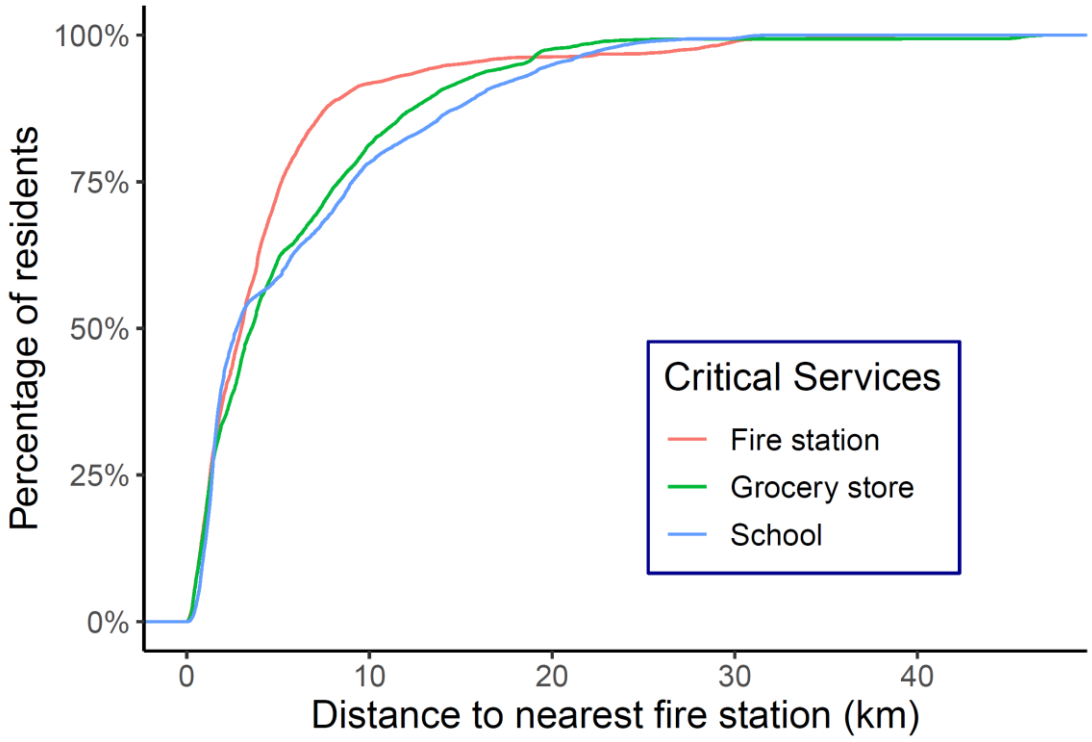

Figure 2.4. ECDF of distance from residents' parcels to the closest critical facilities for each class assuming current mean sea-level.

2.5.2 RSLR

We begin the discussion by examining the fraction of residents that lose accessibility during the 66% likely range of RSLR for different climate scenarios (Table 2.3). By 2030, between 1% and 2% of parcels are expected to lose accessibility to any fire station during periods of mean sea level and greater (even when allowing trucks to traverse 25 cm of water, as opposed to 15 cm as in the other classes of critical services). Between 1% and 4% of parcels are expected to lose accessibility to any grocery store and between 1% and 7% of parcels are expected to lose accessibility to any school. (We do acknowledge that students are assigned to a specific, grade-appropriate school so this figure may be less relevant, though important civic events,

such as voting, typically occur at schools). Because 2030 is relatively soon compared to the other years under consideration and thus, uncertainty surrounding RSLR is less, the range of the percentage of people who lose access in the 66% likely range is fairly narrow (a few percentage points). Most people who lose access to one critical class of services lose access to others, though this is not universally true and depends on where the parcel is located relative to these services.

Table 2.3. The percentage of parcels in Dorchester County, MD, that lose accessibility to the three classes of critical facilities under 66% likely range of RSLR for different climate scenarios. This is reported as a range with the lower end representing the 83% exceedance probability and the upper end representing the 17% exceedance probability.

Year	Emissions Pathway	66% likely range		
		Fire stations	Grocery stores	Schools
2030	**N/A**	1% – 2%	1% – 4%	1% – 7%
2050	**N/A**	2% – 12%	4% – 13%	7% – 15%
2080	**RCP 4.5**	7% – 18%	10% – 19%	10% – 20%
	RCP 8.5	12% – 20%	13% – 20%	15% – 21%
2100	**RCP 4.5**	12% – 20%	14% – 21%	16% – 21%
	RCP 8.5	14% – 22%	18% – 23%	19% – 23%

As time progresses, under all emissions pathways and for all classes of critical facilities, the fraction of parcels that lose accessibility increases. By 2050, the percentage of parcels that are expected to lose access to any fire station is least, in part because there are more fire stations than other critical services, and in part because the threshold through which vehicles are allowed to traverse flood waters is higher for this class of services. The range of the percentage of people to lose access to critical facilities in

2050 is generally wider compared to 2030, mostly due to uncertainty in RSLR. This could make local planning for SLR challenging, requiring a greater consensus for which exceedance probability is selected and used for planning.

By 2080, the emissions pathway that is selected does have an impact - though not always a substantial one - on the expected outcome. The exceedance level that is selected is more consequential. Consider access to any fire station by 2080. Between 7% and 18% of residents are expected to lose accessibility in the 66% most likely range for RCP 4.5 while between 12% and 20% are expected to lose accessibility for RCP 8.5. There is significant overlap between these two climate scenarios, especially at the end of the more consequential exceedance probability (the 17%). I see similar trends for other classes of critical services.

Figure 2.5 shows similar statistics to those shown in Table 2.3, though for a greater range of exceedance probabilities. Each vertical bar represents a different year in the future, except those two bars are shown for 2080 and 2100 to represent the two potential emissions pathways under consideration. The red horizontal line represents the 1% exceedance probability (worst case). The dark green bar represents the 83% exceedance probability, and the orange bar represents the 17% exceedance probability; together, they represent the 66% likely range. The reduction in accessibility is significant between the 17% and 1% exceedance probabilities for all years, classes of critical facilities, and emissions scenarios. For example, in 2100 for RCP 4.5, 20% of parcels are expected to lose access to a fire station for the 17% exceedance probability compared to 25% for the 1% exceedance probability - a difference of about 5% or 934

parcels. This difference jumps to about 7% or 1,264 parcels for RCP 8.5 in 2100. (Note that the difference between the 50% and 17% exceedance probabilities, a probability range that is near twice the range of 1% to 17%, is about 3% of parcels in both cases.) In both 2080 and 2100, for all classes of critical services, there is significant overlap between the emissions scenarios in terms of loss of accessibility. Thus, it is not the emissions scenarios that are driving the variability in possible outcomes in this area; it is the exceedance probabilities. (It is very possible that this is not the case in other regions of the world.)

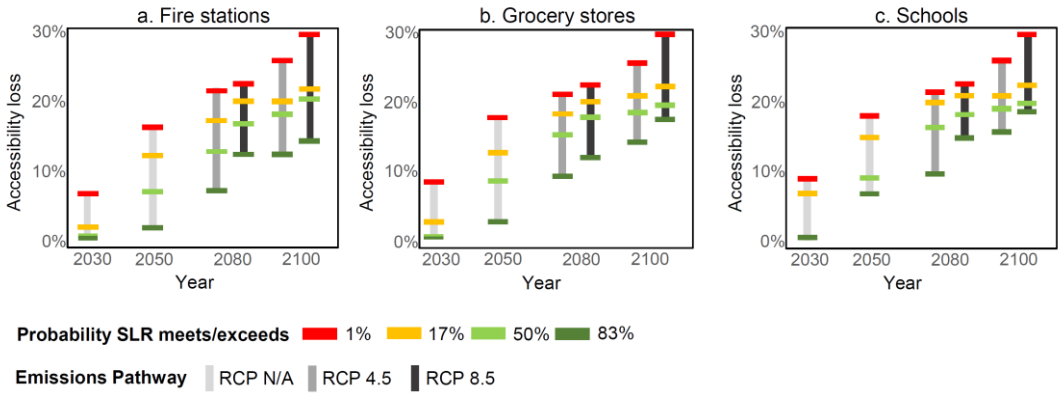

Figure 2.5. Distribution of accessibility loss under different RSLR scenarios to (a) fire stations, (b) grocery stores, and (c) schools. Note that these are not 95% confidence intervals, but rather distributions with key exceedance probabilities identified.

The maps in Figure 2.6 show the spatial patterns of accessibility loss and travel distance change to fire station for the top end of the most likely range (the 17% exceedance probability) for multiple years in the future. Again, each colored square represents a parcel, and the parcels in red lose accessibility to any fire station. The parcels colored in gray represent parcels that are unaffected by RSLR and have no change in their accessibility. Parcels colored in dark green have minor increases in the

distance they would need to travel to reach a fire station (< 1 km) and whereas parcels colored in orange must travel a significant additional distance (10-20 km). Residents living in the peninsulas in the south and west of the county are particularly access-poor, and many parcels will lose consistent access to any fire station by 2030 (assuming that they have not already). This is, in part, driven by a dependence on a few critical but low-lying roads with no alternative routing options.

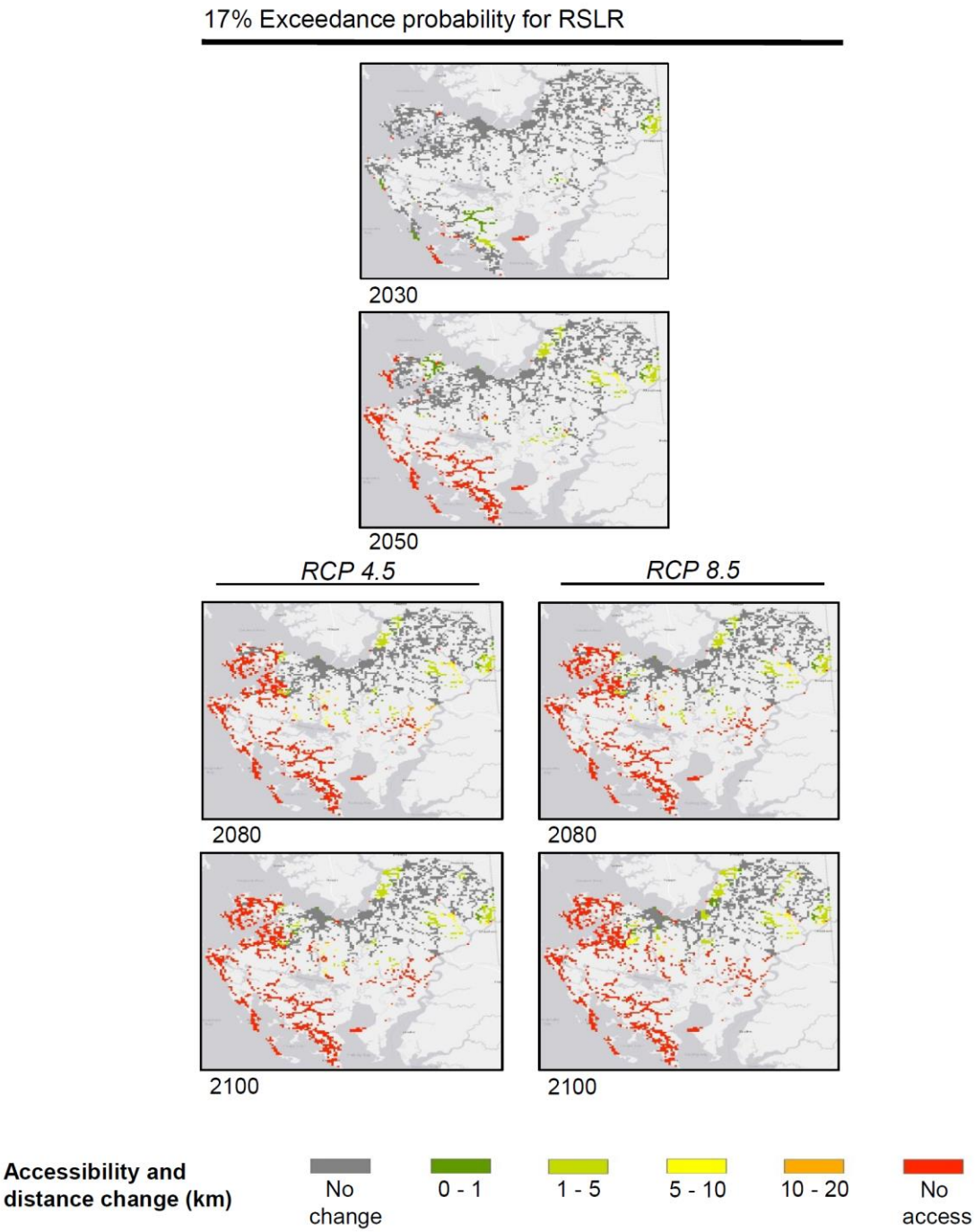

Figure 2.6. Residents' accessibility to their nearest fire stations under different RSLR scenarios using the 17% exceedance probability.

By 2050 of the 3,160 parcels whose accessibility to a fire station is affected by SLR, most will lose access. Specifically, 2,164 of the 18,484 total parcels in Dorchester

County (or 11.7% of existing parcels) lose access and 996 (or 5.4%) maintain access but require longer travel distances. Residents of parcels who need to travel further to reach a fire station generally reside along the Choptank River in the northeast of the county or along the Nanticoke River in the east of the county. By 2080, many parcels along tributaries in the center of the county will require longer distances to reach a fire station and the trend continues through 2100. The majority of parcels which are expected to experience longer travel distance due to inundation are projected to find that the critical facilities that were closest to them without inundation continue to be the closest; it will simply take longer to get to that location.

Table 2.4 shows the average difference between the travel distance to a fire station without inundation and with various RSLR scenarios; the average is over all residents who maintain access to a fire station. The mean difference is relatively small for all RSLR scenarios for a few reasons. First, most parcels are inland, and thus are not impacted by RSLR. Second, of the parcels which will require longer travel to reach a fire station, the additional travel is usually minimal (the green and yellow squares in Figure 2.6). Third, most parcels that are impacted by RSLR lose access to a fire station as opposed to witnessing an increase in travel distance, and these parcels are excluded from the averaging. Figure 2.7 presents selected violin plots that show the distribution over the change in travel distances to a fire station for the residents of parcels who are forced to be rerouted due to inundation (i.e., the green, yellow, and orange parcels in Figure 2.6) By 2030, for the 1% exceedance probability, although very few parcels are required to take longer routes (1,176 parcels), the change in travel distance of these

routes' ranges uniformly between a value close to 0 km and 34 km. For the 17% exceedance probability, fewer parcels are forced to find alternative routes (677 parcels) and those parcels are required to travel less than 5.3 km more. By 2050 for the 1% exceedance probability, the vast majority of the parcels that were forced to find an alternative route in 2030 will have lost access to a fire station altogether. Thus, the range of the density plot is much shorter (about 14 km) with the bulk of the distance change hovering between 0 and 5 km.

Table 2.4. Average difference (in km) between distance from each parcel to its nearest fire station under no inundation scenario and different RSLR scenarios (for parcels that do not lose accessibility).

Year	Emissions Pathway	Exceedance Probability				
		1%	5%	50%	17%	83%
2030	**N/A**	1.04	1.00	0.03	0.06	0.00
2050	**N/A**	0.20	0.16	1.04	0.15	0.06
2080	**RCP 4.5**	0.36	0.21	0.16	0.24	1.05
	RCP 8.5	0.34	0.23	0.20	0.21	0.15
2100	**RCP 4.5**	0.33	0.33	0.26	0.24	0.16
	RCP 8.5	0.36	0.35	0.21	0.33	0.19

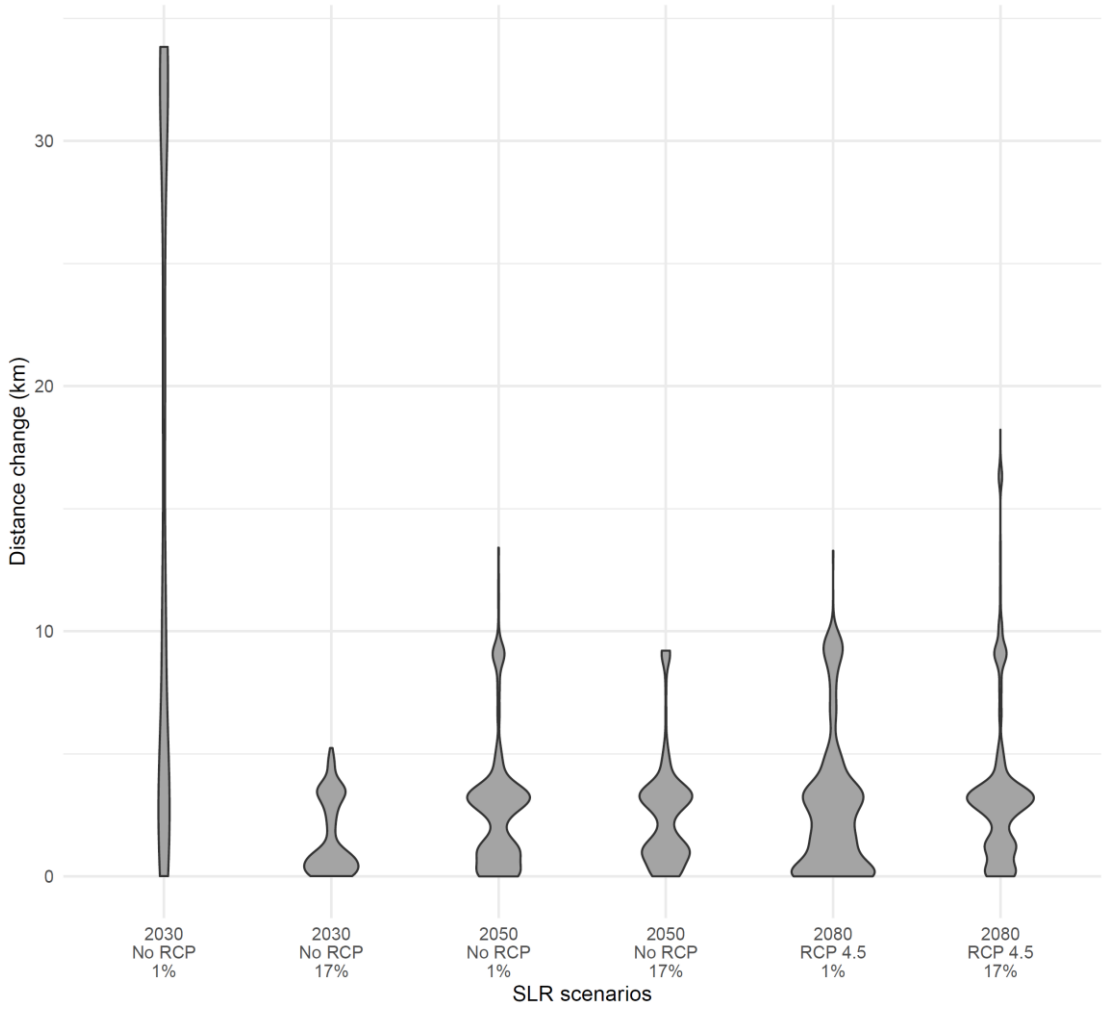

Figure 2.7. Distribution of changes in travel distance to the closest fire station for parcels' whose accessibility is impacted by SLR. This is shown for the 1% and 17% exceedance probabilities for 2030, 2050, and 2080.

Here, I reframe the question to ask in which year is a parcel expected to lose accessibility given the various RSLR scenarios. Understanding this spatial distribution can enable better temporal planning by local and state governments. To answer this question, I assume a linear increase in RSLR between the years for which I have estimates (Note: MD provides estimates to 2150). Figure 2.8 shows this spatial distribution for accessibility loss to fire stations for the 17% exceedance probability

under an RCP 4.5 change scenario. The parcels colored in gray are expected to continue to have access to fire stations through 2150. The red parcels lose accessibility before 2030 and the blue parcels lose accessibility sometime between 2100 and 2150 (assuming no significant adaptation measures are taken). As mentioned previously, residents in the peninsulas in the south and west are particularly access-poor, and those parcels are expected to lose consistent accessibility to any fire station by 2030 due to their dependency on a few low-lying roads with no alternative routing options.

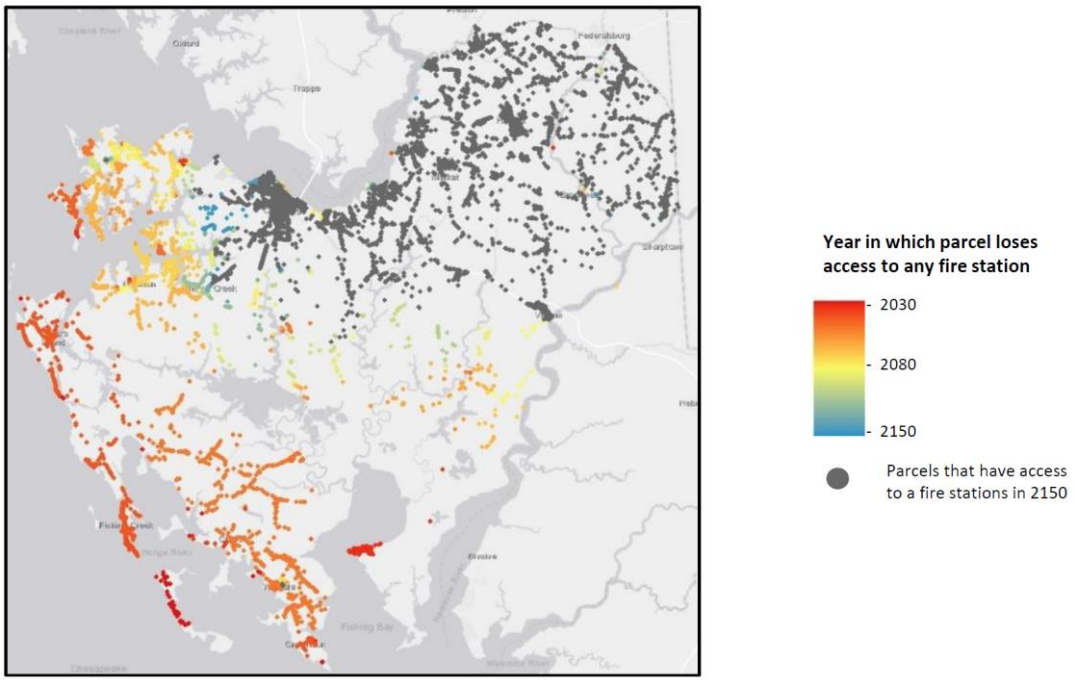

Figure 2.8. Spatial and temporal distribution of accessibility loss to fire stations for an 17% exceedance probability under an RCP 4.5 change scenario.

2.5.3 Parcel inundation

While not central to this research, I additionally evaluate the year in which parcel inundation is expected for different climate scenarios. This allows us to later evaluate the relationship among accessibility loss, changes in travel distances, and

parcel inundation. Figure 2.9 shows the year in which parcel inundation is expected for each parcel using the 17% exceedance probability and RCP 4.5 scenario. As expected, parcels closer to the water are expected to have their centroids be inundated sooner than parcels further inland.

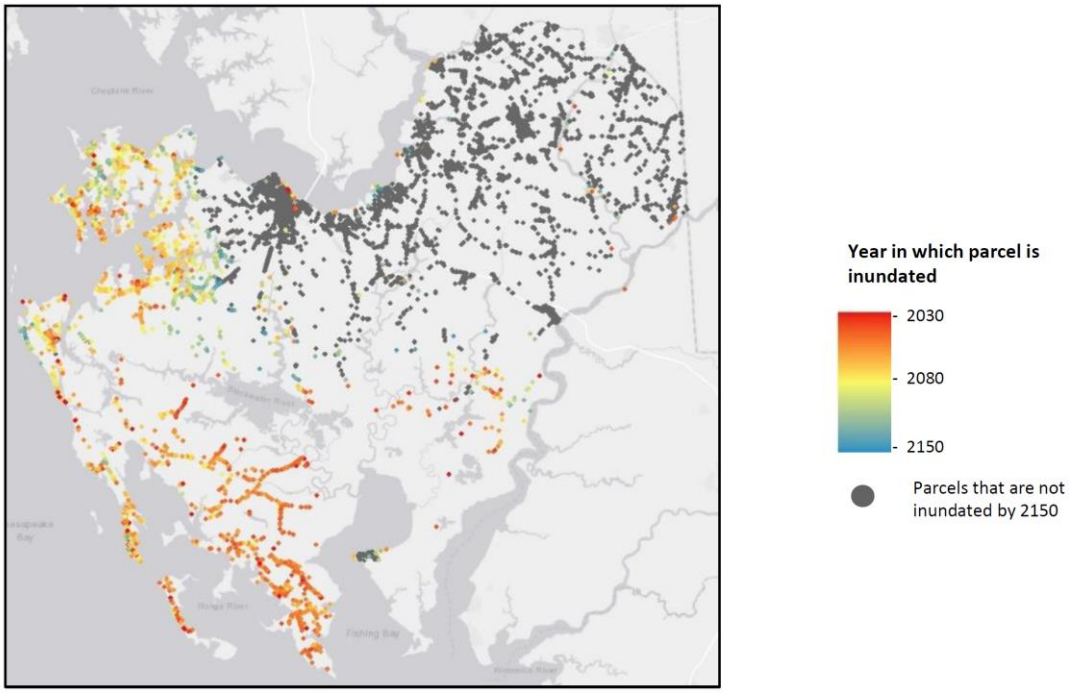

Figure 2.9. Spatial and temporal distribution of parcel inundation for the 17% exceedance probability under an RCP 4.5 change scenario.

2.5.4 Relationship between parcel inundation and accessibility loss

In addition to examining when parcels lose consistent access to critical services, I can compare this to when parcels themselves become inundated from SLR. The idea here is to see, of the parcels that will be inundated, the degree of forewarning that they receive from accessibility issues. If, in practice, a lack of accessibility was to influence retreat decisions in some regions, it may signal retreat sooner than what is expected based on parcel inundation alone. For obvious reasons, numerous confounding factors,

from income and demographics, to place attachment and policy will influence retreat decisions (Binder & Greer, 2016). Comparing roadway and parcel inundation can also inform decisions about SLR adaptation measures such as elevating homes, raising roadway segments, or retreat. For instance, if both roadways and parcels in an area are subject to inundation, retreat may make sense.

We first look at the intersection of the parcels that are inundated by SLR and the parcels that lack accessibility to any fire station for the four candidate years (Table 2.5). Initially, the majority of parcels that lose accessibility to a fire station do not additionally experience parcel inundation. By 2030, using the 1% exceedance probability, only 11% of the parcels that lose accessibility additionally experience parcel inundation. The most likely range would expect that about 5% of parcels that lose access to a fire station are also inundated by SLR - representing only 0.16%-0.21% or 29-39 of all parcels. However, as time passes, this fraction increases. By 2050, of the 4%-11.7% of parcels (or 744 to 2,164 parcels) that lose access to a fire station in the most likely probabilistic range, between 5% and 35% of those parcels will additionally be inundated. By 2080, more than 50% of all parcels that lose accessibility under all exceedance probabilities except for the 83% exceedance probability are additionally inundated.

Table 2.5. Of parcels that lose access to a fire station, the fractions that are also inundated.

Year	Emissions Pathway	Exceedance Probabilities				
		1%	**5%**	**17%**	**50%**	**83%**
2030	**N/A**	11%	7%	5%	5%	5%

2050	**N/A**	58%	51%	35%	11%	5%
2080	**RCP 4.5**	87%	76%	66%	49%	13%
	RCP 8.5	90%	82%	75%	58%	35%
2100	**RCP 4.5**	89%	88%	81%	63%	40%
	RCP 8.5	83%	88%	88%	75%	53%

It is important to additionally understand for parcels that are inundated, how many years prior to inundation that they lose accessibility. This is shown in Figure 2.10 for the 17% exceedance probability and RCP 4.5. Accessibility loss to any fire station is considered. Figure 2.10(a) shows the distribution by decade of the forewarning that comes from losing accessibility. 41% of parcels that are expected to be inundated by 2150 do not experience accessibility loss prior to initial inundation. In the vast majority of these cases, parcel inundation occurs simultaneously to accessibility loss; the road that connects the parcel to the road network becomes inaccessible at the same time as the parcel is inundated. In 12% of parcels that are inundated, the forewarning time is between 1 and 10 years. The median forewarning time is 8 years. Figure 2.10 (b) shows the spatial distribution of the time difference between accessibility loss to a fire station and parcel inundation, assuming a 17% exceedance probability. The parcels which have little forewarning are primarily concentrated along creeks in the northwest and southwest regions. Inland residents and residents along the western coast tend to have decades more forewarning. These results suggest that a local strategy focused solely on residential building mitigation (e.g., elevation) is insufficient for preventing the impacts of flooding to residents. The residents without access to critical facilities may ultimately need to relocate, in some cases, years before parcel inundation.

(a)

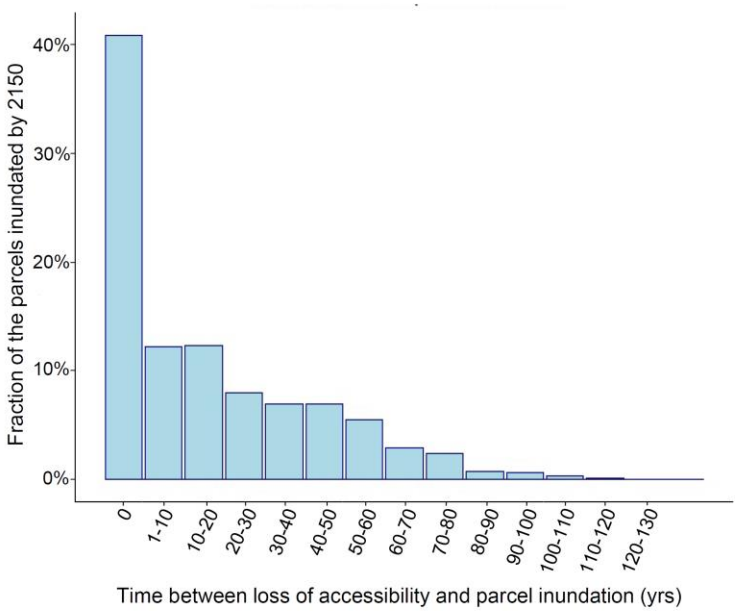

(b)

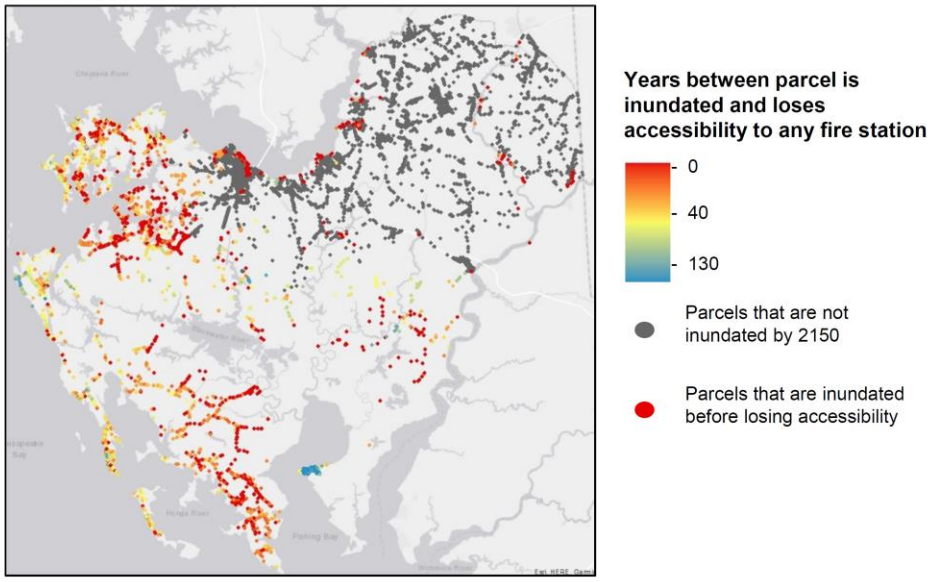

Figure 2.10. (a) Histogram, by decade, of the time between accessibility loss to a fire station and parcel inundation. Zero years indicates that the parcel is expected to be inundated before or simultaneous to accessibility loss. (b) Spatial distribution of the time between accessibility loss and parcel inundation. These plots assume an RCP of 4.5 and an exceedance probability of 17%.

2.6 Conclusion

This paper investigates how sea level rise may impact parcel-level accessibility in rural areas with few options for wide-scale protection - a critical issue often overlooked in climate adaptation literature. Using a case study of Dorchester County, Maryland, I demonstrate the importance of parcel-level assessment, and how modern computers combined with geospatial libraries allow computation of parcel-level access under different climate scenarios relatively quickly. Understanding which parcels might be impacted by SLR, even if the parcel itself is not inundated, is important because it signals when an acute burden of SLR may begin, and when additional support infrastructure, such as electric-power, may become less reliable.

The case study is unique because it is the first of which the authors are aware to compare expected parcel inundation to when residents at the parcels may lose access to critical facilities. The results from the case study suggest that in some regions, the forewarning stemming from accessibility loss could be significant. Projections on regional retreat that focus purely on parcel inundation may overestimate the time until retreat is needed. Obviously, the results for other areas of the country and world are likely to differ and localized evaluations should be conducted. Ultimately, it calls on decision and policy makers to take a more systematic and comprehensive approach to mitigation and adaptation; a strategy that focuses solely on elevating houses, for example, may be ineffective because residents will be unable to travel to key destinations.

The results also indicate that mitigation strategies such as raising roads may not be a permanent solution for Dorchester County residents without a coordinated attempt to also maintain the housing stock (and potentially other infrastructure systems). Focusing on long-term adaptation strategies that are coordinated among infrastructure sectors, such as relocation, could serve as a more collectively advantageous strategy than focusing solely on protecting the transportation system.

While this work focuses on transportation infrastructure, it serves to highlight the importance of considering networked support infrastructures at large that enable parcel occupation when evaluating household retreat due to SLR. Unlike parcels, which are generally not considered networked infrastructure because they lack physical connections to other parcels, electric-power distribution, municipal water infrastructure, and others, are linked by wires, cables, and pipes. A disruption in one section of the network - say due to SLR inundation - can have ripple effects in the network. Sparse networks - say due to being located in a rural area - are often plagued with lower system robustness when critical links are removed (Khademi et al. 2021). The outcome of this work suggests that other networked infrastructure and their proclivity to SLR inundation should be evaluated as well.

Finally, while not a core theme of this paper, the work demonstrates the need for decision and policy makers in a region to reach some level of consensus about assumptions for which possible future is planned when deciding among adaptation strategies. This consensus will likely be driven by the amount of risk the community is able and willing to assume. Failure to build consensus could lead to piecemeal

adaptation strategies in different areas that are collectively inefficient, and potentially even harmful to some (Papakonstantinou et al., 2019). In the case study, while the results varied little between RCP 4.5 and 8.5, the results varied significantly among exceedance probabilities. Thus, in this case, more consensus is required around which exceedance probability is planned for, though this may not be the case in other regions. It also potentially highlights the importance of applying consistent exceedance probabilities for each sector of infrastructure when planning, given their interconnectedness.

There are some significant limitations of this work which could be addressed in the future. First, the work relies on a bathtub inundation model, which lacks accuracy at finer levels of resolutions. Additionally, I did not consider travel time or congestion; while congestion tends to not be an issue in this area, numerous significant changes to route choice could force higher traffic volumes onto roads not designed for them. This presents an opportunity for model enrichment should fine-scale origin-destination data or traffic volume data become available. Finally, while I mentioned the importance of transportation equity when evaluating access, this concept was not formally evaluated. Future work could evaluate the distribution of burdens on various demographics within the region.

3 Chapter 3: Bridging adaptation resources across the urban-rural divide: A comparison of equity-focused roadway investment strategies against flooding

3.1 Introduction

Coastal communities are facing more disruptions than ever from coastal flooding (Krishnamurthy, 2012; Wu et al., 2002). Inundation of transportation assets, such as roadways, is especially challenging because it can impede travel to essential services, such as grocery stores, hospitals, and economic opportunities (Papakonstantinou et al., 2019b). Flooding of only a few road segments may isolate residents or increase their travel distance to these amenities for many (Chang et al., 2010). This is especially problematic in rural areas, which tend to have sparse roadway topology that offers fewer alternative paths for motorists.

In order to preserve access, resources are being directed increasingly to rural areas to armor roads vulnerable to storm surge and sea-level rise (Li et al. 2009). However, given the limited resources combined with the wide-scale threat of flooding, it is likely that many roads will remain unarmored. In these instances, the benefits of protection will accrue unevenly; some fraction of the population may experience longer travel distances or lose the ability to reach their destination altogether while others may experience no impact to travel as a result of interventions. It is important to understand who will benefit and, ultimately for decision-makers, whether it reflects the priorities and values of the region.

A practical approach for guiding armoring resources is to protect roads with higher traffic volumes under threat of inundation or to rehabilitate roads that currently flood periodically. This approach has led, for example, to some segments of roadway in the State of Maryland (the case study location used later in this work) having more than 6 feet of asphalt to merely keep up with the encroaching water (National programs-Maryland public television, 2018). While this approach is practical and politically defensible, it may not offer similar accumulated benefits that other approaches do. More specifically, because it does not take a systems-level perspective, and does not evaluate the ability of all residents to access to key destinations, such as fire stations, while considering how the topology of the road network intersects with the flood hazard, the roads that are selected for protection may offer limited benefits (Alipour et al. 2020; Douglas et al. 2017). In this work, we construct a comparative systems-level framework to inform road-armoring strategies that additionally considers the spatial- and demographic equity of the interventions. It is the first work, to our knowledge, that leverages heuristic optimization approaches to inform strategic road-segment armoring in order to maintain parcel-level access to emergency services.

Arguably, the most efficient engineering strategy would be to armor the combination of road segments that benefit the most people given budget constraints. “Benefit the most people” can have multiple interpretations, including maximizing the number of people who maintain access to some key amenity, such as emergency services, or minimizing the number of motorists forced to take longer paths. However, the justice literature has, for decades, argued that government resources should focus

on equity as opposed to simply being efficient and that efficient solutions could disproportionately benefit some populations while providing little to no benefit for others (Emrich et al., 2020a).

One flashpoint over protection and adaptation resources stems from whether investments serve more rural or urban populations, and how this "should" be balanced. While this is likely to be a national-level issue, it is possible that this divide will additionally materialize on a smaller scale, as there are many rural areas with small urban cores. The cost of protecting rural infrastructure is more expensive on a per capita basis (The White House, 2022). However, evaluating investment in rural infrastructure on a per capita basis ignores the interconnection between rural and urban areas, including knowledge, goods, and capital, and how both need the other to succeed (Dower, 2013). Yet still, spatial inequities of resource distribution exist both within the U.S. and internationally, and this, to some extent, has driven people to move from rural areas to the citiesearch for more opportunities and justice (Tacoli & Mabala, 2010). Ravazzoli & Hoffmann (2020) argue that interactions and exchanges of food, goods, and services, between rural and urban areas build mutual resilience by building human and social capital. This will be even more important in future when climate change exposes more complex societal challenges. This highlights the importance of considering an equitable distribution of infrastructure benefits across urban and rural areas (Pearsall et al., 2021).

Another flashpoint over adaptation resources stems from whether the interventions support socially vulnerable populations. Economically poor

communities, communities of color, indigenous communities, and other disenfranchised populations are often disproportionately impacted by hazards (Emrich & Cutter, 2011). In many instances, this is driven by racial and economic discrimination, forcing them to reside in areas more susceptible to hazards (Cutter & Emrich, 2006). Additionally, socially-vulnerable populations are less likely to have access to resources to support recovery and the political capital to advocate for more local investments and services (Emrich et al., 2020b). Thus, decisions involving adaptation and environmental protection investments require a broader understanding of economic, social, and environmental context, and also how the distributions of the benefits and burdens from such decisions differ across populations (Zamojska & Próchniak, 2017).

In light of this, the work presented here builds a comparative systems-level framework for allocating road armoring resources in ways that balance the distribution of benefits in regions prone to flooding. To do this, we evaluate optimal interventions for a range of budget constraints using multiple equity metrics and other ways to balance resource allocation. This is also then compared to strategies that are often considered "efficient," meaning here, strategies that benefit the most people. Rather than focusing on the vulnerability of individual road segments, the work focuses on strategically protecting links within a network so that residents maintain access to emergency services during floods. This implicitly assumes that residents and emergency vehicles understand how to reroute during times of flooding, and reach their destination, should an alternative route exist. We do not consider, in this work, the

impact of rerouting on congestion or travel time. We then compute the robustness of those strategies under different flood scenarios. The work highlights the tensions that could arise when resources are allocated in accordance with a particular objective, and how the benefits that accrue can be spatially and demographically heterogeneous.

While there has been increased inquiry in recent years into the impact on society from flooding of transportation assets (e.g., Sohn 2006, Change et al. 2010), this work is the first, to the authors' knowledge, to strategically evaluate where road protection should be implemented such that access is maintained and to additionally consider equity in this equation. The comparative framework is illustrated using Dorchester County, Maryland. The county is rural, except for a small population core in the City of Cambridge, and extremely low-lying. Roadway inundation happens frequently. Nearly 60% of the county's landmass is within FEMA's 100-year (Cole, 2008). The county also has a long and fraught history of racial segregation and limited economic and political resources constrain its ability to adapt to environmental threats (Miller Hesed & Paolisso, 2015).

3.2 Literature review

While research into the impacts flooding on transportation infrastructure is relatively limited, the concept of transportation network resilience has existed for more than a decade (Faturechi & Miller-Hooks, 2014). The focus tends to leverage engineering metrics, such as network reliability and robustness, to understand network performance should certain nodes or links fail (e.g., Gu et al., 2020; Johnson et al.,

2021; Snelder et al., 2012). These metrics are limited, however, in that they cannot convey the impact that network degradation may have on users (Jasour et al., 2022). More recently, the impacts on users have been considered, and especially the contribution that flooding may play. This is especially important because knowing the impact on users and residents enables an equity analysis to see who disproportionately benefits and is harmed (Blanchard & Waddell, 2017).

Access is one of the relevant approaches to evaluate the impact on residents. Access is simply the availability of a route that connects an origin (e.g., a parcel) to a desired destination (Litman, 2008). Though access is a more commonly used metric in urban planning (Ermagun et al. 2015), it has been used recently in the resilience literature to understand how individuals will fare after a disruption, and whether they will be able to reach (or be reached by) life-saving emergency services (Lu and Peng, 2011). Travel distance and time changes are alternative metrics for measuring individual impacts and are more commonly used in the roadway flooding literature compared to access (Faturanchi and Miller-Hooks 2014, (Jenelius & Mattsson, 2015). In seminal work by Jacobs et al. (2018), the authors find that over 7,500 miles of roadway in the U.S. are threatened by tidal flooding, which may cause significant travel delays for motorists. However, these travel metrics can mask the extreme consequences of flooding – lack of access to say emergency service – and arguably measure more of the burden caused by flooding. Ultimately, for planning purposes, both approaches (access and travel time/distance) should be considered.

For the sake of brevity, the remainder of the literature review focuses on past work on roadway mitigation (or retrofitting) for floods and work that measures equity of mitigation investments. Jasour et al. (2022) and Alabbad et al. (2021) provides a contemporary review of the literature focusing on flooding and roadways. In summary, the body of work is fairly limited in the range of flooding scenarios that are considered (e.g., 0.5 m of sea-level rise or 100-year flood) and also it often spatially-aggregates origins instead of considering the spatial-heterogeneity of individuals (Fereshtepour et al. 2018; Sun et al. 2020). A significant number of open research questions remain.

One open research question is where roadway mitigation should be conducted in order to reduce the impacts of flooding. While some initial research has been done in this space, no frameworks that inform how such decisions potentially impact the spatial and demographic distribution of access have been built. Of those works that do consider flood mitigation, many do so exogenously. More specifically, the approach has been to iteratively evaluate the impacts on mobility from a predefined set of limited interventions - such as a levee or elevating a key roadway prone to flooding – as opposed to strategically identifying where interventions may offer maximal benefits (Madanat et al. 2019, Suh et al. 2019). For example, Sun et al. (2021) evaluated the impact from three protection strategies (levees in this case), designed to protect the San Francisco Bay transportation infrastructure from sea-level rise using an agent-based modeling approach that additionally considered dynamic rerouting and congestion. While all three strategies lead to net improvements in terms of commute times, the spatial distribution of those benefits was uneven. The work in Hummel et al. (2020)

similarly considers transportation infrastructure in the San Francisco Bay, though carefully demonstrates how shoreline hardening in one county could have delirious impacts on traffic in other counties due to the hydrodynamic response to the barriers. Again, the barriers were evaluated independent of specific objectives.

A recent small, but growing, body of work has developed optimization frameworks to strategically identify where flood mitigation should be conducted. This work builds conceptually from a body of literature that seeks to make mitigation investments to maintain network connectivity given some probability of edge failures and a budget constraint (e.g., Peeta et al., 2010). Work that specifically considers flooding has developed bi-level optimizations that pick road protection strategies in the top level so as to reduce cumulative travel delays in the bottom level (Asadabadi & Miller-Hooks, 2017; Papakonstantinou et al., 2019a). While not an optimization approach, earlier work by Sohn (2006), develops an accessibility index based each link's marginal contribution to regional access before and after a 100-year flood, and this prioritization, they argue, could inform road retrofitting strategy. Due mostly to computational limitations, the networks used in these works are smaller, and they do not consider the distributional impact of interventions on residents.

It should be noted that the concept of roadway mitigation has been considered for other hazards - namely earthquakes (e.g., Chang et al., 2003; Furuta et al., 2011; Peeta et al., 2010). Peeta et al. (2010) focus on pre-disaster strategic highway network protections to maximize the post-disaster connectivity between various origin-destination (O-D) pairs and minimize post-event travel time under a budget constraint.

They used a two-stage stochastic program, where the first stage identifies which links to protect and the second stage finds the minimum travel cost between the O-D pairs. Zhang & Wang (2016) proposed a resilience-based framework to identify and prioritize critical bridges for effective pre-disaster mitigation. To evaluate the resilience-based performance of transportation networks, they use a weighted average number of reliable interdependent pathways between any network O-D pair, the pathways with higher traffic flow and shorter length are weighted heavier.

There are several options that decision-makers have to protect road infrastructure from flooding. The process through which segments are selected is often governed by cost, and arguably, a maximization of positive externalities. The interventions tend to focus on the hardening or "gray infrastructure," - such as raising roadways or building levees (Papakonstantinou et al., 2019a). Levees may have spillover effects and protect additional assets (e.g., homes) behind them; alternatively, they may displace water, and induce more flooding in unprotected areas (Hummel et al., 2021). More recently, there has been an increased emphasis, in practice, on "nature-based infrastructure" as a method for protecting transportation assets, given its relatively low cost, lower carbon footprint, and adaptive capabilities (Feagin et al., 2021). To our knowledge, systems-level research on maintaining mobility during floods using nature-based infrastructure has not been evaluated, though Li et al. (2020) take a step toward this approach by developing an indicators-based tool for identifying priority areas for green infrastructure in urban spaces. In this work, we are, to some degree, agnostic about the type of intervention and rather focus on where interventions

should occur. This makes an implicit assumption that the unit cost for each strategy to achieve the same outcome is identical - an assumption known to be incorrect (ROKS, 2022).

A challenge of understanding the implications of protection strategies is understanding burdens and benefits that each can cause to the communities in order to give decision-makers a comprehensive picture of the proposed strategies. For instance, Sun et al., (2020) evaluated the distribution of impacts stemming from transportation related SLR protection strategies. They found, for example, that some strategies, such as protecting bridges, may improve the net travel time during periods of inundation but may significantly burdensome disadvantaged communities who would experience decreased mobility due to these protections. Besides Sun et al. (2020), the transportation asset protection literature does not evaluate the distribution of benefits, and no work has evaluated protection strategies endogenously as a function of balancing benefits.

While there has been little evaluation of how the benefits of hazard protection strategies may accrue, the transportation literature has given significant credence to equity in other applications. For example, Feng & Zhang (2014) used numerous measures of equity to target link capacity enhancements, while Ermagun & Tilahun (2020) computed the distribution of travel time by public transit to key destinations for all census block groups in Chicago. Equity broadly is defined as the distribution of resources in the fairest manner (Welch, 2013). Equity is divided into two types: horizontal and vertical. Horizontal equity relates to the distribution of resources

between individuals considered equal in ability and need. It avoids favoring one group over another and is all about providing services equally to everyone (Delbosc and Currie, 2011). Vertical equity pertains to the distribution of resources among individuals with different needs and abilities (Litman 2002). There are many metrics to quantify resource equity - from GINI to Atkinson (ATK). These metrics are formally presented and defined in Section 3.3.3

Equity often focuses on whether resources are being delivered to underserved populations, which often translates into a focus on socially vulnerable populations. This is reasonable, given that socially vulnerable populations tend to fare worse. Changes in the transportation system proved to create inequality among communities with different demographic backgrounds (Bills & Walker, 2017; Guo et al., 2018; Sun et al., 2020). To better understand the uneven effects of disasters on communities and quantify human dimensions of hazard vulnerability, researchers introduced the concept of social vulnerability in the 1970s when they realized that socioeconomic factors of the communities also affect community resilience and should be considered as a part of vulnerability (Juntunen, 2004). Vulnerability to hazards is influenced by various demographic and socioeconomic factors, such as age, income, race, and neighborhood characteristics (Gladwin and Peacock, 1997, Green et al., 2007). Race is one of the social vulnerable flood-related characteristics, because it may affect the residential locations in high hazard areas due to the lack of economic resources and discrimination (Clark et al., 1998; Spain & Bianchi, 1996). Moreover, wealth enables impacted communities to absorb losses quickly and respond more effectively due to having

insurance and access to social safety nets (Cutter, 2003). Wealth can be measured by per capita income, median household income, median house values, and median rents (Cutter et al., 2008). The changes in the transportation system during a disruption could cause inequality among communities with different demographic backgrounds (Bills & Walker, 2017; Guo et al., 2018). To maintain the regional development and protect equity, it may be desirable for decision-makers to be aware of the certain vulnerable groups' exposure and to direct investments aimed at reducing exposure in a way to particularly benefit these vulnerable groups (Mattsson & Jenelius, 2015).

3.3 Methodology

3.3.1 Overview

The approach broadly evaluates optimal road armoring strategies to maintain parcel-level access during 10-year and 100-year floods using different equity measures. We then examine the demographic and spatial heterogeneity of those who benefit from the protections. This work considers six different objective functions. They are: (1) to maximize the number of parcels in the county that maintain their access, (2) to minimize the GINI index, and thus provide more equal access among all block groups in the county, (3) and (4) to minimize Atkinson index using two different equity parameters, and thus provide more equal access among all block groups in the county with assigning different weights to block groups with lower accessibility. …; (5) to more evenly balance accessibility loss among the vulnerable and non-vulnerable residents impacted by flooding, and (6) to more evenly balance accessibility loss among

the rural and urban communities impacted by flooding. For each objective, we consider accessibility loss from parcels to emergency services (i.e., fire stations) considering the criticality of constant availability of these services. In principle, other destinations could be considered. This work is conducted in a geospatial computational framework designed and built using R software.

We assume that resources are not infinite, and the strategy that is selected is subject to a budget. The cost to elevate roads and conduct other armoring varies by state, environmental condition, road dimension, and road type. Stanton & Ackerman (2007) estimated that the average cost to elevate 1-meter of road by _<insert height> to be 1,243 USD (2006 dollars) (i.e., $2 million/mile in 2006 dollars). For simplicity, we assume that the unit cost of hardening 1 meter of roadway to withstand 1 meter of flooding is constant throughout the network and independent of the hardening approach. Thus, the budget constraints are defined using the meter-meter unit in this study. This is done to be place more emphasis on adaptation equity and to not be bogged down by differential road armoring costs, though this is admittedly a simplification. The marginal cost of hardening the roadway expected to be increasing, in that pouring a centimeter of asphalt is far less expensive on the margin than elevating a roadway's foundation. This could readily be addressed in future work should construction and roadway maintenance costs be known for each road segment. We considered three budget constraints: 500 m^2, 10,000 m^2, and 100,000 m^2.

3.3.2 Qualifying the impact of storm surge on transportation network

The work specifically considers flooding from coastal storm surges, though the methods could be broadened to additionally consider other forms of flooding, such as inundation from sea-level rise and pluvial flooding. Surge depth data, along with its return periods and confidence limits for water depth, is obtained through the Coastal Hazards System (CHS) database (Coastal Hazards System, 2020). The CHS database is built and maintained by the US Army Engineer Research and Development Center (ERDC), a research organization within the US Army Corps of Engineers (USACE). While probabilistic information is provided for a range of return periods and confidence limits (which describes the epistemic uncertainty around flood depths), we focus only on 10-year and 100-year storm surge using a 50% CL, representing both higher-likelihood-lower-consequence and lower-likelihood-higher-consequence scenarios. As with other sources of flooding, the computational platform is flexible enough to study alternative return periods.

To model the impact of storm surge flooding, water depth raster files from the USACE are overlaid onto a Digital Elevation Model (DEM) of the study region developed using USGS LiDAR data and the elevations are subtracted. Road segments with more than 15 cm of flooding are considered impassible and removed from the road network (unless they are later targeted for protection, in which case, they remain in the road network presuming protection is adequate). Water with a depth greater than 15 cm is more likely to cause loss of vehicle control, depending on water velocity

(SmartDriving, 2021). However, note that no depth of water is considered safe to drive through.

The geographic centroid of each parcel is projected to the closest road segment, and this becomes the origin. Critical services are proxied by fire stations, but in principle, any destination could be used. Then, a shortest path algorithm (i.e., Dijkstra's algorithm) is applied to evaluate whether each parcel is able to reach a fire station or not. It is possible that a parcel is unable to reach a fire station that is closest based on Euclidean distance due to flooding but is able to reach a fire station that is further away. A Genetic Algorithm, described later, is then used to identify the combination of road links to protect that best achieve different equity and resource-efficiency priorities.

We note that some studies that explored the impact of floods on roadways have considered the impact of rerouting on congestion and the impact this might have on travel time (e.g., Feng et al., 2019; Hummel et al., 2018). These studies were conducted in urban regions. We elect to not adopt this approach because it is unable to identify who loses access altogether - an arguably more important metric during extreme events - and because of the rural status of the study region where congestion is not a significant concern. Additionally, it is not obvious that assumptions made in previous studies about user equilibrium being achieved during periods of extreme weather are reasonable (Siri et al., 2020).

3.3.3 Transportation equity and metrics

In this study, transportation equity is explored from two perspectives, horizontal equity and vertical equity. Horizontal equity refers to the equality of the service distribution in the area (Litman, 2002). This is evaluated using the GINI and ATK indicators which are explained in detail in sections 3.3.3.1, and 3.3.3.2. Vertical equity, on the other hand, studies the distribution of services among different groups of the community, such as residents with different demographics (Litman, 2002). To evaluate the vertical equity, I study the balanced accessibility between vulnerable and non-vulnerable communities as well as rural and urban communities (Section 3.3.3.3).

To identify the vulnerable communities, I developed a social vulnerability index (SVI) using five census variables that are available at block group level; age below 17, age above 65, unemployed civilian population, income, and minorities (all races other than white) (Census Bureau, 2020). These variables are chosen among the fifteen variables that Flanagan et al. (2011) used to develop the Center of Disease Control Social Vulnerability Index (CDC-SVI) at the tract level to be used in emergencies. It gives one SVI for each block group level between 0 and 1, with 0 indicating less vulnerable and 1 indicating highly vulnerable. Although skipping the other 10 variables impacts the social vulnerability index I calculated in this study, my focus was to use finer resolution. Moreover, the aggregate SVI at tract level was almost consistent with CDC-SVI results. In this study, the population in the case study classifies into two groups; parcels inside the census block groups with SVI above the regional median, which are considered as a vulnerable population, and parcels in the census block groups with an

SVI below the regional median, that are not considered as vulnerable to disasters, and I call them non-vulnerable in this study.

Rural communities are defined based on population density; the block groups with population density less than 500 people per square mile are considered as rural block groups (USDA ERS, 2021) and the remaining block groups are considered as urban. This definition is consistent with my study area that is mostly rural county with a small urban area in the city of Cambridge in the North.

3.3.3.1 Gini Coefficient

As discussed before, I aim to measure transportation equity in this study using different metrics. One of these metrics is the GINI index, which is by far the most frequently used index for distributions of accessibility. GINI index assesses the spatial equality of distribution of services or accessibility among different groups. The GINI index was first developed to measure income inequality and evaluated as the difference between the perfect equality line (the same share of income for everyone in an area) and the actual line depicting people's income (GINI 1912). A GINI index of zero means perfect equality, and a GINI index of one express minimum equality. In this study, I first evaluate the GINI index under a 10-year and a 100-year flood scenario to see the overall degree of inequality in terms of the access to emergency services in the study area. To be consistent with other indicators, I compare accessibility shares between different block groups. It ranges between 0 and 1, and a lower GINI index indicates a more equitable distribution of access across the block groups. In the last decades, this indicator has been used in transportation equity to evaluate the distribution of

accessibility (Feng and Zhang 2009). For example, (Z. Chen et al., 2019) used the GINI coefficient to evaluate the distribution of benefits of bike-sharing systems in Southern Tampa. Tahmasbi et al. (2019) evaluated the impact of development plans on changes in the accessibility level to urban public facilities and equity impacts using GINI. Mayaud et al. (2019) also adopted the GINI coefficient to evaluate the distributional impacts of accessibility to healthcare via public transit among different vulnerable populations in Vancouver, Seattle, and Portland.

$$E_{GINI} = \frac{1}{2N^2\bar{A}} \sum_{i=1}^{N} \sum_{j=1}^{N} |A_j - A_i| \quad (1)$$

Where E is the equity indicator, A_j is the fraction of the block group j with accessibility to a fire station, $\bar{A}$ is the average accessibility share of the study area, and *N*is the number of the block groups.

3.3.3.2 Atkinson Index

The second equity indicator is ATK, proposed by Atkinson (1970). ATK also evaluates the distribution of access, but it has a parameter that is used to measure changes in different segments of the distribution. Various types of decision-making concerns can be reflected using different values for the parameter ε. As ε increases, the ATK index becomes more sensitive to changes at the lower end of the accessibility block groups. Conversely, as the level of ε approaches 0, the ATK index becomes less sensitive to changes in the lower end of the distribution. In this study, I evaluate the ATK index with two different values for the parameters ε , 0.25, and 0,75. Feng and Zhang (2014) incorporated GINI and ATK and five other indicators into an equity maximization

model to evaluate the performance of accessibility-based equity. They used different values between 0 and 1 for ε to explain the impact of different weights on the final results. Zuo et al. (2020) measured the capability of bicycles as first-and-last mile connectors to improve transit accessibility and equity. They used Atkinson with different values for ε between 0 and 2, and also other equity indicators to evaluate the distributional benefits among different races.

$$E_{atk} = 1 - \frac{1}{\bar{A}}\left[\frac{1}{N}\sum_{j=1}^{N}(A_j)^{1-\varepsilon}\right]^{\frac{1}{1-\varepsilon}}, \text{ when } \varepsilon \neq 1$$
$$E_{atk} = 1 - \frac{1}{\bar{A}}(\prod_{j \in N} A_j)^{\frac{1}{N}}, \qquad \text{when } \varepsilon = 1 \tag{2}$$

Where E is the equity indicator, A_j, $\bar{A}$, and *N*are the same as above (equation 1), and ε is the parameter to reflect decision-making concerns regarding the distribution of accessibility share across block groups.

3.3.3.3 Balanced share of accessibility

The next equity indicator focuses on differences between accessibility distribution in urban and rural areas. To evaluate this indicator, first, I define what portion of rural block groups has access to fire stations under each flood scenario and what is the ratio for urban block groups. The absolute difference between these two ratios is a number between 0 and 1 and defines the equity of distribution of services between two different groups of the study area. To have equitable access between urban and rural communities, I want the absolute difference to be close to zero, with zero meaning perfect equity.

$$E_{Balanced\ access\ Rur,Urb} = \left| \sum_{k=1}^{U} A_k - \sum_{m=1}^{R} A_m \right| , \quad N = U + R \tag{3}$$

Where E is the equity indicator, A_k , A_m are the ratio of urban block groups and rural block groups, respectively with access to fire stations.

The last equity indicator is about the equity distribution of access among vulnerable and non-vulnerable communities. To evaluate this indicator, first, I define the portion of the vulnerable block groups as well as non-vulnerable block groups that have access to fire stations under each flood scenario. The equity is defined as the absolute difference between these two ratios, and it ranges between 0 and 1; being zero means perfect equity.

$$E_{Balanced\ access\ Vul/\ Non-vul} = \left| \sum_{v=1}^{V} A_k - \sum_{n=1}^{NV} A_m \right| , \qquad N = V + NV \tag{4}$$

Where E is the equity indicator, A_v , A_n are the ratio of vulnerable block groups and non-vulnerable block groups respectively, with access to fire stations.

3.3.4 Genetic Algorithm

We apply a genetic algorithm (GA) to overcome the intractability of iteratively evaluating all combinations of road protection strategies for a given objective. GAs are a meta-heuristic optimization method, first introduced in Holland (1975), based on the process of natural selection. They have been widely used in resource-constraint problems involving hazard planning and mitigation for infrastructure. For example,

Dong & Frangopol (2017) employ a bi-objective GA to find cost-effective residential building mitigation strategies under climate change. Along similar lines, Hu et al. (2014) use a bi-objective GA to locate optimal post-earthquake shelter locations that simultaneously minimize cumulative travel time and cost.

GAs generally work as follows. In each iteration, a population of binary strings or "chromosomes" is evaluated using a fitness function. In this case, each binary variable in the chromosome is a link, and a value of one indicates that it is selected for hardening. The population of chromosomes represents different hardening strategies. The strategy that is deemed best by the fitness function (i.e., the strategy that maximizes some measure of parcel-level accessibility) is stored and used in the next iteration. The other chromosomes in the next generation are generated using a binary tournament selection method (Mitchell 1998). Here, parent chromosomes are randomly selected, two at a time, in proportion to their fitness, and a new genetic code (or chromosomes) is made by swapping (or "crossing over") the genetic code of the parents at a random point. A mutator operator then randomly changes the binary variables to their complement with a low probability. This adds genetic variability to prevent the optimization from becoming "stuck" at a local optimum. It is possible that new chromosomes violate one or more constraints. GAs address this by penalizing these strategies through the fitness function.

A few notes about my implementation follow. First, only roads that experience more than 15cm of flooding for the given surge scenario are considered for hardening. This reduces the number of links under consideration. The initial population, P, where

|P| = 100, is built from that subset of links, and each link is randomly assigned a 0 or a 1. Mutations are done by choosing 3% of the population at each iteration and changing a randomly chosen gene from zero to one or vice versa. I also introduce ten new populations to the original population in each iteration to increase diversity and increase the chance of finding a global solution. The fitness functions that I use are described in more depth below, though each treat chromosome (or hardening strategy) that violate the resource constraint is prevented from going to the next generation due to the sorting of result and choosing the first 100 best values. The convergence criterion, which dictates when the algorithm stops, is to have 30 generations passed without any improvement in the best fitness value.

In the end, a relevant fitness function is used to evaluate the performance of responses, and the best chromosome is saved as the optimal solution to the problem (Saeidian et al., 2016). The fitness function measures the satisfaction of each chromosome according to the objective function. The objective functions in this study are to maximize the number of parcels that maintain their access as a result of investments, to maximize the equity distribution of access in study areas using different equity metrics that are discussed in section 3.3.3.

Multiple budget constraints are considered to identify different efficient strategies according to different decision-making concerns. I assumed that road protection means elevating the entirety of the flooded portion of the road so that it is no longer underwater. The cost of doing this is measured by the length of the flooded roadway times the water depth; I assume this is roughly proportional to actual costs.

For example, a road that has 50 meters beneath 10 centimeters of water would require $0.01*50\ m^2 = 0.5m^2$ to be protected. For the purpose of this study, I used three different budget limits, $500m^2$, $10{,}000m^2$, and $100{,}000m^2$.

3.4 Study Area

We focus my study area on Dorchester County, Maryland, and areas of neighboring counties that possess fire stations that serve Dorchester County residents (Figure 3.1). Dorchester is on Maryland's Eastern Shore and, with a population of around 32,500 and a population density of 55 people per square mile, is considered a good representative of a rural site (U.S. Census 2010). It has a small urban core in the City of Cambridge, Maryland. Most residents rely on private vehicles to reach their destination. Tourism and agriculture are among the main industries.

This region sits along the Chesapeake Bay, and large areas of the county sit in low-lying coastal plains. The region is prone to repetitive flooding that often diverts motorists onto alternative roads. Currently, it is not uncommon for some motorists to lose access to key amenities, such as fire stations, altogether due to flooding. Nearly 60% of the county is in the 100-year floodplain (Cole, 2008).

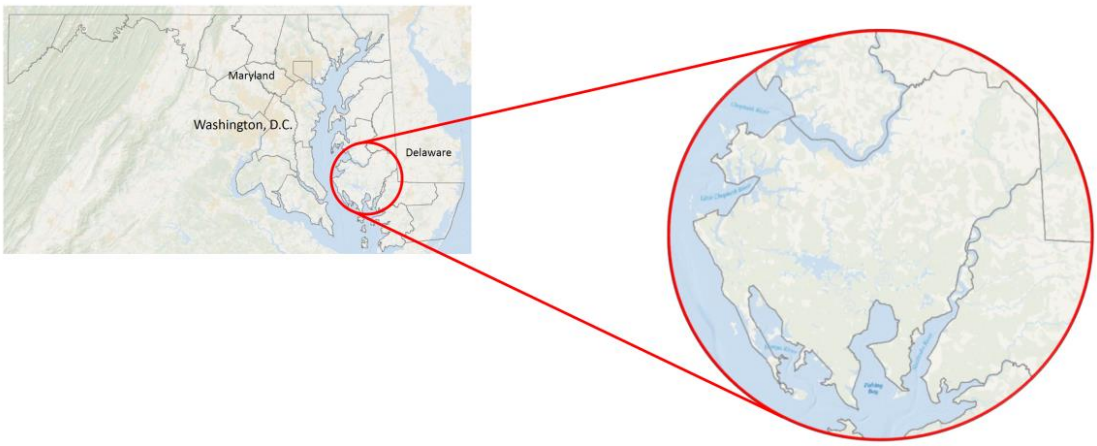

Figure 3.1. Case study location (Esri, 2021)

3.5 Result

To explore the benefits and burdens of each protection strategy and evaluate accessibility equity, I carry out a numerical analysis of Dorchester County. The candidate links to protect are selected from two flood scenarios, 10-year and 100-year storm surges. The results are organized as follows: first, the baseline networks are created, and inundated roads and impacted residents are identified. Then, I present results for protection scenarios under different objectives. Finally, a robustness analysis was conducted for a 10-year flood scenario to evaluate the effectiveness of road protection under different flood scenarios.

3.5.1 Levels of equity without road protection

Figure 3.2 shows the road network of Dorchester County, the inundated road links with flood depth above 15 cm are shown for a 10-year (dark red) and a 100-year (dark red and orange) storm surge flooding. (Cars are reasonably assumed to be able to drive through water of depths less than 15cm). To decrease the number of the roads

from consideration and thus the computational time, I focus on main roads (road types M and S in data) and remove the private roads from the analysis. Under a 10-year storm surge flooding, 284 roads experience a flood depth above 15 cm with a length of 405,295 meters, and this number increases to 334 roads and 492,021 meters under a 100-year storm surge. The percentage of impacted residents in terms of losing their access to any emergency services is provided in Table 3.1. To better understand how flooding impacts are distributed among different groups of the communities, I showed the results for two different categories, rural communities versus urban and vulnerable groups vs. non-vulnerable (others). In total, 4,176 parcels (22.6% of all parcels in Dorchester County) lose their access to any emergency services under a 10-year flood scenario, 21.3% of these parcels live in block groups with SVI equal to or below 0.478 (the region median SVI), and only 1.3% live in block groups with SVI above 0.478, who are considered vulnerable. If I want to consider the impacted residents as rural vs. urban, 2.4% of impacted parcels are located in urban block groups, and 20.2% are located in rural block groups. Overall, results indicate that impacted parcels in Dorchester County are mostly non-vulnerable communities residing in rural areas.

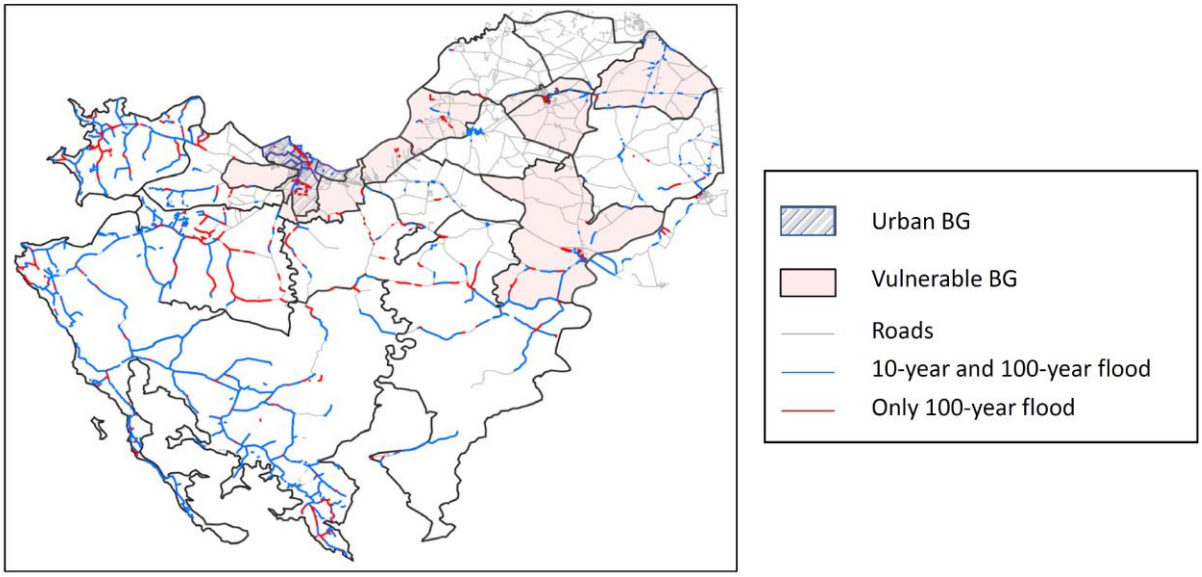

Figure 3.2. Closed roads under a 10-year storm surge (dark red) and a 100-year storm surge (dark red and orange).

Table 3.1. The portion of impacted parcels under different flood scenarios.

Flood scenario	Total impacted roads	Percentage of impacted parcels	Non-Vulnerable	Vulnerable	Urban	Rural
10-year	284	22.60%	21.30%	1.30%	2.40%	20.20%
100-year	334	26.40%	24.00%	2.40%	4.20%	22.20%

To preview the levels of equity measurements, I evaluated the indicators in case of the current situation without any road protection under both flood scenarios. It is found that the levels vary for different equity indicators while all range between 0 and 1. Atkinson indicators change increasingly from 0.04 to 0.22 and 0.27 under 10-year and 100-year flood scenarios, respectively. In the case of Atkinson, a higher value of Ɛ indicates a higher degree of inequity, which means that block groups with low accessibility have higher weights. In this study, I use two different values for Ɛ 0.25 and 0.75 to compare the results.

The first three indicators in Table 3.2 focus on the horizontal spatial distribution of equity; however, there are significant differences among those due to different formulations and different weights that are attached to transfer at different points in the distribution. The values change increasingly from 0.036 and 0.041 to 0.22 and 0.27 under a 10-year and 100-year flood scenarios, respectively, when Ɛ changes from 0.25 to 0.75. Here, a higher level of Ɛ means a higher weight is attached to the zones with low accessibility. The last two indicators look at slightly different equity issues, which are considered vertical equity, and focus on accessibility distribution among groups with different characteristics. The fourth indicator that evaluates the balance of accessibility between rural and urban areas is 0.23 and 0.21 for a 10-year and a 100-year flood scenario, respectively, which means under a 10-year flood scenario, there is a gap of 0.23 between the fraction of parcels with accessibility in rural areas and those in urban areas. The gap decreases by a 100-year flood to 0.21 because a lower amount of flood impacts mostly the rural communities in coastal areas, but a higher amount of flood impacts urban communities in the North. The last indicator that focuses on the balance between vulnerable and non-vulnerable communities areas shows a higher gap of 0.43 and 0.42 for a 10-year and a 100-year flood scenario, respectively, which that means under a 10-year flood scenario, there is a gap of 0.43 between the fraction of parcels with accessibility in vulnerable areas and those in non-vulnerable areas. Since my focus is to provide equitable access for rural and urban communities as well as vulnerable and non-vulnerable communities, I use absolute differences and, in the next section, aim to reduce these numbers to zero.

Table 3.2. Levels of different equity indicators without road protection

Scenario	Indicators	Equity values
10-Year	GINI	0.168
	ATK ($\varepsilon = 0.25$)	0.036
	ATK ($\varepsilon = 0.75$)	0.220
	Balanced Rural/Urban	0.234
	Balanced Vul/Non-Vul	0.428
100-Year	GINI	0.193
	ATK ($\varepsilon = 0.25$)	0.041
	ATK ($\varepsilon = 0.75$)	0.271
	Balanced Rural/Urban	0.213
	Balanced Vul/Non-Vul	0.421

3.5.2 Accessibility and equity maximization

We implemented six single-objective optimization models based on accessibility and equity maximization. The first objective discussed in this study is to maximize the number of parcels that maintain their accessibility to emergency services by protecting the impacted roads. As mentioned before, the analysis is conducted for two storm surge flooding, a 10-year and a 100-year storm surge flooding. Under a 10-year flood scenario with a lower budget, the accessibility of 385 parcels will be maintained, and this number increases to 2934 parcels with 100,000 m^2 budget. The number is different for 100-year flooding events due to the changes in flood depth and the cost to protect the roads and the increase in the number of flooded roads (first column in Table 3.3). The values in Table 3.3 are calculated from the optimal solutions that are based on different protection scenarios. The first column indicates the model I used to optimize equity, and the bold number in the corresponding row is the optimal solution using that model. The other values are indirectly calculated using the other optimal protection strategies. The second column in Table 3.3. shows the number of

parcels that benefits the protection, which means a better strategy results in a larger number. Columns 3 to 7 are about maximizing equity, which means a smaller number close to 0 is the better solution. As expected, the bold numbers in each column (the optimal solution) is the best among other values calculated for that column with respect to the other models. For example, under a 10-year flood scenario, 385 parcels benefit from protection when I optimize model 1. However, this number is 384 when I optimize the protection using the GINI index or 52 when I decide to use model M5 and improve the balance of accessibility between rural and urban communities. The second objective of the meta-heuristic optimization model is to minimize the GINI coefficient, in other words, to maintain the accessibility of parcels in a way that all block groups have the same share of accessibility. The perfect GINI coefficient is zero, which means all block groups have the same share of accessibility but most of the time, due to budget limits, that is impossible. In the case of Atkinson indicators, the objective is to minimize the values to improve equity. However, the results have not changed a lot. Models sixth and seventh focus on optimizing protection benefits by balancing the accessibility distribution among different groups of the community. To have balanced access among different groups, I want all groups to have the same share of benefits, and the difference between the fraction of urban communities with access and rural communities with access gets close to 0. I have the same goal with the vulnerable and non-vulnerable communities. As discussed before, the optimal solution calculated in Table 3.3 with respect to one indicator is not optimal for with respect to other models. You can see the significant differences in accessibility gain for models 2, 3, and 5. The calculated

parcels that benefit from these three models are much smaller than the number of parcels that can benefit if I use model 1. That is due to the different objectives; for example, when model 5 reaches an optimal solution that provides access to rural areas to decrease the fraction of parcels maintaining access in rural and urban areas. Figure 3.3 shows the spatial distribution of the parcels that maintain their access to fire stations; for model 1, that is the optimal numbers, and for other models, they are calculated based on the tagged model. The green block groups in M5 and the pink block groups in M6 show the urban and vulnerable communities, respectively.

The distribution of vulnerable and non-vulnerable communities in Dorchester County makes non-vulnerable block groups more exposed to storm surge flooding than vulnerable groups. The accessibility loss mostly happens among the non-vulnerable communities living in the peninsulas. That results in a smaller portion of the non-vulnerable with accessibility to emergency services and a big difference between them and the portion of vulnerable people with access.

As shown in Table 3.3, the total length of the protected roads and the number of protected roads under each model are calculated. The differences between the numbers explain that based on different objectives, the roads that should be protected may change, and they may benefit different groups of the communities. In reality, decision-makers may decide to use a specific model according to their specific emphasis. One may concentrate on maintaining accessibility for a larger number of parcels and decide to use the first model. While another decision maker may decide to

investigate the available budget in a way that balances the accessibility share between rural and urban communities.

Table 3.3. Optimal and calculated results for accessibility and equity maximization (budget 500 m2).

Flood Scenario	Models	Accessibility gain	Equity metrics					Total road length protected (m)
			GINI	ATK ($\varepsilon = 0.25$)	ATK ($\varepsilon = 0.75$)	Balanced Rural/Urban	Balanced Vul/Non-Vul	
10-year	M1: Accessibility gain	**385**	0.147	0.036	0.218	0.292	0.387	1,519
	M2: GINI	384	**0.147**	0.036	0.218	0.295	0.387	1,879
	M3: ATK ($\varepsilon = 0.25$)	349	0.148	**0.035**	0.218	0.288	0.391	1,335
	M4: ATK ($\varepsilon = 0.75$)	89	0.162	0.035	**0.189**	0.247	0.418	967
	M5: Balanced Rural/Urban	52	0.167	0.036	0.219	**0.230**	0.424	2,182
	M6: Balanced Vuln/Non-Vul	384	0.148	0.036	0.218	0.230	**0.386**	1,718
100-year	M1: Accessibility gain	**984**	0.158	0.036	0.219	0.273	0.409	969
	M2: GINI	891	**0.158**	0.036	0.219	0.343	0.409	939
	M3: ATK ($\varepsilon = 0.25$)	737	0.166	**0.036**	0.219	0.238	0.425	599
	M4: ATK ($\varepsilon = 0.75$)	888	0.158	0.036	**0.218**	0.262	0.409	722
	M5: Balanced Rural/Urban	777	0.167	0.037	0.220	**0.228**	0.421	667
	M6: Balanced Vuln/Non-Vul	901	0.160	0.036	0.219	0.340	**0.408**	946

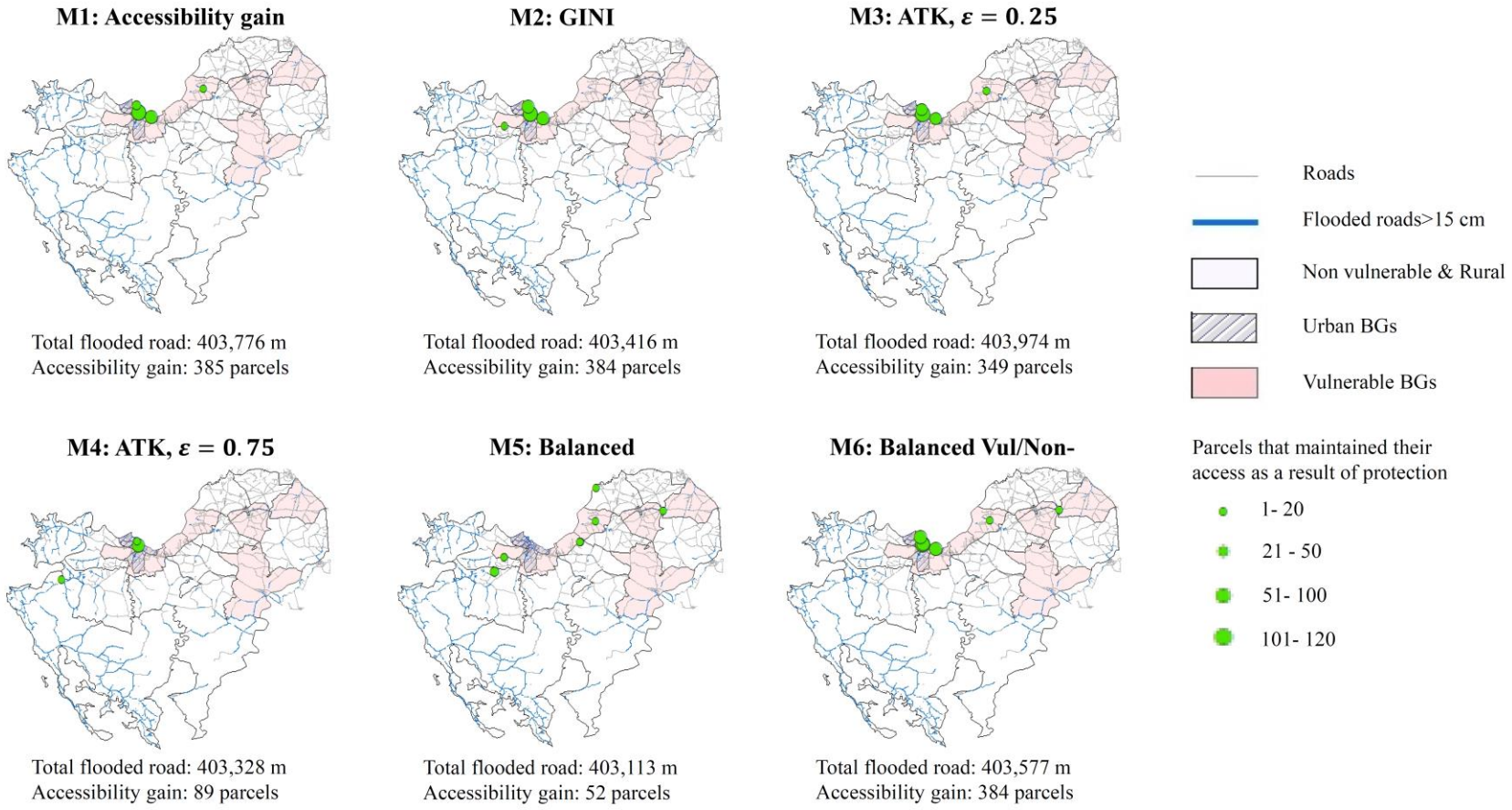

Figure 3.3. Spatial distribution of parcels that maintain their access to at least one fire station under a 10-year storm surge because of road protection prescribed by intervention. Maps are zoomed to the parcels that maintain their access as a result of protection.

Sensitivity analysis

In Dorchester County, the block groups near the coastline have low access to fire stations, and they frequently lose their access due to road inundation. To maintain their accessibility, it is necessary to protect a huge number of roads that require a higher budget limit. That is why the accessibility gain and other equity metrics do not change that much between 500 m^2 budget and 10,000 m^2 but they all changed a lot for both flood scenarios with a 100,000 m^2 budget. Due to budget constraints, it is impossible to protect all roads, but I decided to repeat my analyses for three different budget limits to better understand the sensitivity of the analysis to the allocated budget, the budget limits for this study are 500 m^2, 10,000 m^2, and 100,000 m^2(Table 3.4).

Table 3.4. Results of sensitivity analyses across different objectives.

Flood Scenario	Budget	Accessibility gain	GINI	ATK ($\varepsilon = 0.25$)	ATK ($\varepsilon = 0.75$)	Balanced Rural/Urban	Balanced Vul/Non-Vul
10-Year	500	385	0.147	0.035	0.189	0.230	0.386
	10K	978	0.123	0.020	0.088	0.204	0.351
	100K	2,934	0.049	0.002	0.007	0.037	0.122
100-Year	500	984	0.158	0.036	0.218	0.228	0.408
	10K	1,326	0.142	0.028	0.154	0.215	0.386
	100K	2,351	0.098	0.011	0.036	0.130	0.288

3.5.3 Robustness analysis

Our primary objective was to find the optimal protection strategies for two different flood scenarios. In this section, I evaluate the benefits of adopting one of the

protection strategies I discussed previously. Here, the protection strategy for model M1 under a 10-year flood scenario is adapted to the road network of Dorchester County. To better understand how usable this protection is under other flood scenarios, I evaluate the protected road network under storm surge scenarios with different return periods. For this reason, first, I assume all 13 suggested road links in M1 (Table 3.3, first row) are elevated to the 10-year flood depth; then, using different flood scenarios, I identify the closed roads and impacted parcels that maintain their access to fire stations using the protected road network. Figure 3.4 explains the fraction of parcels that maintain their access as a result of road protection. The largest fraction relates to the 10-year storm surge, which is the one that I optimized my investment based on (Figure 3.4, yellow dashed line). The numbers decrease as the severity of the flood increases to a 10,000-year flood which is intuitively correct; as flood intensity increases water level on the road increases and gets higher than the elevated roads.

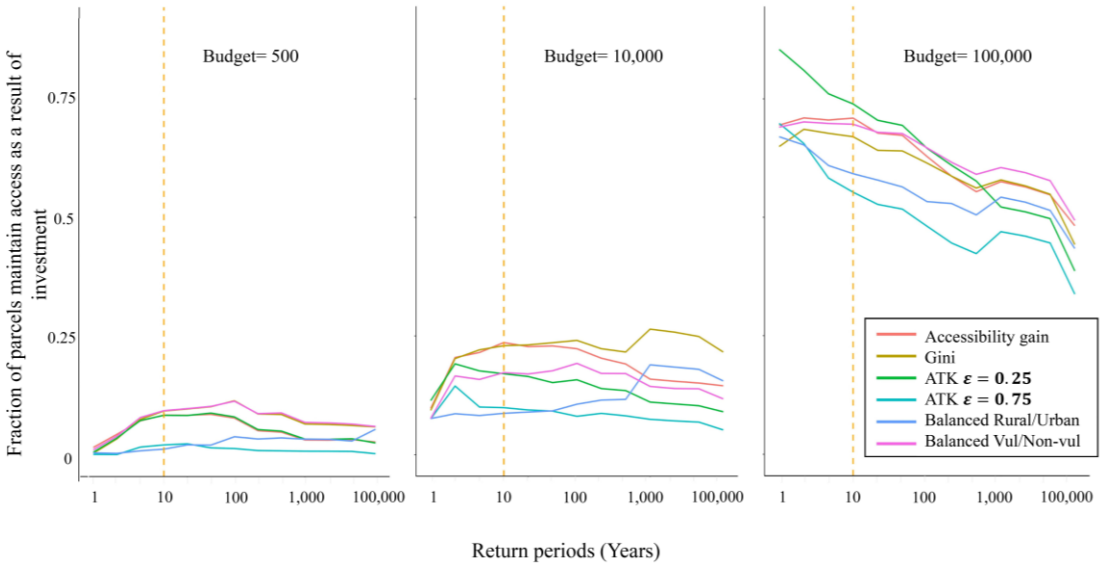

Figure 3.4. Fractions of parcels maintain access to fire stations as a result of protection roads under different storm surge scenarios. The protection strategy is applying M1 (maximizing accessibility) for a 10-year storm surge with a budget limit of 500 m^2.

3.6 Conclusion

The investment in road protection will benefit to increasing accessibility of parcels to critical services; however, it may not automatically lead to an optimal balance of accessibility among different groups of the community as equitable distribution. Although recently more studies have been focused on transportation equity, discussions on the balance accessibility among urban and rural communities as well as vulnerable and non-vulnerable communities are missing (or scarce) in previous studies.

Therefore, in this paper, I investigated how storm surge flooding impacts the parcel-level accessibility in rural areas and measured the spatial equity indicators and proposed an optimization model to describe the trade-offs between equity improvements and the investment of protection strategies under different objectives. The equity was defined by accessibility and represented by indicators, GINI, ATK, balanced accessibility between urban and rural, and balanced accessibility between vulnerable and non-vulnerable block groups. Using the case study of Dorchester County, Maryland, I demonstrate that all of the accessibility-based equity indicators are sensitive to road protection. However, they change on different scales. The sensitivity analyses based on different budget limits and flood scenarios found that the level of equity depends on the severity of the flood and also the extent of road

protection. Moreover, road protection based on one objective would not always result in the same improvement in the other equity metrics or accessibility. In the case study, for a 10-year flood scenario improving balanced accessibility between rural and urban areas could not provide accessibility for a large number of people. The scenarios with the same budget limits select different roads to protect, suggesting the necessity to cautiously select equity indicators in decision-making processes.

There are some limitations of this work that could be addressed in the future. First, I did not consider travel time or congestion in my analysis; congestion does not seem to be a problem in my case study, though the closure of some roads could cause an increase in traffic volume in other road links that are not designed for it. If finer origin-destination data and traffic volume data become available in the future, this limitation can be addressed. For the purpose of simplicity, I assumed in this paper all block groups had the same important weight. However, policymakers may assign different weights to different zones in reality. In this sense, the effect of different weights should be examined in the future.

This type of work could additionally support cost-benefit of where protections strategies should go, such as where U.S. Army Corps of Engineers (USACE) should work. While this study only discussed the hardening road protection strategies to maintain the accessibility of communities, for low-lying coastal areas like Dorchester County, future works could focus on spending available mitigation and adaptation budgets on alternative transportation methods such as water transportation. For example, abandoning the road links that are facing frequent flooding and using a ferry

system to connect communities using these inundated roads to the rest of the county. However, to better understand the most optimal method, the problems with water transportation also need to be discussed, such as the fast corrosion of ferries due to saltwater.

4 Chapter 4: Identification of Critical Road Segments that reduce uncertainty surrounding access to emergency services if monitored

4.1 Introduction

Road networks are a significant body of transportation infrastructures for communities, which provide access to critical services and affect the travel of residents. During disasters and emergency circumstances, road networks are vital resources that play an important role in rescue operations, evacuation, community recovery, and reconstruction. However, they often fail to maintain their original function due to disruptions, and the transportation network performance degrades. This reduction does not happen equally; the failure of certain links can cause significant disruption in network performance. The most challenging issue for decision-makers and stakeholders is to properly assess the losses to communities and physical assets under disruption. Floods are among the most frequent and devastating all-natural hazards that cause frequent disruptions in road networks, especially in coastal areas. To properly evaluate the losses due to flood, several parameters are required, among which flood depth is highly important because it governs the models used to evaluate damages (Cian et al., 2018). The considerable number of flood-related deaths and financial losses reported annually across the world drive attention to improved response to flood consequences. For example, Hurricane Irene in 2011 affected over 2,500 miles of roads (Lunderville, 2011). Without a finer-scale, computationally intensive hydrodynamic modeling understanding the actual consequences is impossible. Therefore, to better

prepare coastal communities for future flooding impacts, better countermeasures could be proposed by studying transportation network vulnerability precisely (Chen et al., 2015).

In order to better inform decision-makers of the criticality of transportation links in case of flooding, this study proposes a two-step framework; first, to identify and select the links with risk of inundation and being closed, and second, to identify the critical links in terms of accessibility among those pre-selected links. In particular, the methodology presented in this paper evaluates the network-wide impacts of certain links failure based on accessibility changes.

Flood maps serve as a critical decision-making tool for different end-users, such as infrastructure developers and disaster-response managers. They indicate the flood depth and the probability of flooding in an area. However, these data with high resolution are not available for all coastal areas due to the extremely high data and computational requirements (Sampson et al., 2015). Recent studies leveraged recent advances in remote sensing and hydrology to construct globally high-resolution data (Sampson et al., 2015), though this data still has a high level of uncertainty. Using this data to evaluate the local impact of flooding results in a high level of uncertainty in results.

Taylor and D'Este (2007) define a link as critical if its removal from the network due to disruption results in a significant reduction in network accessibility

score or losing access to particular nodes. Sohn (2006) also defines a link as critical if its failure reduces the network accessibility score. Sadler et al. (2017) focus on traffic volumes and elevation in their definition, roadways with high traffic volumes (AAWDT>75,000) and low elevation(<3m) are considered the most critical roadways. Sullivan et al. (2010) discuss that critical links are not necessarily those with high traffic volumes, but maybe the links with comparatively high traffic volume and few alternative routes.

To evaluate network performance, Scott et al. (2006) propose a network robustness index (NRI) defined as the total change in vehicle travel time in a network that happens when a link is closed. Sohn (2006) assesses network performance using an accessibility index. He uses distance only and distance-traffic volume criteria to measure the accessibility index to evaluate the criticality of highway links in a transportation network under flood damage. Chang and Nojima (2001) measure network coverage and accessibility to assess network performance post-disaster. Sullivan et al. (2010) discuss a segment as critical if its removal causes a relatively notable increase in the overall network travel time compared to any other segment in the network. This metric is not applicable when there are disconnected parts in the network (travel time for a disconnected O-D is infinite). Jenelius et al. (2006) provide two different criticality measures to solve this problem. They propose quantifying unsatisfied demand for the case when removing a link result in dis-connectivity and network-wide total travel time change for the case that link failure does not cause dis-

connectivity but affects the overall performance of the network. While the previous studies have been focused on identifying critical links by closing a link, Nourzad and Pradhan (2014) quantify the criticality of individual links by computing the impact of reducing the link capacity (using different disruption levels) on network connectivity. Another approach to identifying the critical links in a network is using topological measures such as betweenness centrality, that high betweenness centrality in transportation networks means the link is important, and it is on the largest number of the shortest paths in between network nodes (Furno et al., 2019).

This work expands upon the literature in two ways. First, it selects the links with high variability of flood depth around the defined threshold (25 cm). The identical characteristic of these links is that they all experience a flood depth that is around the threshold to make a road impassable. However, it can happen under different confidence limits (CL). This step helps us to remove the links with a huge amount of water (i.e., that are impassable) as well as the links with shallow water (i.e., that are considered passable due to flood depth below the threshold) from the analysis and improve the computational time. Second, it identifies the group of critical links among the preselected links in terms of accessibility to emergency facilities. Using the traditional entire scan method to find the critical roads can take prohibitive amounts of time (Mattsson & Jenelius, 2015). I use a meta-heuristic optimization method, Genetic Algorithm (GA), to identify the critical links in an appropriate time. This method is demonstrated using a realistic case study in Dorchester County, MD.

4.2 Methodology

The work discussed in this section describes the framework for identifying the critical links to improve hydrodynamic modeling. Through this framework, first, a group of candidate links is selected. The network-wide impact of restricted links on residents' accessibility is evaluated to identify the links that affect the accessibility of a large number of residents. An overview of the approach is presented in Figure 4.1. For this work, I consider a 1-year storm surge which is a more frequent storm surge scenario. The data includes flood depth for four different confidence limits for each flood scenario, 50%, 84%, 95%, and 98%. Since the underlying goal of this analysis is to reduce the uncertainty surrounding access during flood, I consider all road segments with flood depth between 20 sand 30 cm under all different confidence limits for further analysis. For this study, I overlay the water depth for storm surge data for the entire region onto the road network to quantify the amount of flood depth on each road segment in the network. I then evaluate the water level for each link that is flooded to identify the candidate links for the next step. Next, to evaluate the impact of a link failure on network vulnerability, I leverage GA analysis to find the impact of restricting a group of links instead of studying one link at a time. This work is conducted in a geospatial computational framework created in the computer language of R.

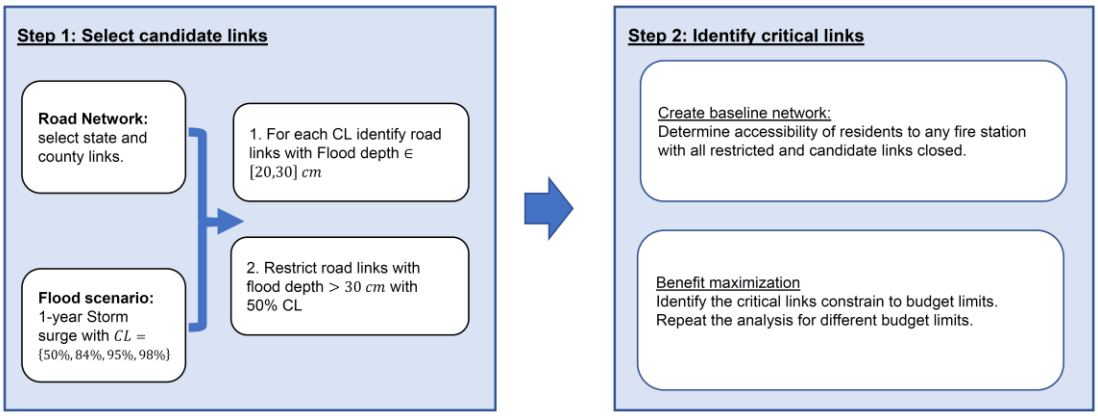

Figure 4.1. Framework

4.2.1 Flood scenarios

I consider the impact of storm surge on road vulnerability in the area. However, this platform is flexible enough to consider alternative or additional sources of flooding. For storm surge, I have multiple probabilistic scenarios. For the purpose of this study, I focus on 1-year storm surge as it is a more frequent scenario. I utilize the probabilistic Coastal Hazards System (CHS) database to model storm surges. This database was built and is maintained by the US Army Engineer Research and Development Center (ERDC) - a research organization within the US Army Corps of Engineers (Coastal Hazards system, 2020). It provides probabilistic storm surge depths with their return periods and confidence limits (50%, 84%, 95%, and 98%) for multiple regions in the United States, such as coastal regions from Maine to Virginia and the coastal regions of Texas and Louisiana and is publicly available and accessible for download. The data is a result of thousands of hydraulic simulation models, and the confidence limits

represent epistemic uncertainty associated with the errors in meteorological and hydrodynamic modeling and astronomical tide variability.

To define which roads flood, this study overlays flood depth raster files with the Digital Elevation Model (DEM) of the study region developed using USGS LiDAR data (Maryland's GIS data catalog, 2019). Then, I use a "bathtub" model, which assumes that all links with elevations less than the surge depth are inundated by water, which is hydrodynamically reasonable in my study area, knowing that it is a large estuary with a shallow slope coastline and numerous streams. This limitation could be addressed in future work. Then, the maximum flood depth for each road segment is computed. In this study, I assume that even if a narrow section of the road has a flood depth above the chosen depth parameter (described below), the road is closed because it is not safe for emergency vehicles. This approach is completed using the "igraph" package in the computing language R.

4.2.2 Road Network

I used the United States Census Bureau (U.S. Census Bureau, 2017) road network data (TIGER/Line Shapefiles) to build the transportation network. This data includes all the federal, state, and local roads in the United States, and it provides information about the road geometry and functionality. I specifically consider household-level mobility to local emergency services, so I assume the parcel to be the origin and the emergency services to be the destination. It is straightforward to consider

additional destinations. For both origins and destinations, I projected them onto the road network at a location that minimizes the distance between the parcel and the road.

Road restriction due to flooding has been addressed in previous studies using a binary variable - flooded or not - which means any road link located in a flooded area is considered close (Sohn 2006; Suarez et al. 2005). Some studies have used a flood depth threshold, whereby travel on the road is restricted once the flood depth is above a prescribed threshold (Fereshtehpour Mohammad et al., 2018; Green et al., 2017; Jotshi et al., 2009, Jasour et al. 2022). This approach is used here. Although speed reduction due to flooded links is also an important factor in transportation, for the purpose of this study, I exclude speed reduction and restrict the roads using a prescribed threshold in the literature.

Many studies have evaluated the "Safe" thresholds for traversing flooded roads while noting that the truly safe threshold is only 0. This threshold for fire trucks is 25 cm, which means they have a tolerance for traversing at most 25 cm of floodwaters depth due to their size, Light, and power (Dawson et al., 2011a; Green et al., 2017; Pregnolato et al., 2017). For the purposes of this study, I focus on emergency vehicles, and I know that there is uncertainty surrounding access during flood due to the lack of local flood depth information, and it's not easy for drivers to identify the exact amount of the flood depth on the road. To identify the inundated road links I focus on a certain bound around the unsafe threshold; the roads with flood depth between 20 and 30 cm are considered as candidate links when considering the accessibility of residents to

emergency services such as fire stations and hospitals; roads with water level less than 20 cm are considered open and passable; roads with flood water greater than 30 cm are considered closed.

Some studies that explore the road criticality in terms of flooding additionally consider demand and traffic congestion changes too (e.g., Feng et al. 2019; Oliveira et al. 2014). This is not included in my analysis because my study region is extremely rural, and congestion is not a significant concern, but accessibility is.

The quickest routing (based on the distance taken to travel between two vertices) is selected to evaluate the accessibility to critical services. Road restrictions contained within the model included flood depth limits to pass the roads. The baseline network is created by restricting all the candidate links explained above and all the links with flood depth above 30 cm under a 1-year storm surge with CL 50%. The quickest routing between all points was then calculated to find the shortest path from each parcel to the nearest fire station under the baseline scenario. The quickest routing between each parcel and the nearest fire station was based on Dijkstra's shortest path algorithm with a network weighted by distance. This algorithm is a widely used approach in solving routing problems and network analysis, and it is also computationally efficient (Sniedovich, 2010). For each parcel, then the closest fire station was chosen to see what the shortest distance from each parcel to its closest fire station is under a 1-year flood scenario.

Then, using GA analysis, I want to identify the group of the links that monitoring simultaneously helps a large number of residents in terms of accessibility to fire stations. In this study, to evaluate the significance of individual network links, I focus on network-wide accessibility, which means I want to identify the links that are likely to experience 20 to 30 cm of floodwater under a 1-year flood scenario, whose a huge number of residents rely on to reach an emergency service. More specifically, the hypothetical disruption of all restricted links due to flood damage is evaluated in terms of accessibility loss and using GA analysis, and I find a group of candidate links whose monitoring can provide more accurate information about the flood depth to a significant number of residents. For example, if a larger group of residents used link one to reach their distance, this means in terms of accessibility, link one is more significant than other links (Sohn 2006). I can extend it to a set of links instead of one link in a network and find the combinations of the links that are considered critical to monitoring.

4.2.3 Genetic Algorithms

I used GA analysis to identify the critical links; GA works with a set of solutions (population) for a given problem. The problem variables are represented as genes in chromosomes in GA; each chromosome consists of a fixed number of genes. In this case, each gene is a candidate link, and 1 means the link is selected to monitor and 0 otherwise.

Initial population: for the purpose of this study, Because I only need to find a small number of the road links to monitor in each model, it is hard to have feasible solutions with a small number of chromosomes in the initial population. Therefore, a large number of initial populations is created randomly, and 100 populations with feasible solutions among them are chosen.

Crossover: this operator is for the mating process (exchange of genes between two chromosomes) that speeds the convergence. It has a crossover rate which is denoted by P_c and shows what portion of the population is used to create new offspring chromosomes. Two parents are chosen from the initial population, and both parents are cut from a random position, and the exchange happens to create two children. In this study, P_c is 0.6 and single-point crossover is selected to create children.

Mutation and immigrants: mutation is another operator to introduce new information. It changes one of the resulted genes, and the overall probability of mutation is called mutation rate and shown by P_m. Immigrants are created the same way as the initial population, and I add them to the generation in each iteration. In this study, P_m= 0.03, and one gene of the chromosome is randomly displaced, then 10 immigrants are added to the new generation each time.

Fitness function: for each chromosome, the satisfaction is measured according to the objective function. The objective function of this study is to maximize the number of residents impacted by monitoring the links. However, due to budget

constraints, I have a limited number of monitors, and for each model, I only want to monitor a specific length of the road links. In this study, I assume each monitor equipment can be used to monitor 50 meters of the link, which means if I have a road with a length of 100 meters, I need two pieces of equipment to monitor.

Selection: the populations with the highest fit among the initial population, the crossover, the mutated, and immigrants are selected and used to generate the next generation.

4.3 Study area

I am applying this study to Dorchester County in Maryland (Figure 4.2). This county, along Maryland's Eastern Shore, is a highly low-lying area and experiences frequent flooding that impacts residents' accessibility and mobility to emergency services. The county is rural with a small urban area in the City of Cambridge in the North. It has several peninsulas and creeks with limited access to the transportation network. As of 2019, the county's population was 31,929. The residents primarily rely on private vehicles. A public transit operator (Delmarva Community Transit) exists in the region, though service is infrequent, and the routes primarily connect the City of Cambridge to towns in adjacent counties.

Almost 60% of the county lies in the 100-year floodplain, which is mostly a tidal floodplain (Cole, 2008). In September 2003, a huge part of the county experienced significant storm surge damage during Tropical Storm Isabel. Since almost half of the

county lies between elevations 2.0 and 4.9, even with minor storm surges that are not related to tropical disturbances, half of the county can experience damage (Cole, 2008). Limited economic and political resources constrain Dorchester County's options for any adaptation strategy (Miller Hesed & Paolisso, 2015), and state and local officials and residents must make challenging decisions regarding what to monitor and what to ignore. While the ethics of this point are debatable, the cost to monitor all roads, the culverts, and ditches that drain them could be highly expensive than the value of the road and the properties that they serve (Cole, 2008), and this happens especially for the roads that serve only a few numbers of residents.

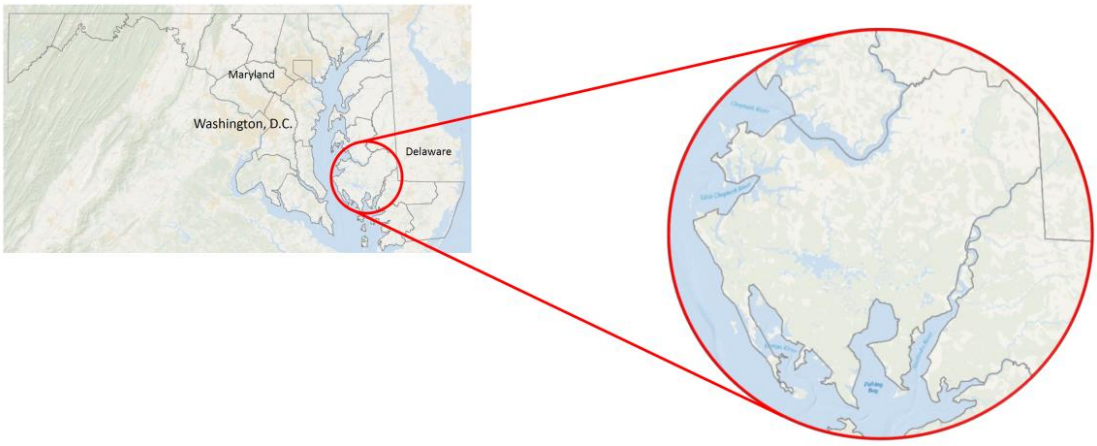

Figure 4.2. Study area.

I include only fire stations as a critical facility in this study to evaluate whether residents at each parcel in Dorchester County are able to access at least one fire station using a road network. As a result of road inundation, there can be no route to any fire station, which means the parcel loses its accessibility to any fire station in the county.

4.4 Result

The results are organized as follows: First, I show the results for the inundated roads under a 1-year storm surge scenario with different confidence limits. This identifies the candidate links for further analysis and forms the baseline model. I then present the results of the road criticality analysis and compare the effect of different budget limits on optimal solutions.

4.4.1 Identify candidate links

Figure 4.3. shows the road network in Dorchester County, the links with flood depth above 30 cm are defined by red and are considered totally closed and impassable under a 1-year storm surge with a confidence limit of 50% (it includes 88.8 km of the roads). The candidate roads are shown in blue in Figure 4.3. Those are the roads that experience flood depth between 20 to 30 cm with a 1-year storm surge flooding with different confidence limits (50%, 84%. 95%, and 98%) with a total length of 117 km. To decrease the number of the roads from consideration, as well as computational time, I focus on main roads only (road types M and S in data) and remove the private roads from the analysis. The map in Figure 4.3 shows all the roads I studied. If I consider all candidate links and flooded links above 30 cm to be closed, it causes 3,921 parcels to lose their access to any fire station. As discussed above, the goal of this study is to define the links that are critical in terms of providing access to fire stations for more residents to maximize information by monitoring them. The network with all inundated links here is considered the baseline for the next section, and I evaluate the benefits of

monitoring different links (by assuming the selected links are passable) for gathering more accurate flood depth data among the candidate links in this network.

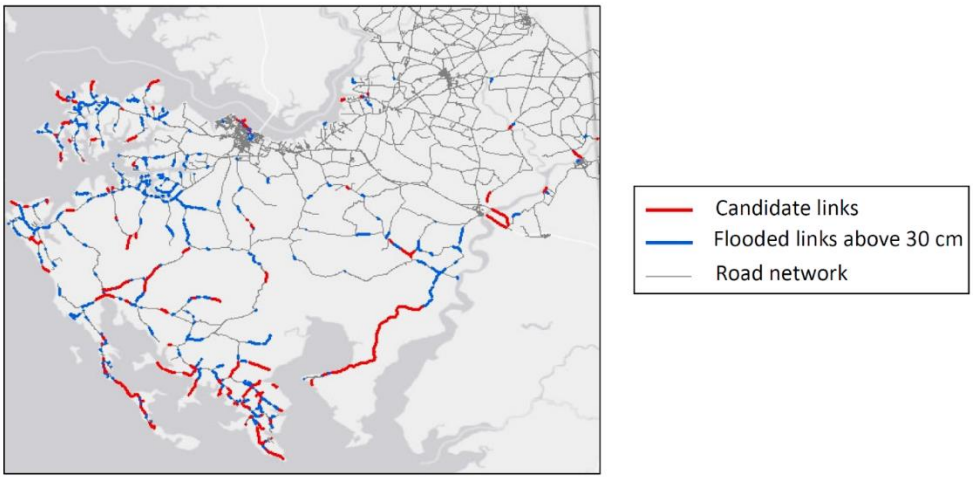

Figure 4.3. Inundated roads under a 1-year storm surge and CL 50% with flood depth above 30 cm (blue) and inundated links under a 1-year storm surge with CL 50%, 84%, 95%, and 98% that experience flood depth between 20 to 30 cm (red).

4.4.2 Benefit maximization

I implemented one single optimization model based on accessibility maximization; the objective is to maximize the number of residents who benefit from closer monitoring of actual hydraulic conditions using the installation of flood monitor equipment in the candidate link. Multiple budget constraints are considered to identify different critical roads according to a different number of flood monitoring equipment. The results could help us to identify the critical links in road network in terms of accessibility to emergency services for further monitoring and gathering local level

flood data. Hence reduce the uncertainty surrounding access to emergency services. The plot in Figure 4.3 shows the number of parcels that benefit from the accurate flood data for the installation of 1 to 10 pieces of monitoring equipment. As mentioned above, I assumed one monitoring equipment could gather data from 50 m of the road, and with more than one piece of equipment, I can gather more accurate data from different links or even one link that has multiple flooded sections or one inundated section that is above 50 m. The first column in Table 4.1 shows the number of monitoring equipment, and columns 2 to 12 demonstrate the candidate links that are selected as the critical links in one or more optimization models (number 1,2, or 3 under each column demonstrate that the how many segments of the link is selected, and 0 means any segment from that link is not selected). For example, two segments of the link L2 are selected when I have two or more pieces of equipment and gathering more accurate flood data from this link benefits 151 parcels, which you can find in under two pieces of equipment. Table 4.1 explains that increasing the budget benefits more parcels. For scenarios with 2 to 8 pieces of equipment, the previous critical links stay in the combinations of selected links and adding to the budget adds a new link to the previous list of selected links. With 9 and 10 pieces of equipment, two new links are selected, and some old links are removed from the list, which demonstrates that increasing the budget does not always add new links to the previously selected links. When the objective is to benefit more parcels, it is possible to spend all of the budgets on one road that can benefit a huge number of parcels instead of different roads that only benefit a small number of parcels.

Figure 4.4 shows the spatial distribution of parcels benefits ten pieces of monitoring equipment. These parcels are mostly located in the middle and north parts of the County because the budget is small, and the model can only focus on the links in high density areas with a small, inundated segment to benefit a larger number of parcels. To benefit the parcels in peninsulas and southwest areas I need to increase the budget.

Table 4.1. Critical link segments selected under each budget scenario and optimal results for the number of parcels benefit the corresponding link monitoring.

	Critical Links											
Numer of equipment	L1	L2	L3	L4	L5	L6	L7	L8	L9	L10	L11	Number of parcels benefit
1	**1**	0	0	0	0	0	0	0	0	0	0	17
2	0	**2**	0	0	0	0	0	0	0	0	0	151
3	**1**	**2**	0	0	0	0	0	0	0	0	0	168
4	**1**	**2**	**1**	0	0	0	0	0	0	0	0	181
5	**1**	**2**	**1**	**1**	0	0	0	0	0	0	0	191
6	**1**	**2**	**1**	**1**	**1**	0	0	0	0	0	0	198
7	**1**	**2**	**1**	**1**	**1**	**1**	0	0	0	0	0	204
8	**1**	**2**	**1**	**1**	**1**	**1**	**1**	0	0	0	0	209
9	**1**	**2**	0	0	0	**1**	0	**2**	**3**	0	0	210
10	**1**	**2**	**1**	**1**	0	0	0	0	0	**2**	**3**	212

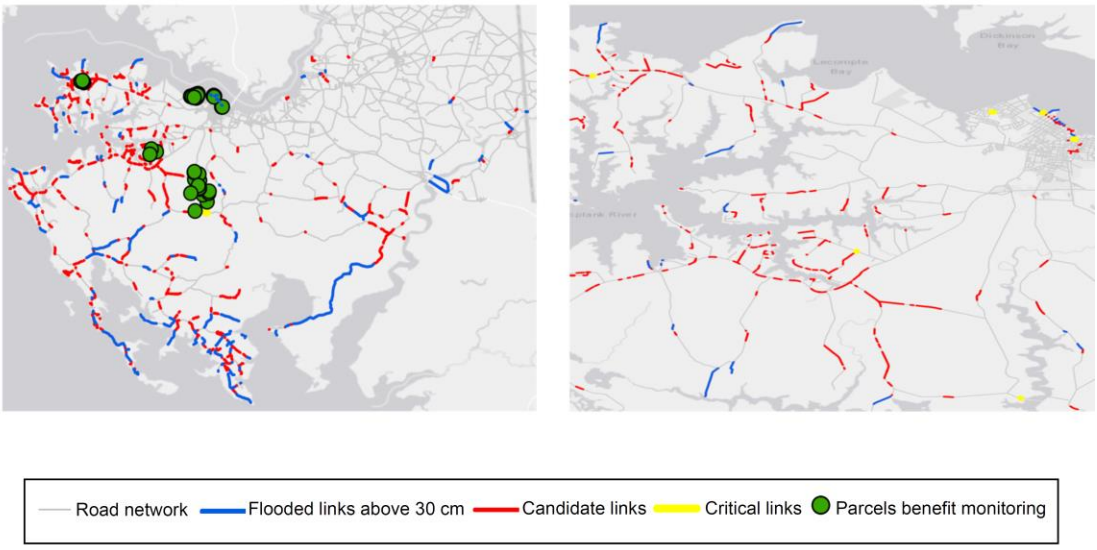

Figure 4.4. Spatial distribution of parcels benefits candidate links monitoring with 10 pieces of monitoring equipment (right plot) and the zoomed map that shows the spatial distribution of critical links in yellow (right plot).

If policy and decision-makers have access to more accurate flood data, they can better evaluate the network-wide impacts of certain links failure based on accessibility changes and leverage the maximum information about the consequences of floods to better be prepared for future flood events.

4.5 Conclusion

Flooding is among the most destructive, widespread, and frequent natural hazards causing extensive damage to infrastructure and communities. The frequency and severity of flooding are increasing due to climate change. As a result, the techniques of monitoring and gathering flood data to improve flood maps are also increasing. However, it is a costly process to maximize flood data information at a local level with closer monitoring for all road segments.

Therefore, in this chapter I investigate where the impacts of floods in a road network could be most consequential and causes more parcel-level accessibility loss to the fire stations. I define these links as critical links. Using the case study of Dorchester County, Maryland, I identify the critical links for different budget limits to monitor closely by evaluating how many parcels rely on them to reach any fire station.

There are some limitations of this work which could be addressed in the future. First, I only focused on accessibility loss as a consequence of floods in a road network, however, flood also impacts travel time. Although in rural regions congestion is not that much of problem but the increase in travel time can be significant due to inundated road links and could be studied if the traffic data gets available in future. While, this study only focuses on 1-year flood scenario, to have more comprehensive understanding of the critical links in the area for improving flood information other flooding scenarios could be studied too. Moreover, this study only focuses on identifying the road links that if monitored, maximize information in terms of access to fire stations but does not study the intersect of flood uncertainties and the road criticality, which can be studied in future.

5 Chapter 5: Conclusion

This dissertation investigates how sea-level rise and coastal flooding may impact parcel-level accessibility in rural areas and what road protection strategies can maximize transportation equity by improving the accessibility of impacted parcels for different groups in the area. Finally, I used the transportation network and accessibility analysis to improve the flood data by identifying the roads that will be flooded and are also critical in terms of providing access to a large number of parcels. This investigation is done under three research questions:

Under the first research question, I evaluated the impact of sea-level rise in a low-lying rural area in terms of accessibility to critical facilities. Using Dorchester County, Maryland, as a suitable case study, I showed the importance of parcel-level accessibility assessment under different sea-level rise scenarios. Moreover, investigating the time that parcels lose their accessibility and also the time that parcels inundation happens provides great information for policy and decision-makers to better allocate the limited budgets on mitigation and adaptation strategies.

Under the second research question, I investigated how transportation equity changes when storm surge flooding impacts parcel-level accessibility and proposed a metaheuristic optimization model to evaluate the trade-offs between investment in road protection strategies and equity improvements under various objectives. Using the case study of Dorchester County, MD, I explained that all the accessibility-based indicators improve with road protection, although they change on different scales, and not all of them maintain accessibility for a large number of residents. Most importantly,

improving balanced accessibility in rural areas may not provide access for a large number of people due to the sparse road network and a large budget to protect longer roads to maintain accessibility.

Under the last research question, I used transportation network and accessibility analysis to improve the accuracy of flood maps in the area. Understanding which roads with risk of inundation are critical in term of accessibility to emergency services help us to improve the data collection equipment and models for those specific roads and provide better localized information about the potential flooding and inform motorists and emergency managers with trip-planning. Using Dorchester County as a case study, I explored the critical roads with the risk of flooding under a 1-year storm surge and different budget limits. The results indicate that having more accurate data about a group of the roads could serve more numbers of residents than focusing solely on individual links independently.

There are some significant limitations of this dissertation that could be addressed in the future. In the first study bathtub inundation model was used to evaluate the impact of sea-level rise on roads, which lacks accuracy at a finer level of resolution. In the second study, I assumed all the block groups have the same weight, which is not always true, and policymakers may assign different weights to different zones in reality. Additionally, in none of the studies, the congestion and travel time have been considered; while congestion tends to not be a problem for the study area, having a large number of inundated roads could force higher traffic volume onto the routes that are not designed for them.

While I mentioned the importance of transportation equity in the first study, I have not conducted it when evaluating access. Future work could evaluate the distribution of burdens on different groups of the community within the region.

Finally, this dissertation demonstrates the need for decision-makers and policymakers in any region to reach some level of consensus about flood scenarios and exceedance probability for which possible future is planned when deciding among adaptation strategies. The amount of risk the communities are able and willing to assume defines this consensus. Failure to build a general agreement results in piecemeal adaptation strategies in different areas that are collectively inefficient for the community and may even be harmful due to their interconnectedness (Papakonstantinou et al., 2019).

6 Chapter 6: Appendix; Climate change and agriculture: Combining publicly available data and machine learning approaches to predict corn yield in State of Maryland

6.1 Abstract

Evaluations of the impacts of climate change on agriculture require accurate yield response models. Typically, yield prediction models use field-collected data and fixed time intervals for weather variables. In this study, I attempt to analyze and compare different machine learning models, as well as parametric and non-parametric methods, to predict corn yield. Corn yield data was collected from the U.S. census bureau for years between1950 and 2012, and the meteorological data was obtained from the National Oceanic and Atmospheric Administration (NOAA-NCDC, 2018) for the corresponding year in the state of Maryland. Different growing stages, different spatial grouping, and different predictive modeling give us 60 various models to compare. I assessed the out-of-sample predictive ability of the candidate models using *K*-fold cross-validation to choose the best model based on R^2 (e.g., for Allegany County, the best model is SVM predictive model using the four stages and county-level data with $RMSE$, MAE, and R^2 are 0.16, 0.14, and 0.75, respectively). Results explain that spatial grouping and mostly clustering based on precipitation improves the accuracy of the predictions in most of the counties.

Introduction

Climate change is causing worldwide impacts on water resources, food security, and the production of agricultural products such as maize (Arora, 2019; Chami &

Moujabber, 2016; Karimi et al., 2018; Malek et al., 2018). If the current situation of climate change continues, then by the end of the century, the production of major cereal crops such as maize yields will experience a significant decline (20-45%) (FAO, 2016). Recent research has focused specifically on the impact of climatic variables (e.g., precipitation) on crop production. The rationale is that by understanding the relationship between climatic variables and production, researchers and farmers can better forecast the impact of climate change on future yields. This information can support long-term adaptation planning in agricultural and related sectors. Further, computationally efficient models that leverage readily available public information can help planners understand how climate is likely to change infrastructure needs in agriculture-dependent regions.

The first step in understanding the impact of climate change on agricultural production is understanding the relationship between historic climate variables and production. The predictive capabilities of a model that explains this historical relationship can then be validated to assess its ability to forecast the impact of possible future changes in climatic variables on agricultural yield.

The bulk of existing literature focusing on the relationship between climatic variables and crop yields relies on ordinary least-squared (OLS) regression to perform the analysis. While OLS regression is a powerful tool with highly interpretable results, issues exist that limit the insights and forecasting capabilities under future climate conditions. First, OLS regression makes an assumption that the response variable (i.e., production) is a monotonic and linear function of the predictor variable. This is unlikely

to be true. For example, Huong et al. (2019) examined the effect of temperature changes and rainfall on farming in Northwest Vietnam. Their study found a non-linear relationship between weather variables and farmers' revenue. Second, these OLS regression models are generally assessed using measures of performance tied to the assessment of fit (i.e., the ability of models to capture variations associated with prior observations) rather than "out of sample" predictive capability (i.e., the ability to forecast the values of the response variable under "unseen" values of the predictor). That is, they tend to focus on establishing a relationship that reflects past data, but not whether this relationship is robust under conditions that differ from the past. Newer statistical modeling techniques offer opportunities to model more complex mathematical relationships that may or may not be readily explained parametrically. The model validation approaches typically used in conjunction with these newer techniques often focus specifically on assessing "out of sample" predictive capability rather than on measures of fit.

The contribution of this paper is two-fold. First, this paper leverages recent advances in machine learning as well as parametric and non-parametric statistical modeling to develop predictive models of crop yield under climate forcing for the State of Maryland using readily available public data. Second, in addition to presenting state-specific results, this paper outlines a general framework for model development and validation to support long-term infrastructure planning in geographic regions for which agriculture represents a significant source of economic activity and is a driver of infrastructure needs.

6.2 Context

Agriculture plays a critical role in the economy of the state of Maryland. Corn for grain is among the state of Maryland's top five agricultural products. In 2017 56,940,000 bushels of corn had been harvested from 390,000 acres of land. Corn was the highest value crop in the state. Because of corn's economic importance, I seek to determine the impacts of climate change on corn yield to develop possible adaptation strategies.

To date, there is no established predictive model for forecasting regional yields for the State of Maryland using climatological and hydrometeorology factors. That is, there are no studies that go beyond building an explanatory relationship between yield and climate factors to a paradigm where the model is fully validated based on its predictive accuracy on out-of-sample data. I hypothesize that tree-based models such as random forests or more complex data-miners such as support vector machines work better than linear regression to predict the corn yield.

Because data limitations present challenges in developing the proposed predictive models, this paper focuses on boosting the predictions of corn yield using models developed at different spatial and temporal scales. Using historical county-level data from across Maryland, I develop and validate multiple types of parametric and non-parametric models that allow for relationships between predictor and response variables to be non-linear and non-monotonic. The value of these models is that they provide insight into the factors that are most important in predicting yield and provide the factor's marginal influence over its entire domain. In assessing model performance,

my focus is not on model fit (e.g., "R^2"), which provides no information on a model's predictive abilities but instead on how accurate the model is at forecasting out-of-sample data (e.g., root mean square error).

Specifically, this study demonstrates how using different machine learning strategies at varying spatial and temporal scales can improve prediction when available data are limited. While this study focuses on Maryland, the overall approach demonstrates how the development of models at different spatial and temporal scales can lead to improvements in predictive modeling abilities.

6.3 Review of Existing Studies

Data-driven methods are empirical methods that do not require in-depth knowledge about the physical mechanisms that produce the data. These methods have frequently been applied for several decades to predict the yield prediction in agriculture using classical statistics such as linear regression (Dixon et al., 1994). For example, Schlenker and Roberts (2006) used OLS regression to examine the relationship between temperature and corn yield. They found a non-linear behavior for corn yield, which varies with temperature changes. Their result shows yield increases with temperature in the moderate range but decreases once the temperature exceeds 86^{o} F. Studies have also sought to improve model performance by leveraging a range of data sources. For example, remote sensing data such as climate factors, MODIS (Moderate Resolution Imaging Spectroradiometer), and NDVI (Normalized Difference Vegetation Index) have been widely used in the estimation of crop yields by adopting

statistical methods such as regression model (Das et al., 2020; Drummond et al., 2003; González Sánchez et al., 2014; Matsumura et al., 2015; Schlenker & Roberts, 2006; Wang et al., 2020). Expanding beyond standard regression techniques, machine learning methods have been used to estimate crop yield in the last years (Gandhi et al., 2016; Jaikla et al., 2008; Roel & Plant, 2004; Nari & Yang-Won, 2016). Table 4.1 provides a summary of existing research that has leveraged machine-learning and conventional statistical modeling methods to predict agricultural yields.

A number of studies have emphasized the potential modeling improvements that can be achieved through the application of machine-learning methods. Focusing specifically on the State of Maryland (which is the focus of this study), Kaul et al. (2005) studied the effectiveness of Artificial Neural Network (ANN) models in predicting Maryland corn and soybean yields for typical climatic conditions. They compared the prediction capability of their models at state, regional, and local levels. They used available rainfall data and nine different soil types for five locations in Maryland and created ANN and multiple regression models with various model inputs at the state and few regionals and local levels. Their comparison between ANN and multiple linear regression models indicates that ANN models consistently produce more accurate predictions than regression models, and local level models predicted yield more accurately than the region and state models for both corn and soybean. In this work, I consider several alternate machine-learning modeling approaches and systematically consider several options of spatial and temporal aggregation of data

across the State of Maryland. I leverage the publicly available data to study all counties in Maryland instead of focusing on a few locations with available data.

More broadly, Nari and Yang-Won (2016) used machine learning methods to estimate corn yield in Iowa. They applied Support Vector Machine (SVM), Random Forest (R.F.), Extremely Randomized Trees (ERT), and Deep Learning (DL) technique. Their analysis indicates that the DL technique provides more stable results. Leng and Hall (2020) assessed the effect of climate change (global warming) on corn yield in the United States using machine learning methods, regression models, and process-based models. They found that machine learning models are able to explain 93% of observed yield variability; however, regression models and process-based models only explain 51% and 42% of variability, respectively.

The aforementioned studies focused on the assessment of the fit of models to past data. However, validation of the model on an "unseen" data set (typically referred to as a "test set" or "hold outset") is important when developing a predictive model. This test (holdout) data set is a set of data not used for training the model. It is reserved (held out) for testing predictive accuracy, i.e., the model's ability to forecast future or unseen data.

Wang et al. (2020) compared the performance of linear models with machine learning methods such as SVM, R.F., and DNN on wheat yield with climate, soil data, and vegetable indices at the county-level for the counties with available data in the conterminous United States. They trained the models on a dataset from 2008 to 2016 and evaluated the dataset from 2017 and 2018 using metrics such as $RMSE$, MAE, R^2.

Their results indicate machine learning methods perform better than linear regression models. Gonzalez-Sanchez et al. (2014) compared the capabilities of linear regression and ML techniques for predicting the crop yield in ten crop datasets using metrics such as $RMSE$, MAE, $RRSE$, and R^2. Nari et al. (2016) used one-year-out cross-validation to examine the accuracy of corn yield estimation using machine learning methods. Schwalbert et al. (2006) used one-year-out cross-validation and MAE, $RMSE$, and MSE to assess the accuracy of their model's output.

The use of machine learning methods described above for yield prediction improves the accuracy of the yield prediction relative to more conventional approaches. However, most of the models have sought to improve model performance through consideration of additional predictor variables. For example, several studies have used soil data obtained from laboratory analyses or field collection (Drummond et al., 2003; Pantazi et al., 2016). However, the creation and collection of such data are time-consuming and expensive. Existing studies have not attempted to utilize the spatial and temporal grouping techniques to "boost" the accuracy of predictive models that leverage only limited publicly available data. The aim of this study is to overcome the limitations of the above-mentioned linear and non-linear approaches for predicting the yield by integrating the spatial and temporal grouping and validating the range of candidate predictive models (as well as a "mean-only" null model) using *K*-fold validation.

Table 6.1. A selection of articles in agriculture research that used machine learning and conventional statistical modeling methods.

Article	Crop type	Location	Modeling technique	X variables
Drummond et al. (2003)	Grain	Three fields near Centralia in central Missouri	Stepwise multiple linear regression and neural network models	Soil properties and climatological data
Roel and Plant (2004)	Grain	Two rice fields near Marysville, CA	Cluster analysis, classification, and regression trees (CART) methods	Soil data
Kaul et al. (2005)	Corn and soybean	Maryland	ANN and multiple linear regression models	Climate conditions
Schlenker and Roberts (2006)	Corn	2000 USA counties	OLS regression	Temperature
Jaikla et al. (2008)	Rice	Thailand	Support vector regression method (SVR)	Day from planting to harvesting, temperature, and precipitation
Schlenker and Roberts (2006)	Corn, wheat, soybean, and cotton	USA Counties east of the 100-degree meridian	Regression analysis	Temperature and precipitation
Gonzalez-Sanchez et al. (2014)	Corn	Mexico	Linear regression and ML techniques (M5-Prime regression trees, N.N., Support vector regression, and k-nearest neighbor method)	Planting area, irrigation water depth, cumulative rainfall, cumulative global solar radiation, temperatures, and duration of the season-duration cultivar
Matsumura et al.(2015)	Maize yield	Jilin province, China	Multiple linear regression, non-linear ANN models	Climate conditions (precipitation) and fertilizer
Pantazi et al. (2016)	Wheat	A field at Duck End Farm, UK	Counter-propagation artificial neural network, XY-fused networks, and supervised Kohonen networks	Online multi-layer soil data
Gandhi et al. (2016)	Rice	27 districts of Maharashtra, India	SVM, the sequential minimal optimization (SMO) classifier algorithm using the WEKA tool.	Precipitation, minimum, maximum, average temperature, reference crop evapotranspiration, and area
Mokarram and Bijanzadeh (2016)	Barley	Online available data from	Multiple linear regression, ANN including multi-layer	Water E.C., irrigation regime, Nitrogen applied,

		different literatures	perceptron (MLP) and radial basis function (RBF)	Phosphorous applied, Potassium applied, plant density, rainfall amount, …
Nari and Yang-Won (2016)	Corn	Iowa	SVM, R.F., Extremely Randomized Trees (ERT), and deep learning (DL)	Remote sensing climate data
Andrade et al. (2018)	Corn	Near Bushland, TX	Artificial Neural Network	Data from the soil, water, plant, weather using (ISCCADAS).
Cai et al. (2019)	Wheat	Australia	Regression method (LASSO as a benchmark) and machine learning methods (SVM, R.F., neural network)	Satellite data (vegetation index, solar-induced chlorophyll fluorescence as metrics to approximate crop productivity)
Das et al. (2020)	Coconut	Fourteen districts of the West coast of India.	Different linear models such as stepwise multiple linear regression (SMLR), PCA-SMLR, least absolute shrinkage, and selection operator (LASSO), and elastic net (ELNET) with non-linear models, namely ANN and PCA-ANN	Weather indices using monthly cumulative rainfall, the monthly average value for maximum and minimum temperature, relative humidity, wind speed, and solar radiation
de Oliveira and Antunes Rodrigues (2020)	Sugarcane	Brazil	Mechanistic, regression, machine learning	Daily minimum, maximum, and medium temperature. Pest and inspection data and fertilizers and agrochemicals.
Leng and Hall (2020)	Maize yield	The U.S.	Process-based models, regression model, and a machine learning algorithm	Climate data
Schwalbert et al. (2006)	Soybean	Brazil	Multivariate OLS linear regression, random forest, and Long-short term memory (LSTM) neural network	Satellite imagery and weather data
Wang et al. (2020)	Wheat	Conterminous United States	Ordinary least square (OLS), Least absolute shrinkage and selection operator (LASSO), SVM, R.F., Adaptive	Climate data, Soil data, vegetation indices (VIs)

			Boosting (AdaBoost), and deep neural network (DNN).	
Wolanin et al. (2020)	Wheat	Indian Wheat Belt	Deep neural network	Multivariate time series of vegetation variables and meteorological data such as minimum, maximum, average temperature, precipitation, and day-length.

6.4 Data Collection and Processing

In the current study, multiple machine-learning and statistical approaches are used to develop predictive models of corn yield for counties in the State of Maryland. Specifically, I consider a mean-only (null) model, a linear regression model, and three machine learning models (i.e., random forest, bagged CART, support vector machine). These models are described further in Section 6.5.3. For the implementation of this approach, crop yield and meteorological (e.g., temperature and precipitation) data for each county were gathered from online publicly available sources. The state of Maryland has twenty-three counties with agricultural data available. Baltimore city is not among those counties and is thus excluded from the analysis. Additional details regarding data collection and processing are provided in Sections 6.4.1.

6.4.1 Crop Yield Data Collection and Processing

The response variable (i.e., the variable to be predicted) is the area-normalized corn yield for all counties of the State of Maryland. Corn has two different usages in

the state: (1) corn for grain and (2) corn for silage or green chop. In this study, I focus on corn for grain.

We collected agricultural census data for the harvested product and the harvested land area from the United States Department of Agriculture (USDA, 2018) and used it to compute the area-normalized corn yield in county i and year t ($Y_{i,t}$):

$$Y_{i,t} = \frac{P_{i,t}}{A_{i,t}}, \quad i = 1, \dots, N_C;\ t = 1, \dots, N_t \tag{1}$$

Where $P_{i,t}$ and $A_{i,t}$ are the total harvested product and the harvested area of the county i in year t, respectively.

USDA agriculture census data are available every five years. To account for general agricultural trends over time (e.g., due to changes in technology), the state-specific data have been normalized using the corn yield for the U.S. The area-normalized corn yield for county i in year t was divided by the area normalized corn yield for the U.S. in the corresponding year:

$$Y_{i,t}^{[N]} = \frac{Y_{i,t}}{Y_{US,t}} = \frac{P_{i,t} \times A_{US,t}}{P_{US,t} \times A_{i,t}} \tag{2}$$

Where $P_{US,t}$ and $A_{US,t}$ are the total harvested product and the harvested area of the U.S. year t.

6.4.2 Climate Data Collection and Processing

The explanatory variables are the meteorological variables that affect the corn yield, which may change over time due to climate change. Data considered in this study include daily minimum and maximum temperatures and daily precipitation in the years

for which corn data is available between the years 1950 and 2012. These data were obtained from the National Oceanic and Atmospheric Administration (NOAA-NCDC, 2018) for the 402 stations in the state of Maryland shown in.

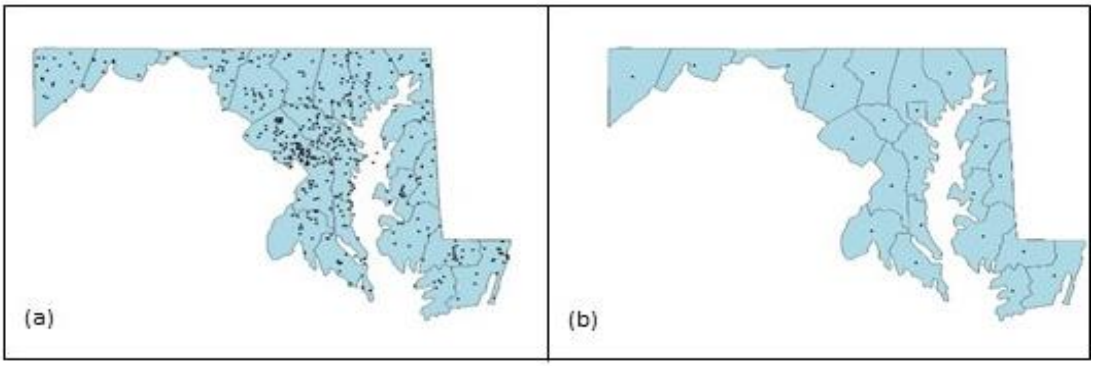

Figure 6.1. (a) Geographical location of weather stations (b) the geocentroid of each county in Maryland.

Consistent with the existing state of practice, I processed "raw" climate data in several ways to produce indices that better reflect the physical relationship between weather and plant growth. In general, the temperature is considered the most important factor controlling the rate of plant development, although other factors such as water and light availability are also important. There are established "bands" of temperature associated with growth, and crops can experience shock below and above those thresholds. For corn, this temperature band is between 50°F and 86°F (NDAWN center, 2018).

A useful temperature index to estimate plant growth is growing degree days (GDD), which is calculated using daily maximum and minimum air temperature. In this work, I calculate daily corn growing degree days for day d in county i in year t ($GDD_{i,t}$) as:

$$GDD_{i,t}^{[d]} = \begin{cases} 50, T_{min,i,t}^{[d]} \leq 50 \\ \left[\left(\frac{T_{max,i,t}^{[d]} + T_{min,i,t}^{[d]}}{2}\right) - T_{Base}\right], 50 < T_{max,i,t}, T_{min,i,t} < 86 \\ 86, T_{max,i,t}^{[d]} \geq 86 \end{cases} \quad (3)$$

Where $T_{max,i,t}^{[d]}$ and $T_{min,i,t}^{[d]}$ are the maximum and minimum temperature on day d for county i in year t. For corn, the base temperature (T_{Base}) is 50 degree-Fahrenheit. (NDAWN center, 2018).

Building off the above, accumulated daily growing degree days (AGDD) through the day d^* of the growing season can be calculated beginning with the day after the specified planting date and continuing until the specified ending date. Specifically, A$GDD_{i,t}^{[d^*]}$ for county i and year, t is computed as the sum of daily $GDD_{i,t}^{[d]}$ from the first post-planting day (i.e., $d = 1$) to the specified end day ($d = d^*$):

$$AGDD_{i,t}^{[d^*]} = \sum_{d=1}^{d^*} GDD_{i,t}^{[d]} \quad (4)$$

Where: $GDD_{i,t}^{[d]}$ is computed as in equation 3.

In this study, the planting time (i.e., day $d = 0$) was selected as 14 days after the last frost in the spring for each county (Boeckmann, 2020). The threshold for frost is 30 degree-Fahrenheit.

As an example, Figure 6.2 shows the time series plot for daily $GDD_{i,t}^{[d]}$ for Anne Arundel County in 2012. (top) shows the accumulated GDD for Anne Arundel

County. Based on the last frost in the spring, the planting date for Anne Arundel in 2012 is selected as March 25.

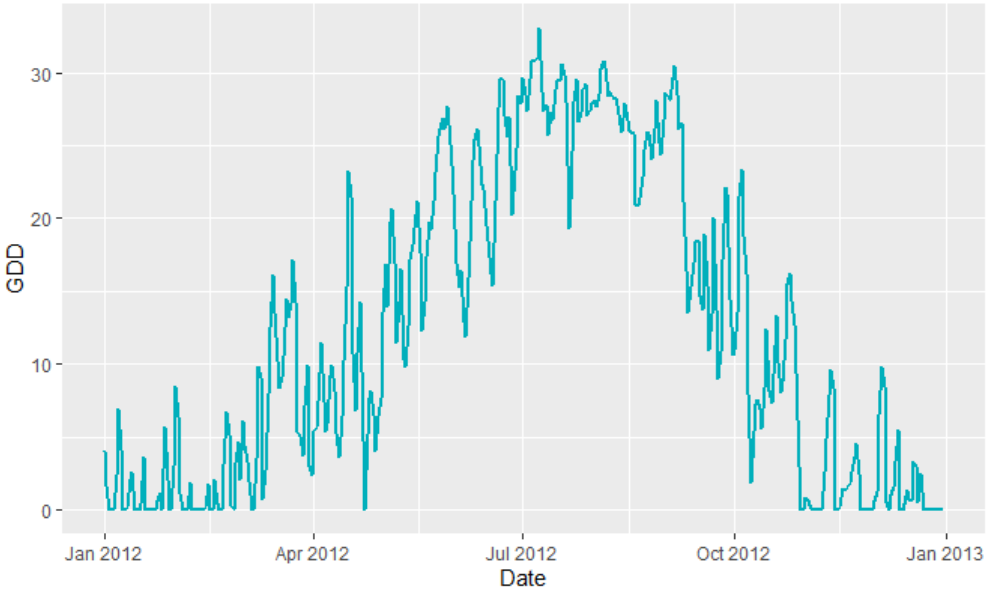

Figure 6.2. Daily growing degree days for Anne Arundel County in 2012.

We likewise "processed" precipitation data to generate accumulated daily precipitation time-series using daily precipitation data for each county:

$$PRC_{i,t}^{[d^*]} = \sum_{d=1}^{d^*} prc_{i,t}^{[d]} \tag{5}$$

Where $PRC_{i,t}^{[d^*]}$ is the sum of daily $prc_{i,t}^{[d]}$ (i.e., precipitation on day d) for county i in year t from planting day to day d^*. (bottom) shows the accumulated precipitation for Anne Arundel County in 2012. The starting point to accumulate the precipitation is the planting date, which was March 25 for Anne Arundel County in 2012.

6.5 Model Development

The objective of this study is to build predictive models for estimating corn yields under varying climatic conditions using conventional modeling approaches and supervised (machine) learning methods. The response variable (i.e., the variable to be predicted) is the area-normalized corn yield for each county in the State of Maryland. The explanatory variables are meteorological variables that affect the corn yield and which may change over time due to climate change. The predictive model takes the following form:

$$\hat{Y}_i^{[N]} = f\left(\mathbf{X}_{M_i}\right), i = 1, \dots, N_C \quad (6)$$

Where: $\hat{Y}_{i,t}^{[N]}$ is a predicted value of normalized corn yield for county i, and $\mathbf{X}_{M_i}$ is a vector of explanatory variables related to meteorological variables for county i. In this study, explanatory meteorological variables include the number of days with a temperature below 50°F, the number of days with a temperature above 86°F, and accumulated precipitation.

Figure 6.3 shows a flow chart of the overall process I used for building $N_{model} = 60$ candidate predictive models with a range of modeling assumptions. The logic tree in Figure 6.4 summarizes the combinations of candidate modeling assumptions I considered. These modeling assumptions relate to four key areas, which correspond to the "branching points" of the logic tree shown in Figure 6.4:

- The number of growing stages is used to temporally partition the data in each year (1-stage, 4-stage, and 8-stage).
- The strategy for aggregating data spatially (state-level, county-level, and clustered).
- The clustering approach is used (applicable only to spatial aggregation using clustering).
- The supervised learning approach was used to build the predictive model (linear regression, bagging, random forest, and support vector regression).

Regardless of the specific model assumptions, the overall process for model development follows Figure 6.3. The model development process begins with the collection and processing of county-level yield and climate data, as described previously in Section 6.4. Then, for each candidate model $i = 1, \ldots N_{model}$, the following key steps were executed:

Data was temporally partitioned according to the number of growing stages defined for the specific candidate model i, and all necessary prediction and response parameters were created. Additional information regarding growing stages and the creation of prediction and response variables are provided in Section 6.4.2.

Data were randomly partitioned into model training and testing sets to support model cross-validation. The cross-validation approach uses holdout sets containing a single year of data across all counties, as described in Section 6.5.2.

County-level data were spatially aggregated according to the spatial resolution associated with model i. If clustering is used for spatial aggregation, a clustering model is developed using training data and applied to testing data. Additional information regarding spatial grouping and the development of clustering models is provided in Section 0.

Training data are used to train and optimize supervised learning models. Section 6.5.36.5.3 provides additional information regarding candidate models.

The trained, supervised learning model is applied to the testing (holdout) data to create out-of-sample predictions, and performance is assessed using several measures. Performance measures and results are presented in Section 6.6

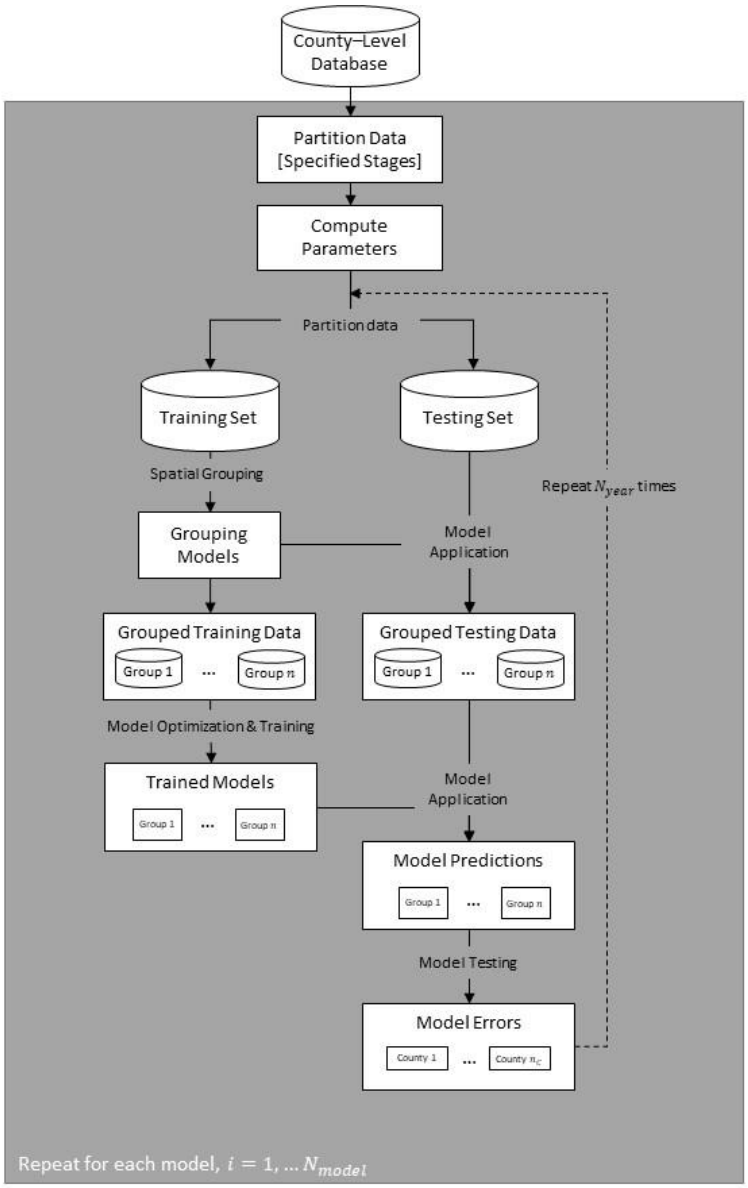

Figure 6.3. The process of predictive modeling

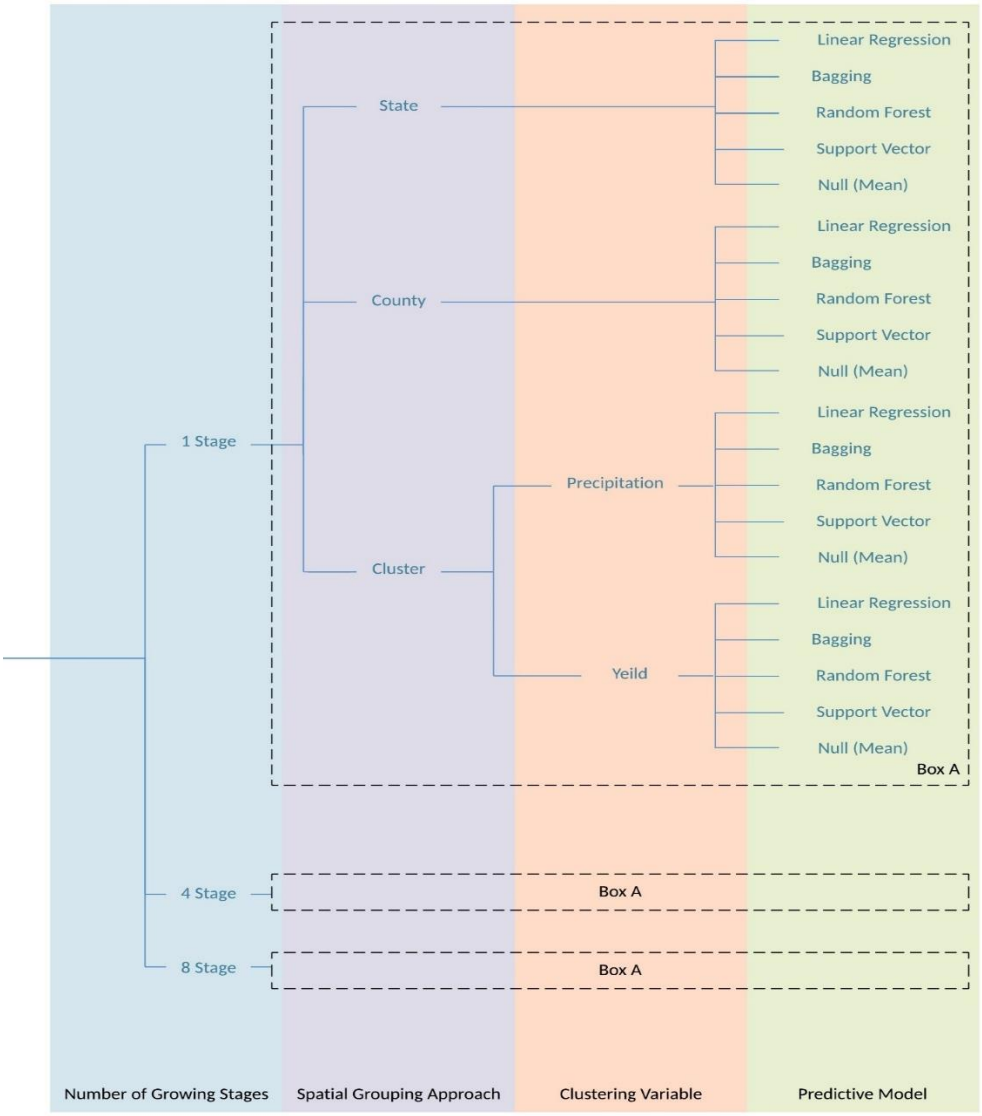

Figure 6.4. The Logic tree of creating predictive models

6.5.1 Temporal Grouping and Parameter Definition

There are four main growth stages for corn: emergence and stand establishment; rapid growth and dry matter accumulation; pollination; and grain fill (Dekalb, 2020). To reach a certain stage of maturity, a corn plant generally requires a

certain number of growing degree days. Extremely cold or hot temperatures in each stage may cause a yield reduction. However, the sensitivity of corn to moisture and heat stress differs by stage, with plants being more sensitive in the early and late stages.

In this study, I selected predictors based on the four primary stages of corn growth. Table 6.2 explains these stages. The first column of Table 6.2 identifies the four primary stages of corn growth and the second column shows a conventional notation used to denote a more-refined breakdown of corn growing substages. The third column identifies the AGDD threshold for each of the substages (Nafziger, 2009). To illustrate the four primary growth stages, the vertical red lines in separate the four primary growth stages for Anne Arundel County in 2012 based on when the computed AGDD reaches the thresholds identified in Table 6.2 (i.e., AGDD equal to 795, 1180, and 1400 degrees, respectively, for the three lines).

In model development, I consider three options for partitioning the corn growth period. The 1-stage option does not partition the growth period. The 4-stage option considers the four main stages of corn growth. The 8-stage option breaks down the "grain fill" stage into a series of sub-stages. The 8-stage option is intended to study the effect of heat and moisture stresses at the last growing stage. These three stage-breakdown options are identified in the 4^{th}, 5^{th}, and 6^{th} columns of Table 6.2, along with the associated AGDD thresholds.

Table 6.2. Corn stages are based on growing degree days and three different sub-stages of a corn growth period for this study.

Stages	GDD	1-Stage	4- Stages	8- Stages

Emergence and stand establishment (VE to V9)	VE[1]-V9	795		795	795
Rapid growth and dry matter accumulation (V10 to V17)	V10-V17	1180		1180	1180
Pollination (V18 to R1)	V18	1220		1400	
	VT[2]	1350			1350
	R1[3]	1400			
Grain fill (R2 to R6)	R2	1660			
	R3	1925			1920
	R4	2190			2190
	R5	2450		2700	2450
	R6	2700	2700		2700

1. Vegetable emergence
2. Vegetable tasseling
3. Reproductive

For the purpose of building a predictive model, I consider two temperature variables: (1) the number of the days that the temperature in stage s in county i in year t is above the optimal temperature growing range for corn ($x_{NDA_{s,t,i}}$) and (2) the number of the days in stage s in county i in year t that temperature is below the optimal temperature growing range for corn ($x_{NDB_{s,t,i}}$). For example, the horizontal dashed lines in (middle) show the lower and the upper limits of the optimal temperature grow range for corn (upper threshold is 86°F and the lower is 50°F). The points of the curve above the upper dashed line define the number of days that the temperature is above the threshold (x_{NDA}) and the points of the curve below the lower dashed line define the number of the days that temperature is below the threshold (x_{NDB}). In this example, there is not any point below the lower line between the first, second, and the third red

lines, which means the number of days that the temperature is below the threshold (x_{NDB}) is zero for both substages two and three.

To study the sensitivity to the moisture, the accumulated precipitation in stage s in county i in year t ($x_{PRC_{s,t,i}}$) is created for each sub-stages in each group of the data. The lowest plot in shows the accumulated precipitation in corn's growing period for Anne Arundel County in 2012.

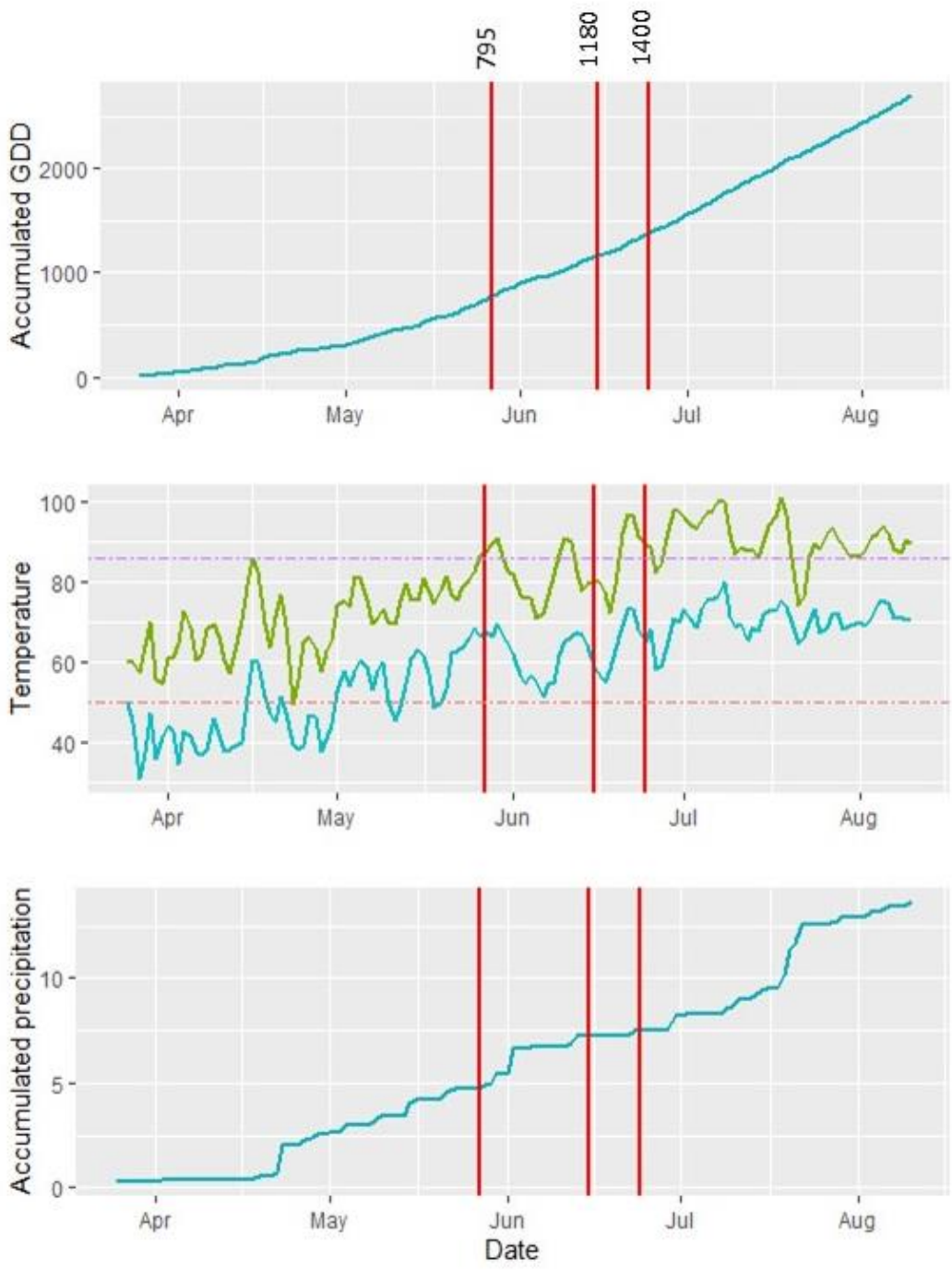

Figure 6-5. The process of creating the variables for Anne Arundel County and in 2012 for different stages of the corn. Figure 6.5 (top) shows the accumulated GDD from planting until the harvesting time (blue lines) and the dates used to separate the four different stages of the corn growth period (red vertical lines). Figure 6.5 (middle) shows the minimum and the maximum temperature (blue and green lines, respectively) and the upper and lower temperature thresholds (purple and red

dashed lines). Figure 6.5 (bottom) shows the accumulated precipitation curve for predictive models in the next section.

6.5.2 Data Partitioning and Cross-validation

We use *K*-fold cross-validation to assess the out-of-sample predictive ability of the candidate models considered in this study. This approach begins by splitting the data into K subsets. In this study, I partitioned the data by year, i.e., $K = 14$ is the number of the years in the dataset. Then, for each year $t = 1, \dots, K$, the data for year t is "holdout" (reserved) while a predictive model is trained (developed) using the remaining ($K - 1 = 13$) years of data. For example, for the first iteration, one year of the dataset is selected as the holdout (testing) set and the remaining 13 years of data represent the training data (Hastie et al., 2009).

Using the training set, spatial grouping (see Section 0) is performed, and all candidate models (see Section 6.5.3) are developed for that spatial group. The trained model is then applied to the holdout (testing) year of data, and measures of error/performance are computed at the county level. That is, for each county, the model predictions for the held-out year are compared against that year's observed values in the dataset. The process is repeated K times, incrementally "holding out" each subset (year) of data. This holdout validation provides an assessment of the ability of each candidate model to predict corn yield for "unseen" years. The computed performance metrics are used to compare candidate models.

Spatial grouping

In this study, I seek to build models to predict corn yield at the county level. In building these models, there is a trade-off between geographic specificity and data availability. To address this, I consider three different spatial model resolutions by developing state-level, county-level, and cluster models:

For the *state-level modeling approach*, all the data for Maryland (23 counties) are combined and used to train a single model for each fold of the cross-validation. The single state-level model is then applied to predict corn yields in each county for the holdout year using the county-specific explanatory variables. The performance metrics are then calculated for each county.

The *county-level modeling approach* builds and tests a predictive model for each of the 23 counties in Maryland using yield and meteorological variables for that county. Although available data for each county is limited, focusing on one county may capture local geographic effects and reduce the error due to spatial correlation between data.

The *cluster-level modeling approach* seeks to balance geographic specificity and data availability by creating geographic clusters of counties in the state. I do this using k-mean time-series clustering based on (1) total precipitation in the growth period and (2) yield. I used a hierarchical method, 4 clusters, and dynamic time wrapping (DTW) distance for both clustering options. To implement the cluster-level modeling approach, k-means clustering (using either total precipitation or yield) is applied to the training data for each cross-validation partition t, $i = 1, \dots, K$ and the counties are clustered. Then, each of the remaining candidate model assumptions are used to train

models for each cluster. To assess performance, the clusters determined using the training data are applied to partition the testing data, and the trained models are applied to generate estimates for each county. The performance metrics are calculated for each county.

6.5.3 Candidate predictive models

Predictive models can be simple, like a linear model and logistic regression, which are relatively easy to interpret but limited in the types of variable interactions they can capture. Predictive models can also involve more complex models that capture the influence of multiple interacting factors, often leading to more accurate results but with the trade-off of being harder to interpret. This study considers both conventional parametric regression and statistical learning (non-parametric) approaches to build candidate numerical models. Specifically, I considered linear regression, support vector machine, random forest, and bagged classification and regression tree (CART). I also included a simple null model (i.e., a simple average of the response variable) as a baseline against which the other models can be compared. In this way, I seek to understand the advantages of modeling, such as the high interpretability of linear models or tree-based models' ability to capture the structure of the data. Table 6.3 provides a brief description of each model. Different growing stages, different spatial grouping, and different predictive modeling give us 60 different models to compare (see Figure 6.4). Table 6.4 provides all abbreviations for the models, stages, and spatial grouping approaches used in the rest of the paper and plots.

Table 6.3. Descriptions of candidate predictive models.

Model		Description
Null	Mean	A simple average of the response variable can be used as a baseline to compare other models against it.
Parametric	Linear regression	Appropriate for observations with a linear relationship between the explanatory and response variables.
Non-Parametric	Random forest	An ensemble learning technique by integrating a large set of decision trees for classification or regression. In R.F. regression, a random set of variables and a sample of the dataset are selected for each tree. It reduces the bias brought by a single decision tree due to randomness.
	Support vector machine (SVM)	A class of algorithms characterized by the usage of Kernels and acting on margins. In the SVM regression, first, input is mapped to a higher dimensional feature space using a kernel function. Then a linear model is built in the feature space to balance between reducing the errors and overfitting.
	Bagged CART	A classification and regression (CART) model is a decision tree model with high variance, and the bagging technique can decrease its variance and improve its performance by combining the prediction from different machine learning methods together to make more accurate predictions than an individual model.

Table 6.4. Models' abbreviations and descriptions.

Model		Stage		Spatial	
LR	Linear regression	S1	1 stage	ST	State
SVM	Support vector machine	S4	4 stages	CNT	County
RF	Random forest	S8	8 stages	CLP	Cluster based on Precipitation
B.G.	Bagged CART			CLY	Cluster-based on Yield
Null	Mean				

6.6 Result

In this section, the best predictive models for each county are identified based on the three out-of-sample predictive performance measures.

The *mean absolute error* (***MAE***) is the mean of the absolute residuals taken across all holdout sets (years):

$$MAE_i = \frac{\sum_{t=1}^{K} |y_{i,t} - \hat{y}_{i.t}|}{K} \qquad (7)$$

Where $y_{i,t}$ is the actual (observed) value in year t for county i, $\hat{y}_{i,t}$ is the predicted value of the observation in year t for county i, and K is the number of holdout sets (years).

The root means square error ($\boldsymbol{RMSE}$) is the square root of the mean of the squared errors:

$$RMSE_i = \frac{\sum_{t=1}^{K}(y_{i,t} - \hat{y}_{i,t})^2}{K} \quad (8)$$

Where quantities are as defined for equation (7).

The $\boldsymbol{R^2}$ conventionally used to measure fit can also be used as a predictive measure if holdout data are used to calculate it.

$$R^2{}_i = 1 - \frac{\sum_{t=1}^{K}(y_{i,t} - \hat{y}_{i,t})^2}{\sum_{t=1}^{K}(y_{i,t} - \bar{y}_i)^2} \quad (9)$$

Where $\bar{y}_i$ is the average of actual (observed) value in year t, and other quantities are as defined for equation (7.

These performance metrics are computed for each county and explored from several perspectives. Section 6.6.1 identifies the "best model" for each county, while Section 6.6.2 explores temporal and spatial patterns of performance. Section 6.6.3 investigates variable importance and influence.

6.6.1 Selection of the best model for each county

We computed each of three performance metrics for each of the 60 candidate models. Figure 6.6 plots observed yield (y-axis) versus my model estimates (x-axis) for each county in the state of Maryland for the model with the highest R^2. The model with

the highest R^2 is identified in the titled for each plot under the county name. Figure 6.6 also lists the MAE, $RMSE$, and R^2 for the presented model. For example, for Allegany County, the best model based on R^2 is SVM/S4/CNT which means using SVM predictive model and the 4 stages and county level data gives the lowest errors and performs better than all the other combinations of the models and data grouping. $RMSE$, MAE, and R^2 are 0.16, 0.14, and 0.75, respectively. In these plots, if the model predictions were perfect, the black points would lie along the red 1:1 line. For example, for Allegany County, the SVM/S4/CNT model overestimated for lower yield and underestimated for higher yield.

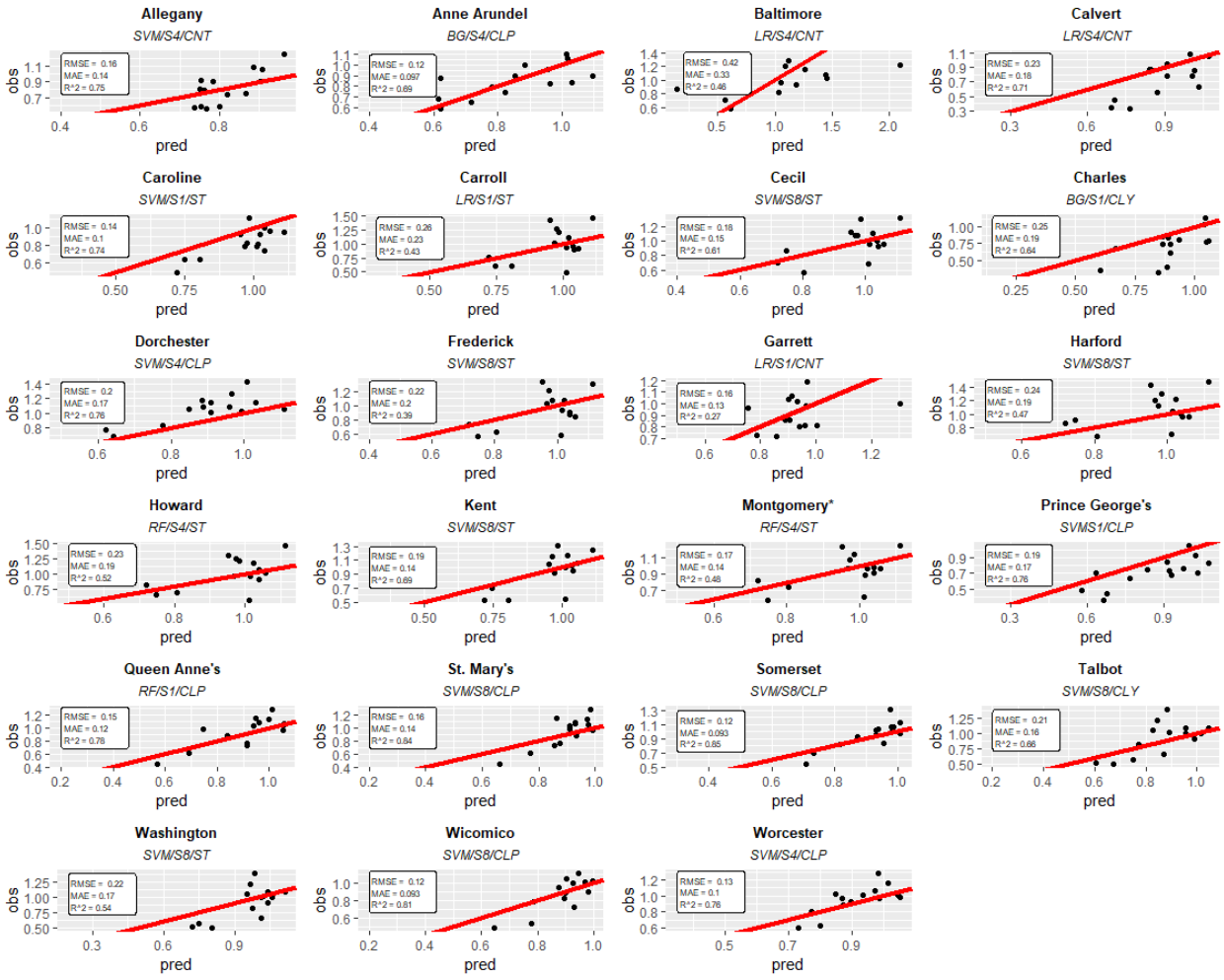

Figure 6.6. Observed corn yield for each county in the state of Maryland during study time (1950-2012) vs. predictions made using the model with the best R^2.

6.6.2 The best model, temporal, and spatial selection pattern for each county

To better understand spatial patterns in the data, Figure 6.7 uses colors to identify the modeling approach (first row of maps), the model stage (second row of maps), and the spatial grouping approach (third row) of maps that yields the highest R^2 (first column of maps), lowest MAE (second column of maps) and lowest $RMSE$ (third column of maps) for each county.

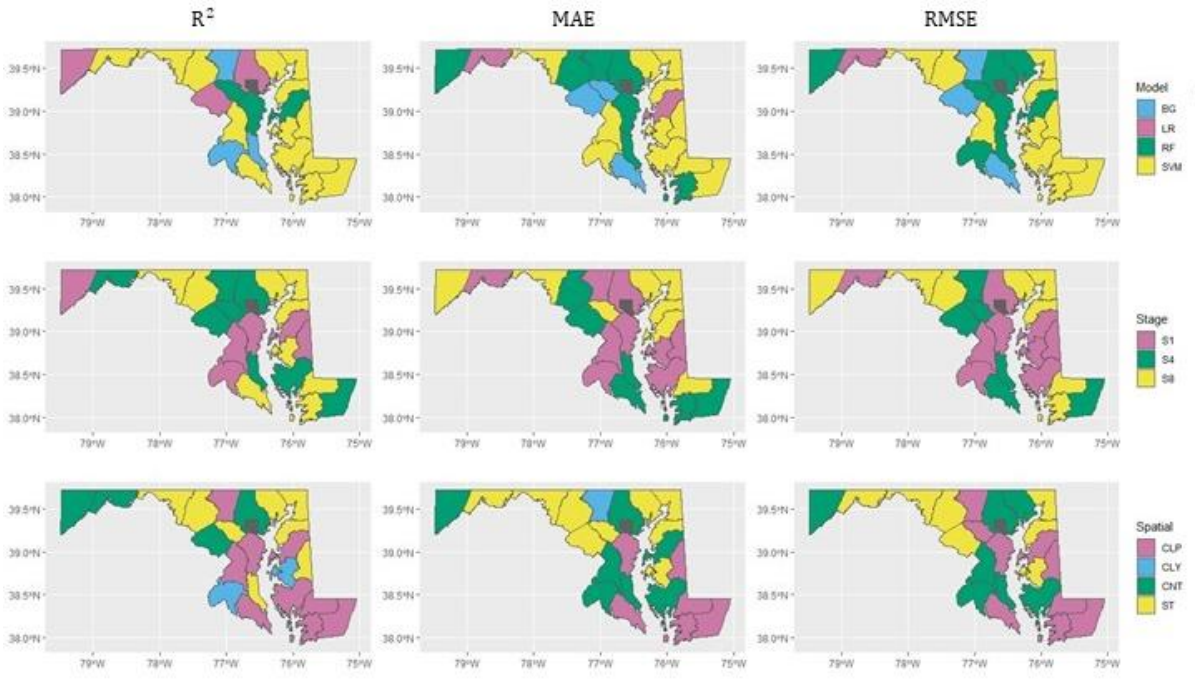

Figure 6.7. The characteristics of the "best models" for each county when considering four predictive models (first row of maps), three different temporal groupings (second row of maps), and four different spatial groupings (third row of maps). The best models for each county have been chosen based on the best R^2 (first column of maps), MAE (second column of maps) and the RMSE (third column of maps).

Looking across the first row, the SVM modeling approach "wins" in a large number of counties and while random forest comes "second." SVM consistently performs best for the counties along the Chesapeake Bay (coastal areas in the right-middle portion of the state). Results are somewhat mixed for the model stages, with the stage 1 model producing the best performance most frequently. Looking across the last row of maps, the plots do not show that any particular spatial grouping strategy performs consistently well.

Figure 6.8 depicts a map of the performance metrics (MAE, $RMSE$, and R^2) associated with the "best performing model" (where "best" is selected based on the

respective metric) for each county, as well as a map of the average yield for each county taken across the study time period. For all performance metrics, the darker color indicates better performance (i.e., smaller $RMSE$ and MAE, larger R^2). Larger agriculture production in Maryland is found in counties located along the Eastern Shore of the Chesapeake Bay and in the region north of the Bay. Better model performance (darker colors) is observed for counties located along the Chesapeake Bay, and particularly along the Eastern shore. However, weaker performance is seen in the northern region, potentially suggesting a weaker relationship between climate and agriculture productivity changes.

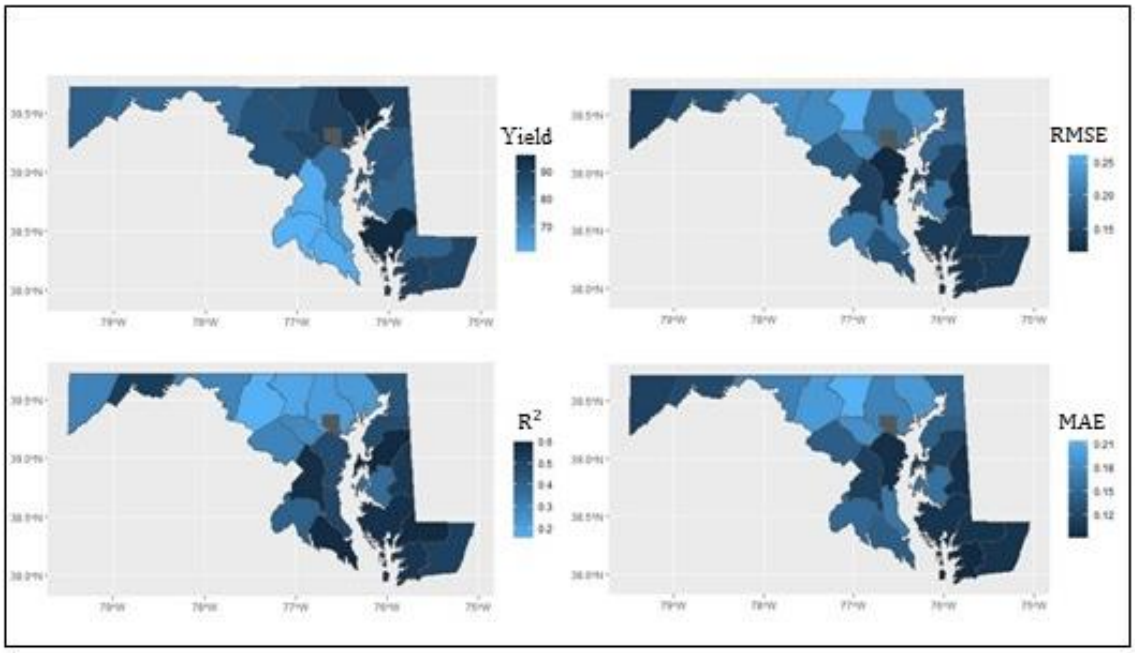

Figure 6.8. The average yield for each county in studying years and the error metrics for the best model for each county.

6.6.3 Variable importance and influence

To further explore the relationship between climate variables and agricultural yield, the "best" performing models (selected based on R^2) for Anne Arundel and Wicomico are selected for further analysis. Both counties were associated with relatively strong predictive model performance (i.e., there appears to be predictive power of climate variables and agriculture yield). The model with the best performance for Anne Arundel is a random forest model with 1 stage data and counties clustered by precipitation. The best performing model for Wicomico is an SVM model with eight stages and counties clustered by precipitation. Figure 6.9 a-b depicts the relative importance of each of the explanatory variables in these two models. Because of the large number of explanatory variables (24) shown in Figure 6.9 a, I focus on the two most important variables for further analysis: number of the days with temperature above threshold in substage 7 (x_{NDA7}) and the accumulated precipitation in substage 4 (x_{PRC4}).

The second variable importance plot (Figure 6.9. b) for Anne Arundel County is based on a model that only has three variables. The number of days with temperatures above the threshold and accumulated precipitation is the most important variable, with number of days with temperatures below the threshold having little importance.

For non-parametric models, partial dependence plots show the relationship between a covariate and the response variable by showing how the predicted quantity changes with changes in an input variable (holding all other quantities at their mean). The partial dependence plots (PDP) in Figure 6.9 c and Figure 6.9 d show the marginal

effect of the two selected variables (x_{NDA7} and X_{PRC4} for Wicomico and x_{PRC} and x_{NCD} for Anna Arundal) on predicted outcome (normalized yield). Figure 6.9 e and Figure 6.9 f present conceptually analogous plots but varying two quantities at a time. The plotted relationship between variables and the predicted outcome can be linear, monotonic, or more complex. For example, in Figure 6.9 c, when I applied an SVM model, the single variable partial dependence plot shows a smooth monotonic relationship; however, in Figure 6.9 d, the relationship is much more complicated for the random forest model. Similar patterns of simplicity versus complexity are observed in the two-variable partial dependence plots (Figure 6.9 e-f) with SVM yield a smoothly varying surface. The random forest model yielded a more complicated surface with the "plaid-like" pattern apparent in the graph reflecting the tree-like structure used in the regression model. These two models provide an interesting example of better performance by a complex model using a small number of explanatory variables versus a "simpler model" mixed with many explanatory variables.

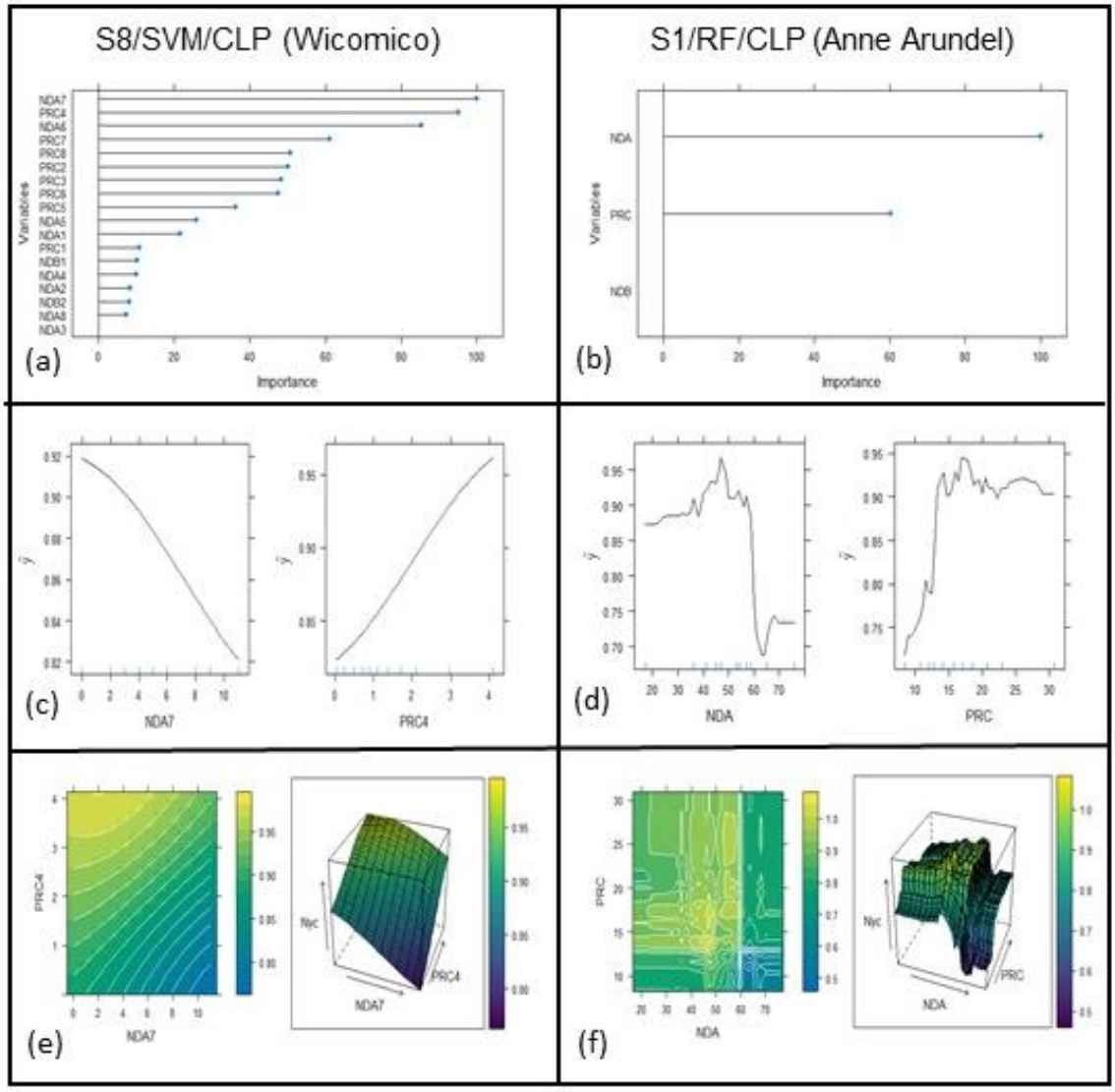

Figure 6.9. Variable importance and partial dependence plot for the two most important variables for Anne Arundel and Wicomico County. 9. a.

6.7 Discussion

Accurate predictive models could provide valuable information for understanding the potential impacts of climate on the agriculture industry. Computationally efficient models that leverage readily available public information (rather than, for example, proprietary crop data) can help infrastructure and community

planners working in agriculture-dependent regions understand how climate is likely to change agriculture in the region and the associated infrastructure needs. Previous studies use site surveys and sample data to improve their models. However, this study shows how using various machine learning strategies, spatial groupings, and temporal can improve prediction when my available data is limited to publicly available climate and agriculture data, as may be the case for infrastructure and community planners.

In the current research, I used data-driven approaches to predict corn yield in Maryland counties based on climate and precipitation data. I considered a null (mean; baseline) model, a linear regression approach, and three different machine learning methods. To help improve the accuracy of the models, I leveraged the spatial and temporal grouping. To have a more comprehensive and reliable measure of predictive capabilities used cross-validation. I found that machine learning methods performed better than linear regression in most of the counties. I found that spatial grouping and mostly clustering based on precipitation improves the accuracy of the predictions in most of the counties. I also explored variable importance and provided commentary on the potential trade-offs in modeling, including spatial specificity versus data quantity and the number of variables included in the model versus the inherent complexity of the modeling approach (algorithm).

We judge that the modeling framework created in this study to predict the corn yield at the county level is applicable to other crops and geographic contexts.

Bibliography

Alabbad, Y., Mount, J., Campbell, A. M., & Demir, I. (2021). Assessment of transportation system disruption and accessibility to critical amenities during flooding: Iowa case study. *Science of The Total Environment*, *793*, 148476. https://doi.org/10.1016/j.scitotenv.2021.148476

Alipour, A., Ahmadalipour, A., & Moradkhani, H. (2020). Assessing flash flood hazard and damages in the southeast United States. *Journal of Flood Risk Management*, *13*(2), e12605. https://doi.org/10.1111/jfr3.12605

Andersson, S., & Stålhult, S. (2014). *Hospitals exposed to flooding in Manila City, Philippines: GIS analyses of alternative emergency routes and allocation of emergency service and temporary medical centre*. http://urn.kb.se/resolve?urn=urn:nbn:se:kau:diva-33042

Andrade, M. A., Evett, S. R., & O'Shaughnessy, S. A. (2018). *Machine learning algorithms applied to the forecasting of crop water stress indicators*. 13.

Andreucci, R., & Aktas, C. B. (2017). Vulnerability of coastal Connecticut to sea level rise: Land inundation and impacts to residential property. *Civil Engineering and Environmental Systems*, *34*(2), 89–103. https://doi.org/10.1080/10286608.2017.1325878

Arora, N. K. (2019). Impact of climate change on agriculture production and its sustainable solutions. *Environmental Sustainability*, *2*(2), 95–96. https://doi.org/10.1007/s42398-019-00078-w

Asadabadi, A., & Miller-Hooks, E. (2017). Assessing strategies for protecting transportation infrastructure from an uncertain climate future. *Transportation Research Part A: Policy and Practice*, *105*, 27–41. https://doi.org/10.1016/j.tra.2017.08.010

Atkinson, A. B. (1970). On the measurement of inequality. *Journal of Economic Theory*, *2*(3), 244–263. https://doi.org/10.1016/0022-0531(70)90039-6

Azevedo de Almeida, B., & Mostafavi, A. (2016). Resilience of Infrastructure Systems to Sea-Level Rise in Coastal Areas: Impacts, Adaptation Measures, and Implementation Challenges. *Sustainability*, *8*(11), 1115. https://doi.org/10.3390/su8111115

Bier, V. M., Zhou, Y., & Du, H. (2020). Game-theoretic modeling of pre-disaster relocation. *The Engineering Economist*, *65*(2), 89–113. https://doi.org/10.1080/0013791X.2019.1677837

Bills, T. S., & Walker, J. L. (2017). Looking beyond the mean for equity analysis: Examining distributional impacts of transportation improvements. *Transport Policy*, *54*, 61–69. https://doi.org/10.1016/j.tranpol.2016.08.003

Binder, S. B., & Greer, A. (2016). The Devil Is in the Details: Linking Home Buyout Policy, Practice, and Experience After Hurricane Sandy. *Politics and Governance*, *4*(4), 97–106. https://doi.org/10.17645/pag.v4i4.738

Blanchard, S. D., & Waddell, P. (2017). Assessment of Regional Transit Accessibility in the San Francisco Bay Area of California with UrbanAccess. *Transportation Research Record*, *2654*(1), 45–54. https://doi.org/10.3141/2654-06

Boeckmann, C. (n.d.). *Growing Corn*. Old Farmer's Almanac. Retrieved November 9, 2020, from https://www.almanac.com/plant/corn

Boesch, D. F., Atkinson, L. P., Boicourt, W. C., Boon, J. D., Cahoon, D. R., Dalrymple, R. A., Ezer, T., Horton, B. P., Johnson, Z. P., & Kopp, R. E. (2013). *Updating Maryland's sea-level rise projections*.

Boesch, D. F., Boicourt, W. C., Cullather, R. I., Ezer, T., Galloway Jr, G. E., Johnson, Z. P., Kilbourne, K. H., Kirwan, M. L., Kopp, R. E., & Land, S. (2018). *Sea-level rise: Projections for Maryland 2018*.

Boon, J. D. (2012). Evidence of Sea Level Acceleration at U.S. and Canadian Tide Stations, Atlantic Coast, North America. *Journal of Coastal Research*, *28*(6), 1437–1445. https://doi.org/10.2112/JCOASTRES-D-12-00102.1

Bremmer D, Cotton KC, Cotey D, Prestrud CE, Westby G. Measuring Congestion: Learning from Operational Data. Transportation Research Record. 2004;1895(1):188-196. doi:10.3141/1895-24

Brody, S., Blessing, R., Sebastian, A., & Bedient, P. (2014). Examining the impact of land use/land cover characteristics on flood losses. *Journal of Environmental Planning and Management*, *57*(8), 1252–1265.

Brody, S. D., Highfield, W. E., Blessing, R., Makino, T., & Shepard, C. C. (2017). Evaluating the effects of open space configurations in reducing flood damage along the Gulf of Mexico coast. *Landscape and Urban Planning*, *167*, 225–231.

Bruneau, M., Chang, S. E., Eguchi, R. T., Lee, G. C., O'Rourke, T. D., Reinhorn, A. M., Shinozuka, M., Tierney, K., Wallace, W. A., & Von Winterfeldt, D. (2003). A framework to quantitatively assess and enhance the seismic resilience of communities. *Earthquake Spectra*, *19*(4), 733–752.

Bukvic, A., & Harrald, J. (2019). Rural versus urban perspective on coastal flooding: The insights from the U.S. Mid-Atlantic communities. *Climate Risk Management*, *23*, 7–18. https://doi.org/10.1016/j.crm.2018.10.004

Cai, Y., Guan, K., Lobell, D., Potgieter, A. B., Wang, S., Peng, J., Xu, T., Asseng, S., Zhang, Y., You, L., & Peng, B. (2019). Integrating satellite and climate data to predict wheat yield in Australia using machine learning approaches. *Agricultural and Forest Meteorology*, *274*, 144–159. https://doi.org/10.1016/j.agrformet.2019.03.010

Calil, J., Beck, M. W., Gleason, M., Merrifield, M., Klausmeyer, K., & Newkirk, S. (2015). Aligning natural resource conservation and flood hazard mitigation in California. *PLoS One*, *10*(7), e0132651.

Castrucci, L., & Tahvildari, N. (2017). Hydrodynamic modeling of storm surge flooding in the transportation infrastructure in southeast virginia. *OCEANS 2017 - Anchorage*, 1–8.

Castrucci, L., & Tahvildari, N. (2018). Modeling the impacts of sea level rise on storm surge inundation in flood-prone urban areas of Hampton Roads, Virginia. *Marine Technology Society Journal*, *52*(2), 92–105.

Chami, D. E., & Moujabber, M. E. (2016). Drought, climate change and sustainability of water in agriculture: A roadmap towards the NWRS2. *South African Journal of Science*, *112*(9–10), 1–4. https://doi.org/10.17159/sajs.2016/20150457.

Chang, H., Lafrenz, M., Jung, I.-W., Figliozzi, M., Platman, D., & Pederson, C. (2010). Potential Impacts of Climate Change on Flood-Induced Travel Disruptions: A Case Study of Portland, Oregon, USA. *Annals of the Association of American Geographers*, *100*(4), 938–952. https://doi.org/10.1080/00045608.2010.497110

Chang, S. E., & Nojima, N. (2001). Measuring post-disaster transportation system performance: The 1995 Kobe earthquake in comparative perspective. *Transportation Research Part A: Policy and Practice*, *35*(6), 475–494. https://doi.org/10.1016/S0965-8564(00)00003-3.

Chang, S. E. (2003). Transportation planning for disasters: an accessibility approach. *Environment and Planning A*, 35(6), 1051-1072.

Change, I. P. O. C. (2014). Ipcc. *Climate Change*.

Chanse, V. (2016). Engaging Stakeholders in the Sea Level Rise Design Process: A Pilot Project on Maryland's Eastern Shore. *International Journal of Climate Change: Impacts & Responses*, *8*(3).

Chen, X.-Z., Lu, Q.-C., Peng, Z.-R., & Ash, J. E. (2015). Analysis of Transportation Network Vulnerability under Flooding Disasters. *Transportation Research Record*, *2532*(1), 37–44. https://doi.org/10.3141/2532-05

Chen, Z., Guo, Y., Stuart, A. L., Zhang, Y., & Li, X. (2019). Exploring the equity performance of bike-sharing systems with disaggregated data: A story of southern Tampa. *Transportation Research Part A: Policy and Practice*, *130*, 529–545. https://doi.org/10.1016/j.tra.2019.09.048

Cian, F., Marconcini, M., Ceccato, P., & Giupponi, C. (2018). Flood depth estimation by means of high-resolution SAR images and lidar data. *Natural Hazards and Earth System Sciences*, *18*(11), 3063–3084. https://doi.org/10.5194/nhess-18-3063-2018

Clark, G. E., Moser, S. C., Ratick, S. J., Dow, K., Meyer, W. B., Emani, S., Jin, W., Kasperson, J. X., Kasperson, R. E., & Schwarz, H. E. (1998). Assessing the vulnerability of coastal communities to extreme storms: The case of Revere, MA., USA. *Mitigation and Adaptation Strategies for Global Change*, *3*(1), 59–82.

Climate change widespread, rapid, and intensifying – *IPCC* — (2021). Retrieved September 14, 2021, from https://www.ipcc.ch/2021/08/09/ar6-wg1-20210809-pr/

Costal Hazard System (2019). Retrieved 2019 from https://chs.erdc.dren.mil/Login/Login?ReturnUrl=%2fStorm%2fIndex

Cole, W. D. (2008). *Sea level rise: Technical guidance for Dorchester County*. Maryland Eastern Shore Resource Conservation & Development Council.

Coles, D., Yu, D., Wilby, R. L., Green, D., & Herring, Z. (2017). Beyond 'flood hotspots': Modelling emergency service accessibility during flooding in York, UK. *Journal of Hydrology*, *546*, 419–436. https://doi.org/10.1016/j.jhydrol.2016.12.013

Cox, D., Arikawa, T., Barbosa, A., Guannel, G., Inazu, D., Kennedy, A., Li, Y., Mori, N., Perry, K., Prevatt, D., Roueche, D., Shimozono, T., Simpson, C., Shimakawa, E., Shimura, T., & Slocum, R. (2019). Hurricanes Irma and Maria post-event survey in US Virgin Islands. *Coastal Engineering Journal*, *61*(2), 121–134. https://doi.org/10.1080/21664250.2018.1558920

Crowell, M., Coulton, K., Johnson, C., Westcott, J., Bellomo, D., Edelman, S., & Hirsch, E. (2010). An Estimate of the U.S. Population Living in 100-Year Coastal Flood Hazard Areas. *Journal of Coastal Research*, *26*(2), 201–211. https://doi.org/10.2112/JCOASTRES-D-09-00076.1

Csardi, G., & Nepusz, T. (2006). The igraph software package for complex network research. *InterJournal, Complex Systems*, *1695*(5), 1–9.

Cutter, S. (2016). The landscape of disaster resilience indicators in the USA. *Natural Hazards: Journal of the International Society for the Prevention and Mitigation of Natural Hazards*, *80*(2), 741–758.

Cutter, S. L. (2003). *Social Vulnerability to Environmental Hazards*—Cutter—2003—Social Science Quarterly—Wiley Online Library*. https://onlinelibrary.wiley.com/doi/epdf/10.1111/1540-6237.8402002

Cutter, S. L. (2013). *Building disaster resilience: Steps toward sustainability. Challenges in Sustainability, 1, 72+*.

Cutter, S. L. (2014). Building Disaster Resilience: Steps toward Sustainability. *Challenges in Sustainability*, *1*(2), 72–79. https://doi.org/10.12924/cis2013.01020072

Cutter, S. L., Barnes, L., Berry, M., Burton, C., Evans, E., Tate, E., & Webb, J. (2008). A place-based model for understanding community resilience to natural disasters. *Global Environmental Change*, *18*(4), 598–606. https://doi.org/10.1016/j.gloenvcha.2008.07.013

Cutter, S. L., Burton, C. G., & Emrich, C. T. (2010). Disaster resilience indicators for benchmarking baseline conditions. *Journal of Homeland Security and Emergency Management*, *7*(1).

Cutter, S. L., & Emrich, C. T. (2006). Moral Hazard, Social Catastrophe: The Changing Face of Vulnerability along the Hurricane Coasts. *The ANNALS of the American Academy of Political and Social Science*, *604*(1), 102–112. https://doi.org/10.1177/0002716205285515

Das, B., Nair, B., Arunachalam, V., Reddy, K. V., Venkatesh, P., Chakraborty, D., & Desai, S. (2020). Comparative evaluation of linear and nonlinear weather-based models for coconut yield prediction in the west coast of India. *International Journal of Biometeorology*, *64*(7), 1111–1123. https://doi.org/10.1007/s00484-020-01884-2

Dawson, R. J., Peppe, R., & Wang, M. (2011a). An agent-based model for risk-based flood incident management. *Natural Hazards*, *59*(1), 167–189.

Dawson, R. J., Peppe, R., & Wang, M. (2011b). An agent-based model for risk-based flood incident management. *Natural Hazards*, *59*(1), 167–189. https://doi.org/10.1007/s11069-011-9745-4

Dekalb. (2020). *Corn Growth Stages and Growing Degree Units*. https://www.dekalbasgrowdeltapine.com/en-us/agronomy/corn-growth-stages-and-gdu-requirements.html

Delbosc, A., & Currie, G. (2011). Using Lorenz curves to assess public transport equity. *Journal of Transport Geography*, 19(6), 1252-1259.

Department of Range and Watershed Management, Agriculture College and Natural Resources of Darab, Shiraz University, Iran, Mokarram, M., Bijanzadeh, E., & Department of Agroecology, Agriculture College and Natural Resources of Darab, Shiraz University, Iran. (2016). Prediction of biological and grain yield of barley using multiple regression and artificial neural network models. *Australian Journal of Crop Science*, *10*(6), 895–903. https://doi.org/10.21475/ajcs.2016.10.06.p7634

Deshmukh, A., Ho Oh, E., & Hastak, M. (2011). Impact of flood damaged critical infrastructure on communities and industries. *Built Environment Project and Asset Management*, *1*(2), 156–175. https://doi.org/10.1108/20441241111180415

Dixon, B. L., Hollinger, S. E., Garcia, P., & Tirupattur, V. (1994). Estimating Corn Yield Response Models to Predict Impacts of Climate Change. *Journal of Agricultural and Resource Economics*, *19*(1), 58–68. JSTOR.

Dong, Y., & Frangopol, D. M. (2017). Adaptation optimization of residential buildings under hurricane threat considering climate change in a lifecycle context. *Journal of Performance of Constructed Facilities*, *31*(6), 04017099.

Donner, W., & Rodríguez, H. (2008). Population Composition, Migration and Inequality: The Influence of Demographic Changes on Disaster Risk and

Vulnerability. *Social Forces*, *87*(2), 1089–1114. https://doi.org/10.1353/sof.0.0141

Douglas, E., Jacobs, J., Hayhoe, K., Silka, L., Daniel, J., Collins, M., Alipour, A., Anderson, B., Hebson, C., & Mecray, E. (2017). Progress and challenges in incorporating climate change information into transportation research and design. *Journal of Infrastructure Systems*, *23*(4), 04017018.

Douglass, S. L., & Krolak, J. (2008). *Highways in the coastal environment: Hydraulic engineering circular 25*. United States. Federal Highway Administration. Office of Bridge Technology.

Douglass, S. L., Webb, B. M., Kilgore, R., & Keenan, C. (2014). *Highways in the coastal environment: Assessing extreme events*. United States. Federal Highway Administration.

Dower, M. (2013). Rural development in the New Paradigm. *New Paradigm in Action–on Successful Partnerships. Ministry of Regional Development, Warsaw*, 30–50.

Driving emergencies—Driving through flood water. (2021). Smart Driving. https://smartdriving.co.uk/Driving/Driving_emergencies/Floods.htm

Drummond, S. T., Sudduth, K. A., Joshi, A., & Birrell, S. J. (2003). *Statistical and Neural Methods for Site-Specific Yield Prediction*. *46*, 12.

Emanuel, K. (2005). Increasing destructiveness of tropical cyclones over the past 30 years. *Nature*, *436*(7051), 686–688.

Emrich, C. T., & Cutter, S. L. (2011). Social Vulnerability to Climate-Sensitive Hazards in the Southern United States. *Weather, Climate, and Society*, *3*(3), 193–208. https://doi.org/10.1175/2011WCAS1092.1

Emrich, C. T., Tate, E., Larson, S. E., & Zhou, Y. (2020a). Measuring social equity in flood recovery funding. *Environmental Hazards*, *19*(3), 228–250. https://doi.org/10.1080/17477891.2019.1675578

Emrich, C. T., Tate, E., Larson, S. E., & Zhou, Y. (2020b). Measuring social equity in flood recovery funding. *Environmental Hazards*, *19*(3), 228–250. https://doi.org/10.1080/17477891.2019.1675578

Ermagun, A., & Tilahun, N. (2020). Equity of transit accessibility across Chicago. *Transportation Research Part D: Transport and Environment*, *86*, 102461. https://doi.org/10.1016/j.trd.2020.102461.

Ermagun, A., Levinson, D., 2015. Accessibility and Transit Performance. Retrieved from https://conservancy.umn.edu/bitstream/handle/11299/179832/AccessibilityTransitPerformance.pdf?sequence=1&isAllowed=yFang, J., Wahl, T., Fang, J., Sun, X., Kong, F., & Liu, M. (2020). Compound flood potential from storm surge and heavy precipitation in coastal China. *Hydrology and Earth System Sciences Discussions*, 1–24. https://doi.org/10.5194/hess-2020-377

FAO (Ed.). (2016). *Climate change, agriculture and food security*. FAO.

Faturechi, R., & Miller-Hooks, E. (2014). Travel time resilience of roadway networks under disaster. *Transportation Research Part B: Methodological*, *70*, 47–64. https://doi.org/10.1016/j.trb.2014.08.007

Feagin, R. A., Bridges, T. S., Bledsoe, B., Losos, E., Ferreira, S., Corwin, E., Lodder, Q., Beck, M. W., Reguero, B., Sutton-Grier, A., Figlus, J., Palmer, R., Nelson, D. R., Smith, C., Olander, L., Silliman, B., Pietersen, H., Costanza, R., Gittman, R. K., … Guidry, T. (2021). Infrastructure investment must incorporate Nature's lessons in a rapidly changing world. *One Earth*, *4*(10), 1361–1364. https://doi.org/10.1016/j.oneear.2021.10.003

Feng, H., Bai, F., & Xu, Y. (2019). Identification of critical roads in urban transportation network based on GPS trajectory data. *Physica A: Statistical Mechanics and Its Applications*, *535*, 122337.

Feng, T., & Zhang, J. (2014). Multicriteria evaluation on accessibility-based transportation equity in road network design problem. *Journal of Advanced Transportation*, *48*(6), 526–541. https://doi.org/10.1002/atr.1202

Fereshtehpour Mohammad, Burian Steven J., & Karamouz Mohammad. (2018). Flood Risk Assessments of Transportation Networks Utilizing Depth-Disruption Function. *World Environmental and Water Resources Congress 2018*, 134–142. https://doi.org/10.1061/9780784481431.014

Flanagan, B. E., Gregory, E. W., Hallisey, E. J., Heitgerd, J. L., & Lewis, B. (2011). A social vulnerability index for disaster management. *Journal of Homeland Security and Emergency Management*, *8*(1), 000010220215477355179 2.

Freudenberg, R., Calvin, E., Tolkoff, L., & Brawley, D. (2016). *Buy-in for buyouts: The case for managed retreat from flood zones*. Lincoln Institute of Land Policy Cambridge, MA.

Furno, A., El Faouzi, N.-E., Sharma, R., & Zimeo, E. (2019). Fast Approximated Betweenness Centrality of Directed and Weighted Graphs. In L. M. Aiello, C. Cherifi, H. Cherifi, R. Lambiotte, P. Lió, & L. M. Rocha (Eds.), *Complex Networks and Their Applications VII* (pp. 52–65). Springer International Publishing. https://doi.org/10.1007/978-3-030-05411-3_5

Furuta, H., Frangopol, D. M., & Nakatsu, K. (2011). Life-cycle cost of civil infrastructure with emphasis on balancing structural performance and seismic risk of road network. *Structure and Infrastructure Engineering*, *7*(1–2), 65–74.

Gandhi, N., Armstrong, L. J., Petkar, O., & Tripathy, A. K. (2016). Rice crop yield prediction in India using support vector machines. *2016 13th International Joint Conference on Computer Science and Software Engineering (JCSSE)*, 1–5. https://doi.org/10.1109/JCSSE.2016.7748856

Gillespie-Marthaler, L., Nelson, K., Baroud, H., & Abkowitz, M. (2019). Selecting indicators for assessing community sustainable resilience. *Risk Analysis*, *39*(11), 2479–2498.

Gini, C. (1912). Variabilità e mutabilità. Reprinted in Memorie di metodologica statistica (Ed. Pizetti E.

Gladwin, H. (1997). Warning and evacuation: A night for hard houses. *Hurricane Andrew: Ethnicity, Gender and the Sociology of Disasters*, 52–74.

González Sánchez, A., Frausto Solís, J., & Ojeda Bustamante, W. (2014). Predictive ability of machine learning methods for massive crop yield prediction. *Spanish Journal of Agricultural Research (2171-9292), 12(2)*. http://repositorio.imta.mx/handle/20.500.12013/1927

Green, D., Yu, D., Pattison, I., Wilby, R., Bosher, L., Patel, R., Thompson, P., Trowell, K., Draycon, J., & Halse, M. (2017). City-scale accessibility of emergency responders operating during flood events. *Natural Hazards and Earth System Sciences*, *17*(1), 1–16.

Gu, Y., Fu, X., Liu, Z., Xu, X., & Chen, A. (2020). Performance of transportation network under perturbations: Reliability, vulnerability, and resilience. *Transportation Research Part E: Logistics and Transportation Review*, *133*, 101809. https://doi.org/10.1016/j.tre.2019.11.003

Guo, Y., Chen, Z., Stuart, A., Li, X., & Zhang, Y. (2018). *Measuring Impact of Emerging Transportation Technologies on Community Equity in Economy, Environment and Public Health* [Report]. https://ecommons.cornell.edu/handle/1813/69733

Haimes, Y. Y. (2002). *A risk assessment methodology for critical transportation infrastructure.* Virginia Transportation Research Council.

Hardy, R. D., Milligan, R. A., & Heynen, N. (2017). Racial coastal formation: The environmental injustice of colorblind adaptation planning for sea-level rise. *Geoforum*, *87*, 62–72. https://doi.org/10.1016/j.geoforum.2017.10.005

Hastie, T., Tibshirani, R., & Friedman, J. (2009). *The Elements of Statistical Learning Data Mining, Inference, and Prediction* (Second).

Hauer, M. E., Evans, J. M., & Mishra, D. R. (2016). Millions projected to be at risk from sea-level rise in the continental United States. *Nature Climate Change*, *6*(7), 691–695.

Hausfather, Z., & Peters, G. P. (2020). Emissions – the 'business as usual' story is misleading. *Nature*, *577*(7792), 618–620. https://doi.org/10.1038/d41586-020-00177-3

Hecht, J. S., & Kirshen, P. H. (2019). Minimizing Urban Floodplain Management Regrets under Deeply Uncertain Climate Change. *Journal of Water Resources Planning and Management*, *145*(2), 04018096. https://doi.org/10.1061/(ASCE)WR.1943-5452.0001012

Highfield, W. E., & Brody, S. D. (2013). Evaluating the effectiveness of local mitigation activities in reducing flood losses. *Natural Hazards Review*, *14*(4), 229–236.

Highfield, W. E., Brody, S. D., & Blessing, R. (2014). Measuring the impact of mitigation activities on flood loss reduction at the parcel level: The case of the clear creek watershed on the upper Texas coast. *Natural Hazards*, *74*(2), 687–704. https://doi.org/10.1007/s11069-014-1209-1

Hijmans, R. J., Etten, J. van, Sumner, M., Cheng, J., Baston, D., Bevan, A., Bivand, R., Busetto, L., Canty, M., Fasoli, B., Forrest, D., Ghosh, A., Golicher, D., Gray, J., Greenberg, J. A., Hiemstra, P., Hingee, K., Geosciences, I. for M. A., Karney, C., … Wueest, R. (2021). *raster: Geographic Data Analysis and Modeling* (3.4-10) [Computer software]. https://CRAN.R-project.org/package=raster

Holland: Adaptation in natural and artificial systems:... - Google Scholar. (n.d.). Retrieved December 28, 2021, from https://scholar.google.com/scholar_lookup?title=Adaptation%20in%20natural%20and%20artificial%20systems&publication_year=1992&author=J.H.%20Holland

Hosseini Nourzad Seyed Hossein & Pradhan Anu. (2016a). Vulnerability of Infrastructure Systems: Macroscopic Analysis of Critical Disruptions on Road Networks. *Journal of Infrastructure Systems*, *22*(1), 04015014. https://doi.org/10.1061/(ASCE)IS.1943-555X.0000266

Hosseini Nourzad Seyed Hossein & Pradhan Anu. (2016b). Vulnerability of Infrastructure Systems: Macroscopic Analysis of Critical Disruptions on Road Networks. *Journal of Infrastructure Systems*, *22*(1), 04015014. https://doi.org/10.1061/(ASCE)IS.1943-555X.0000266

Hu, F., Yang, S., & Xu, W. (2014). A non-dominated sorting genetic algorithm for the location and districting planning of earthquake shelters. *International Journal of Geographical Information Science*, *28*(7), 1482–1501. https://doi.org/10.1080/13658816.2014.894638.

Hummel, M. A., Griffin, R., Arkema, K., & Guerry, A. D. (2021). Economic evaluation of sea-level rise adaptation strongly influenced by hydrodynamic feedbacks. *Proceedings of the National Academy of Sciences*, 118(29).Hummel, M. A., Siwe, A. T., Chow, A., Stacey, M. T., & Madanat, S. M. (2020). Interacting Infrastructure Disruptions Due to Environmental Events and Long-Term Climate Change. *Earth's Future*, *8*(10), e2020EF001652. https://doi.org/10.1029/2020EF001652

Huong, N. T. L., Bo, Y. S., & Fahad, S. (2019). Economic impact of climate change on agriculture using Ricardian approach: A case of northwest Vietnam. *Journal of the Saudi Society of Agricultural Sciences*, *18*(4), 449–457. https://doi.org/10.1016/j.jssas.2018.02.006

Jacobs, J. M., Cattaneo, L. R., Sweet, W., & Mansfield, T. (2018). Recent and Future Outlooks for Nuisance Flooding Impacts on Roadways on the U.S. East Coast. *Transportation Research Record*, *2672*(2), 1–10. https://doi.org/10.1177/0361198118756366

Jacobs, P., Blom, G., & van der Linden, T. (2000). Keynote Paper 2 Climatological Changes in Storm Surges and River Discharges: The Impact on Flood Protection and Salt Intrusion in the Rhine-Meuse Delta. *ECLAT-2*, 35.

Jaikla, R., Auephanwiriyakul, S., & Jintrawet, A. (2008). Rice yield prediction using a Support Vector Regression method. *2008 5th International Conference on Electrical Engineering/Electronics, Computer, Telecommunications and*

Information Technology, *1*, 29–32. https://doi.org/10.1109/ECTICON.2008.4600365

Jasour, Z. Y., Reilly, A. C., Tonn, G. L., & Ferreira, C. M. (2022). Roadway flooding as a bellwether for household retreat in rural, coastal regions vulnerable to sea-level rise. *Climate Risk Management*, *36*, 100425. https://doi.org/10.1016/j.crm.2022.100425

Jenelius, E., & Mattsson, L.-G. (2012). Road network vulnerability analysis of area-covering disruptions: A grid-based approach with case study. *Transportation Research Part A: Policy and Practice*, *46*(5), 746–760. https://doi.org/10.1016/j.tra.2012.02.003.

Jenelius, E., & Mattsson, L. G. (2015). Road network vulnerability analysis: Conceptualization, implementation and application. *Computers, environment and urban systems*, 49, 136-147.

Jenelius, E., Petersen, T., & Mattsson, L.-G. (2006). Importance and exposure in road network vulnerability analysis. *Transportation Research Part A: Policy and Practice*, *40*(7), 537–560.

Johnson, C. A., Reilly, A. C., Flage, R., & Guikema, S. D. (2021). Characterizing the robustness of power-law networks that experience spatially-correlated failures. *Proceedings of the Institution of Mechanical Engineers, Part O: Journal of Risk and Reliability*, *235*(3), 403–415. https://doi.org/10.1177/1748006X20974476

Jotshi, A., Gong, Q., & Batta, R. (2009). Dispatching and routing of emergency vehicles in disaster mitigation using data fusion. *Socio-Economic Planning Sciences*, *43*(1), 1–24.

Ju, Y., Lindbergh, S., He, Y., & Radke, J. D. (2019). Climate-related uncertainties in urban exposure to sea level rise and storm surge flooding: A multi-temporal and multi-scenario analysis. *Cities*, *92*, 230–246.

Juntunen, L. (2004). *Addressing social vulnerability to hazards* [PhD Thesis]. University of Oregon Eugene.

Karimi, V., Karami, E., & Keshavarz, M. (2018). Climate change and agriculture: Impacts and adaptive responses in Iran. *Journal of Integrative Agriculture*, *17*(1), 1–15. https://doi.org/10.1016/S2095-3119(17)61794-5

Kaul, M., Hill, R. L., & Walthall, C. (2005). Artificial neural networks for corn and soybean yield prediction. *Agricultural Systems*, *85*(1), 1–18. https://doi.org/10.1016/j.agsy.2004.07.009

Kermanshah, A., & Derrible, S. (2017). Robustness of road systems to extreme flooding: Using elements of GIS, travel demand, and network science. *Natural Hazards*, *86*(1), 151–164.

Kim Nari & Lee Yang-Won. (2016). *Machine Learning Approaches to Corn Yield Estimation Using Satellite Images and Climate Data: A Case of Iowa State - Journal of the Korean Society of Surveying, Geodesy, Photogrammetry and Cartography | Korea Science*. https://www.koreascience.or.kr/article/JAKO201625752504104.page

Kirshen, P., Knee, K., & Ruth, M. (2008). Climate change and coastal flooding in Metro Boston: Impacts and adaptation strategies. *Climatic Change*, *90*(4), 453–473. https://doi.org/10.1007/s10584-008-9398-9

Krishnamurthy, P. K. (2012). Disaster-induced migration: Assessing the impact of extreme weather events on livelihoods. *Environmental Hazards*, *11*(2), 96–111. https://doi.org/10.1080/17477891.2011.609879

Leng, G., & Hall, J. W. (2020). Predicting spatial and temporal variability in crop yields: An inter-comparison of machine learning, regression and process-based models. *Environmental Research Letters*, *15*(4), 044027. https://doi.org/10.1088/1748-9326/ab7b24.

Li, L., Uyttenhove, P., & Van Eetvelde, V. (2020). Planning green infrastructure to mitigate urban surface water flooding risk–A methodology to identify priority areas applied in the city of Ghent. *Landscape and Urban Planning*, *194*, 103703.

Li, Q., Zhang, Y. H., & Zhang, J. (2009). Practice and enlightenment of coordinated development between urban and rural areas in foreign countries. *World Agriculture*, *6*, 25-28.

Litman, T. (2008). Evaluating accessibility for transportation planning. *Victoria Transport Policy Institute, Victoria, Canada*.

Litman, T. (2012). *Evaluating accessibility for transportation planning: Measuring people's ability to reach desired goods and activities*. Victoria Transport Policy Institute.

Logan, T. M., Williams, T. G., Nisbet, A. J., Liberman, K. D., Zuo, C. T., & Guikema, S. D. (2019). Evaluating urban accessibility: Leveraging open-source data and analytics to overcome existing limitations. *Environment and Planning B: Urban Analytics and City Science*, *46*(5), 897–913.

Longenecker, H. E. (2019). *Evaluating the Effects of Induced Development on Flood Hazards and Losses in U.S. Communities with Levees* [Ph.D., University of Colorado at Boulder]. https://www.proquest.com/docview/2299814349/abstract/DA63194F1249485APQ/1

Lu, B., & Lu, M. B. (2018). *Package 'shp2graph.'*

Lu, Q.-C., & Peng, Z.-R. (2011). Vulnerability analysis of transportation network under scenarios of sea level rise. *Transportation Research Record*, *2263*(1), 174–181.

Lu, Q.-C., Peng, Z.-R., & Zhang, J. (2015). Identification and Prioritization of Critical Transportation Infrastructure: Case Study of Coastal Flooding. *Journal of Transportation Engineering*, *141*(3), 04014082. https://doi.org/10.1061/(ASCE)TE.1943-5436.0000743

Lunderville, N. (2011). Irene recovery report. *A Stronger Future. A Report to the Governor of Vermont. State of Vermont, Montpelier, Vermont.*

Malek, K., Adam, J. C., Stöckle, C. O., & Peters, R. T. (2018). Climate change reduces water availability for agriculture by decreasing non-evaporative

irrigation losses. *Journal of Hydrology*, *561*, 444–460. https://doi.org/10.1016/j.jhydrol.2017.11.046

Madanat, S. M., Papakonstantinou, I., & Lee, J. (2019). The benefits of cooperative policies for transportation network protection from sea level rise: A case study of the San Francisco Bay Area. *Transport Policy*, 76, A1-A9.

Maryland's GIS Data Catalog. (2020). Retrieved April 9, 2021, from https://data.imap.maryland.gov/

Matsumura, k, C. F. Gaitan, K. Sugimoto, & A.J. Cannon. (2015). *Maize yield forecasting by linear regression and artificial neural networks in Jilin, China | The Journal of Agricultural Science | Cambridge Core*. https://www.cambridge.org/core/journals/journal-of-agricultural-science/article/maize-yield-forecasting-by-linear-regression-and-artificial-neural-networks-in-jilin-china/18FABBC7B735E5237CBC8D23B4AD7416

Mattsson, L.-G., & Jenelius, E. (2015). Vulnerability and resilience of transport systems–A discussion of recent research. *Transportation Research Part A: Policy and Practice*, *81*, 16–34.

Mayaud, J. R., Tran, M., & Nuttall, R. (2019). An urban data framework for assessing equity in cities: Comparing accessibility to healthcare facilities in Cascadia. *Computers, Environment and Urban Systems*, *78*, 101401. https://doi.org/10.1016/j.compenvurbsys.2019.101401

McLean, R. F., Tsyban, A., Burkett, V., Codignotto, J. O., Forbes, D. L., Mimura, N., Beamish, R. J., & Ittekkot, V. (2001). Coastal zones and marine ecosystems. *Climate Change*, 343–379.

McMichael, C., Barnett, J., & McMichael, A. J. (2012). An Ill Wind? Climate Change, Migration, and Health. *Environmental Health Perspectives*, *120*(5), 646–654. https://doi.org/10.1289/ehp.1104375

Meerow, S., Newell, J. P., & Stults, M. (2016). Defining urban resilience: A review. *Landscape and Urban Planning*, *147*, 38–49.

Mendelsohn, R., Emanuel, K., Chonabayashi, S., & Bakkensen, L. (2012). The impact of climate change on global tropical cyclone damage. *Nature Climate Change*, *2*(3), 205–209. https://doi.org/10.1038/nclimate1357

Miller Hesed, C. D., & Paolisso, M. (2015). Cultural knowledge and local vulnerability in African American communities. *Nature Climate Change*, *5*(7), 683–687. https://doi.org/10.1038/nclimate2668

Mitchell: An introduction to genetic algorithms—Google Scholar. (n.d.). Retrieved December 28, 2021, from https://scholar.google.com/scholar_lookup?title=An%20introduction%20to%20genetic%20algorithms&publication_year=1996&author=M.%20Mitchell

Mora, C., Frazier, A. G., Longman, R. J., Dacks, R. S., Walton, M. M., Tong, E. J., Sanchez, J. J., Kaiser, L. R., Stender, Y. O., Anderson, J. M., Ambrosino, C. M., Fernandez-Silva, I., Giuseffi, L. M., & Giambelluca, T. W. (2013). The projected timing of climate departure from recent variability. *Nature*, *502*(7470), 183–187. https://doi.org/10.1038/nature12540

Morrow, V. (1999). Conceptualising social capital in relation to the well-being of children and young people: A critical review. *The Sociological Review*, *47*(4), 744–765.

Moser, S. C., Davidson, M. A., Kirshen, P., Mulvaney, P., Murley, J. F., Neumann, J. E., Petes, L., Reed, D., Melillo, J. M., & Richmond, T. T. (2014). Coastal zone development and ecosystems. *Climate Change Impacts in the United States: The Third National Climate Assessment*, *579*, 591.

Nafziger, E. (2009). Corn. In *Illinois Agronomy Handbook*.

Nagurney, A., & Qiang, Q. (2012). Fragile networks: Identifying vulnerabilities and synergies in an uncertain age. *International Transactions in Operational Research*, *19*(1–2), 123–160.

National programs (2018, February 5). *High tide in Dorchester*. [video]. YouTube. https://www.youtube.com/watch?v=XNA7nopSESQ&t=7s.

Scribbr. (2020, August 20). Develop a theoretical framework in three steps [Video]. YouTube. https://youtu.be/4y1BAqOnhMM

NDAWN center. (2018). *NDAWN Corn Growing Degree Days Information*. NDAWN Center. https://ndawn.ndsu.nodak.edu/help-corn-growing-degree-days.html

New Hampshire Coastal Risk and Hazards Commission. (2016). *Preparing New Hampshire for Projected Storm Surge, Sea-Level Rise, and Extreme Precipitation: Final Report and Recommendations*.

Nicholls, R. J. (2011). Planning for the impacts of sea level rise. *Oceanography*, *24*(2), 144–157.

NOAA-NCDC. (2018). *Select a Location | Data Tools | Climate Data Online (CDO) | National Climatic Data Center (NCDC)*. NOAA. https://www.ncdc.noaa.gov/cdo-web/datatools/selectlocation

Nourzad, S. H. H., & Pradhan, A. (2014). Resiliency of Intelligent Transportation Systems to Critical Disruptions: An Eigenvalue-Based Viewpoint. *Computing in Civil and Building Engineering (2014)*, 1731–1738. https://doi.org/10.1061/9780784413616.215

Oliveira, E. L. de, Portugal, L. da S., & Junior, W. P. (2014). Determining Critical Links in a Road Network: Vulnerability and Congestion Indicators. *Procedia - Social and Behavioral Sciences*, *162*, 158–167. https://doi.org/10.1016/j.sbspro.2014.12.196

Oliveira, M. P. G. de, & Rodrigues, L. H. A. (2020). How good are the models available for estimating sugar content in sugarcane? *European Journal of Agronomy*, *113*, 125992. https://doi.org/10.1016/j.eja.2019.125992

Pantazi, X. E., Moshou, D., Alexandridis, T., Whetton, R. L., & Mouazen, A. M. (2016). Wheat yield prediction using machine learning and advanced sensing techniques. *Computers and Electronics in Agriculture*, *121*, 57–65. https://doi.org/10.1016/j.compag.2015.11.018

Papakonstantinou, I., Lee, J., & Madanat, S. M. (2019a). Optimal levee installation planning for highway infrastructure protection against sea level rise. *Transportation Research Part D: Transport and Environment*, *77*, 378–389.

Papakonstantinou, I., Lee, J., & Madanat, S. M. (2019b). Game theoretic approaches for highway infrastructure protection against sea level rise: Co-opetition among multiple players. *Transportation Research Part B: Methodological*, *123*, 21–37. https://doi.org/10.1016/j.trb.2019.03.012

Paudel, B., Acharya, B. S., Ghimire, R., Dahal, K. R., & Bista, P. (2014). Adapting Agriculture to Climate Change and Variability in Chitwan: Long-Term Trends and Farmers' Perceptions. *Agricultural Research*, *3*(2), 165–174. https://doi.org/10.1007/s40003-014-0103-0

Peacock, W. G. (2003). Hurricane Mitigation Status and Factors Influencing Mitigation Status among Florida's Single-Family Homeowners. *Natural Hazards Review*, *4*(3), 149–158. https://doi.org/10.1061/(ASCE)1527-6988(2003)4:3(149)

Pearsall, H., Gutierrez-Velez, V. H., Gilbert, M. R., Hoque, S., Eakin, H., Brondizio, E. S., Solecki, W., Toran, L., Baka, J. E., Behm, J. E., Brelsford, C., Hinrichs, C., Henry, K. A., Mennis, J., Roman, L. A., Rosan, C., South, E. C., & Valletta, R. D. (2021). Advancing equitable health and well-being across urban–rural sustainable infrastructure systems. *Npj Urban Sustainability*, *1*(1), 1–6. https://doi.org/10.1038/s42949-021-00028-8

Peeta, S., Sibel Salman, F., Gunnec, D., & Viswanath, K. (2010). Pre-disaster investment decisions for strengthening a highway network. *Computers & Operations Research*, *37*(10), 1708–1719. https://doi.org/10.1016/j.cor.2009.12.006

Pistrika, A. K., & Jonkman, S. N. (2010). Damage to residential buildings due to flooding of New Orleans after hurricane Katrina. *Natural Hazards*, *54*(2), 413–434.

Pregnolato, M., Ford, A., Wilkinson, S. M., & Dawson, R. J. (2017). The impact of flooding on road transport: A depth-disruption function. *Transportation Research Part D: Transport and Environment*, *55*, 67–81. https://doi.org/10.1016/j.trd.2017.06.020

Pugh, D. (2004). *Changing sea levels: Effects of tides, weather and climate*. Cambridge University Press.

R Core Team. (2019). *R: A language and environment for statistical computing*.

Rao, N. S., Ghermandi, A., Portela, R., & Wang, X. (2015). Global values of coastal ecosystem services: A spatial economic analysis of shoreline protection values. *Ecosystem Services*, *11*, 95–105. https://doi.org/10.1016/j.ecoser.2014.11.011

Ravazzoli, E., & Hoffmann, C. (2020). *Fostering Rural Urban Relationships to Enhance More Resilient and Just Communities* (pp. 1–7). https://doi.org/10.1007/978-3-319-71061-7_109-1

Reiner, M., & McElvaney, L. (2017). Foundational infrastructure framework for city resilience. *Sustainable and Resilient Infrastructure*, *2*(1), 1–7. https://doi.org/10.1080/23789689.2017.1278994

Roel, A., & Plant, R. E. (2004). Spatiotemporal Analysis of Rice Yield Variability in Two California Fields. *Agronomy Journal*, *96*(1), 77–90. https://doi.org/10.2134/agronj2004.7700

ROCKS, 2022. retrieved from https://www.doingbusiness.org/content/dam/doingBusiness/media/Special-Reports/road-costs-knowledge-system-Updated.pdf.

Ross, W. (1999). Personal mobility or community accessibility: A planning choice with social, environmental and economic consequences [Phd, Murdoch University]. In *Ross, William <https://researchrepository.murdoch.edu.au/view/author/Ross, William.html> (1999) Personal mobility or community accessibility: A planning choice with*

social, environmental and economic consequences. PhD thesis, Murdoch University. https://researchrepository.murdoch.edu.au/id/eprint/52758/

Sadler, J. M., Haselden, N., Mellon, K., Hackel, A., Son, V., Mayfield, J., Blase, A., & Goodall, J. L. (2017). Impact of Sea-Level Rise on Roadway Flooding in the Hampton Roads Region, Virginia. *Journal of Infrastructure Systems*, *23*(4), 05017006. https://doi.org/10.1061/(ASCE)IS.1943-555X.0000397

Saeidian, B., Mesgari, M. S., & Ghodousi, M. (2016). Evaluation and comparison of Genetic Algorithm and Bees Algorithm for location–allocation of earthquake relief centers. *International Journal of Disaster Risk Reduction*, *15*, 94–107.

Sampson, C. C., Smith, A. M., Bates, P. D., Neal, J. C., Alfieri, L., & Freer, J. E. (2015). A high-resolution global flood hazard model. *Water Resources Research*, *51*(9), 7358–7381. https://doi.org/10.1002/2015WR016954

Schlenker, W., & Roberts, M. J. (2006). Nonlinear Effects of Weather on Corn Yields. *Applied Economic Perspectives and Policy*, *28*(3), 391–398. https://doi.org/10.1111/j.1467-9353.2006.00304.x

Scott, D. M., Novak, D. C., Aultman-Hall, L., & Guo, F. (2006). Network Robustness Index: A new method for identifying critical links and evaluating the performance of transportation networks. *Journal of Transport Geography*, *14*(3), 215–227. https://doi.org/10.1016/j.jtrangeo.2005.10.003

Sharifi, A. (2016). A critical review of selected tools for assessing community resilience. *Ecological Indicators*, *69*, 629–647. https://doi.org/10.1016/j.ecolind.2016.05.023

Siders, A. R. (2019). Managed Retreat in the United States. *One Earth*, *1*(2), 216–225. https://doi.org/10.1016/j.oneear.2019.09.008

Siri, E., Siri, S., & Sacone, S. (2020). Network performance evaluation under disruptive events through a progressive traffic assignment model. *IFAC-PapersOnLine*, *53*(2), 15017–15022.

Snelder, M., van Zuylen, H. J., & Immers, L. H. (2012). A framework for robustness analysis of road networks for short term variations in supply. *Transportation*

Research Part A: Policy and Practice, *46*(5), 828–842. https://doi.org/10.1016/j.tra.2012.02.007

Sniedovich, M. (2010). *Dynamic programming: Foundations and principles*. CRC press.

Sohn, J. (2006). Evaluating the significance of highway network links under the flood damage: An accessibility approach. *Transportation Research Part A: Policy and Practice*, *40*(6), 491–506. https://doi.org/10.1016/j.tra.2005.08.006

Song, J., & Peng, B. (2017). Should We Leave? Attitudes towards Relocation in Response to Sea Level Rise. *Water*, *9*(12), 941. https://doi.org/10.3390/w9120941

Spain, D., & Bianchi, S. (1996). *Balancing act: Motherhood, marriage, and employment among American women*. Russell Sage Foundation.

Stanton, E. A., & Ackerman, F. (2007). Florida and climate change: The costs of inaction. *Florida and Climate Change: The Costs of Inaction.*

State of California Sea-Level Rise Guidance. (2018). 84.

Suarez, P., Anderson, W., Mahal, V., & Lakshmanan, T. R. (2005). Impacts of flooding and climate change on urban transportation: A systemwide performance assessment of the Boston Metro Area. *Transportation Research Part D: Transport and Environment*, *10*(3), 231–244.

Suh, J., Siwe, A. T., & Madanat, S. M. (2019). Transportation infrastructure protection planning against sea level rise: Analysis using operational landscape units. *Journal of Infrastructure Systems*, 25(3), 4019024.

Sullivan, J. L., Novak, D. C., Aultman-Hall, L., & Scott, D. M. (2010). Identifying critical road segments and measuring system-wide robustness in transportation networks with isolating links: A link-based capacity-reduction approach. *Transportation Research Part A: Policy and Practice*, *44*(5), 323–336. https://doi.org/10.1016/j.tra.2010.02.003

Sun, J., Chow, A. C. H., & Madanat, S. M. (2020). Multimodal transportation system protection against sea level rise. *Transportation Research Part D: Transport and Environment*, *88*, 102568. https://doi.org/10.1016/j.trd.2020.102568

Sun, J., Chow, A. C., & Madanat, S. M. (2021). Equity concerns in transportation infrastructure protection against sea level rise. *Transport Policy*, *100*, 81–88.

Tacoli, C., & Mabala, R. (2010). Exploring mobility and migration in the context of rural—urban linkages: Why gender and generation matter. *Environment and Urbanization*, *22*(2), 389–395. https://doi.org/10.1177/0956247810379935

Tahmasbi, B., Mansourianfar, M. H., Haghshenas, H., & Kim, I. (2019). Multimodal accessibility-based equity assessment of urban public facilities distribution. *Sustainable Cities and Society*, *49*, 101633. https://doi.org/10.1016/j.scs.2019.101633

Taylor, M. A. P., & D'Este, G. M. (2007). Transport Network Vulnerability: A Method for Diagnosis of Critical Locations in Transport Infrastructure Systems. In A. T. Murray & T. H. Grubesic (Eds.), *Critical Infrastructure: Reliability and Vulnerability* (pp. 9–30). Springer. https://doi.org/10.1007/978-3-540-68056-7_2

Taylor, M. A. P. & Susilawati. (2012). Remoteness and accessibility in the vulnerability analysis of regional road networks. *Transportation Research Part A: Policy and Practice*, *46*(5), 761–771. https://doi.org/10.1016/j.tra.2012.02.008.

The White House, 2022. Strengthening the rural economy-strengthening rural infrastructure. Retrieved from , https://obamawhitehouse.archives.gov/administration/eop/cea/factsheets-reports/strengthening-the-rural-economy/strengthening-rural-infrastructure

Twigger-Ross, C., Great Britain, Environment Agency, Great Britain, & Department for Environment, F. & R. A. (2005). *The impact of flooding on urban and rural communities*. Environment Agency.

US Census Bureau. (2017). *TIGER/Line Shapefiles*. The United States Census Bureau. https://www.census.gov/geographies/mapping-files/time-series/geo/tiger-line-file.html

USDA. (2018). *USDA - National Agricultural Statistics Service—Statistics by Subject*. https://www.nass.usda.gov/Statistics_by_Subject/index.php

Vromans, M. J., Dekker, R., & Kroon, L. G. (2006). Reliability and heterogeneity of railway services. *European Journal of Operational Research*, *172*(2), 647–665.

Wang, Y., Zhang, Z., Feng, L., Du, Q., & Runge, T. (2020). Combining Multi-Source Data and Machine Learning Approaches to Predict Winter Wheat Yield in the Conterminous United States. *Remote Sensing*, *12*(8), 1232. https://doi.org/10.3390/rs12081232

Warner, K., Ranger, N., Surminski, S., Arnold, M., Linnerooth-Bayer, J., Michel-Kerjan, E., Kovacs, P., & Herweijer, C. (2009). Adaptation to climate change: Linking disaster risk reduction and insurance. *United Nations International Strategy for Disaster Reduction, Geneva*.

Warren-Myers, G., Aschwanden, G., Fuerst, F., & Krause, A. (2018). Estimating the Potential Risks of Sea Level Rise for Public and Private Property Ownership, Occupation and Management. *Risks*, *6*(2), 37. https://doi.org/10.3390/risks6020037

Weiss, J. L., Overpeck, J. T., & Strauss, B. (2011). Implications of recent sea level rise science for low-elevation areas in coastal cities of the conterminous U.S.A. *Climatic Change*, *105*(3), 635–645. https://doi.org/10.1007/s10584-011-0024-x

Welcome to the NOAA Institutional Repository (2020). Retrieved December 9, 2020, from https://repository.library.noaa.gov/view/noaa/2565

Wilbanks, T. J., & Fernandez, S. (Eds.). (2014). *Climate Change and Infrastructure, Urban Systems, and Vulnerabilities*. Island Press/Center for Resource Economics. https://doi.org/10.5822/978-1-61091-556-4

Wolanin, A., Mateo-García, G., Camps-Valls, G., Gómez-Chova, L., Meroni, M., Duveiller, G., Liangzhi, Y., & Guanter, L. (2020). Estimating and understanding crop yields with explainable deep learning in the Indian Wheat Belt. *Environmental Research Letters*, *15*(2), 024019. https://doi.org/10.1088/1748-9326/ab68ac

Wu, S.-Y., Yarnal, B., & Fisher, A. (2002). Vulnerability of coastal communities to sea-level rise: A case study of Cape May County, New Jersey, USA. *Climate Research*, *22*(3), 255–270.

Zamojska, A., & Próchniak, J. (2017). Measuring the social impact of infrastructure projects: The case of Gdańsk International Fair Co. *Journal of Entrepreneurship, Management and Innovation*, *13*(4), 25–42.

Zhang, W., & Wang, N. (2016). Resilience-based risk mitigation for road networks. *Structural Safety*, *62*, 57–65. https://doi.org/10.1016/j.strusafe.2016.06.003

Zuo, T., Wei, H., Chen, N., & Zhang, C. (2020). First-and-last mile solution via bicycling to improving transit accessibility and advancing transportation equity. *Cities*, *99*, 102614. https://doi.org/10.1016/j.cities.2020.102614.